

23613643



This is to certify that the

dissertation entitled

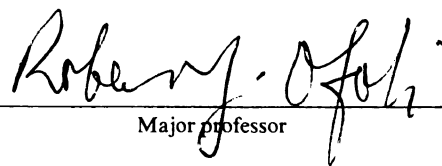
Starch Liquefaction by Thermostable Alpha-Amylase
During Reactive Extrusion

presented by

Vanee Komolprasert

has been accepted towards fulfillment
of the requirements for

Ph.D. degree in Agricultural Engineering

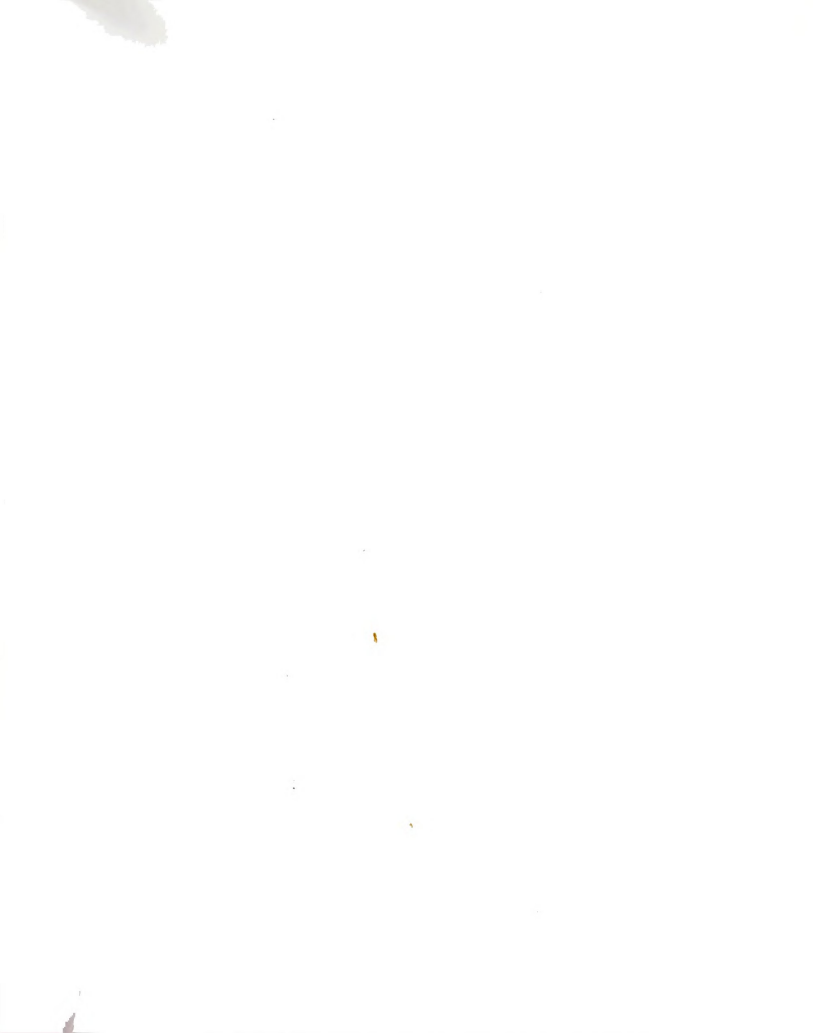

Major professor

Date 12-11-1989

**PLACE IN RETURN BOX to remove this checkout from your record.
TO AVOID FINES return on or before date due.**

DATE DUE	DATE DUE	DATE DUE
_____	_____	_____
_____	_____	_____
_____	_____	_____
_____	_____	_____
_____	_____	_____
_____	_____	_____
_____	_____	_____

MSU Is An Affirmative Action/Equal Opportunity Institution



**STARCH LIQUEFACTION BY THERMOSTABLE ALPHA-AMYLASE
DURING REACTIVE EXTRUSION**

By

Vanee Komolprasert

A DISSERTATION

Submitted to
Michigan State University
in partial fulfillment of the requirements
for the degree of

DOCTOR OF PHILOSOPHY

in

Agricultural Engineering

Department of Agricultural Engineering

1989

6054523

ABSTRACT

STARCH LIQUEFACTION BY THERMOSTABLE ALPHA-AMYLASE DURING REACTIVE EXTRUSION

By

Vanee Komolprasert

An MPF-50D Baker-Perkins twin screw extruder was used as a bioreactor for liquefaction of pre-gelatinized corn starch by thermostable α -amylase. A one-dimensional axial dispersion model was used to predict the extent of liquefaction, and was evaluated using data from several experimental extrusion runs.

An initial rate study at low starch concentration (1-8% w/w) showed that the kinetics of α -amylase follows the classical Michaelis-Menten model. At a starch concentration of 40%, a continuous rate study was used. Results from this study showed that the enzyme kinetics could be described by a modified first order equation with a rate constant of 0.033 min^{-1} at 95°C and a pH of 6.0.

The effect of shear on enzyme activity was studied in both a Haake viscometer and the extruder. While loss of activity was found to depend significantly on strain history alone in the viscometer, loss of activity in the extruder depended on the combination of strain history, shear rate and specific energy consumption (SEC). The loss of enzyme activity in the extruder was small (20%), possibly due to the shielding effect of soy polysaccharide (SPS) which was used as a carrier for the enzyme.

Corn syrup (Newtonian), 7% SPS in honey and 2.5% methocel in water were used to determine the effect of rheological behavior on the dispersion of fluids during extrusion. The extruder was modeled as a tube, using the hydraulic diameter as a characteristic dimension. The Taylor-Aris dispersion model for laminar tube flow was used to describe the effect of molecular diffusion and velocity profile on the dispersion

coefficient. Results showed that the Taylor-Aris model is applicable to the SPS-honey mixture and to corn syrup. Effect of velocity was dominant in comparison to that of molecular diffusion.

The extent of starch liquefaction depended significantly on moisture content, residence time and enzyme dosage. Dispersion numbers were calculated from residence time distribution (RTD) data and used in the axial dispersion model. The dispersion number decreased with increased length of reaction zone but increased with increased screw rpm. The axial dispersion equation was solved analytically and compared to experimental data, with very good agreement. The maximum fractional conversion was 0.3 at a residence time of 11 minutes.



ACKNOWLEDGMENTS

I would like to express my sincere gratitude and appreciation to Dr. Robert Y. Ofoli, my major professor, for giving me financial support throughout my program, and enabling me to pursue my degree. Many thanks for his guidance, encouragement and for all his hard work in the preparation of this dissertation. Without his guidance and support, this would not have been possible.

Thanks to Dr. K. Jayaraman (Associate Professor of Chemical Engineering) for his suggestions in experimental design and analyses, and for helping me learning more about viscoelasticity. Thanks to Dr. D. Miller (Associate Professor of Chemical Engineering) who helped me extend my knowledge of kinetics and for his assistance in analyzing the kinetic data. Thanks also to Dr. K. Berglund (Associate Professor of Chemical Engineering and Agricultural Engineering) and Dr. Bruce R. Harte (Associate Professor of the School of Packaging) for their advice and willingness to serve on my guidance committee.

Thanks to Dr. Badal Saha (Senior Scientist of the Michigan Biotechnology Institute) for his suggestions on analytical procedures. Thanks to Steve Hull, John Keenan and Drew Van-Norman for their help in all the extrusion runs, and to all my friends for their help in making my study possible.

Special thanks to my mother in Thailand for her love, support and encouragement throughout my study. Thanks to the Gingas family for their love and care, and for making me feel at home during my stay in Michigan.

Support for this work from the Research Excellence Fund (REF) of the State of Michigan is gratefully acknowledged.

TABLE OF CONTENTS

LIST OF TABLES	viii
LIST OF FIGURES	x
1 INTRODUCTION	1
2 OBJECTIVES	3
3 LITERATURE REVIEW	4
3.1 The Nature of Starch	4
3.1.1 Starch components and structure	4
3.1.2 Starch gelatinization	6
3.2 Amylolytic Enzymes	7
3.3 Processes for Producing Sweeteners	9
3.4 Enzyme Kinetics	10
3.5 Legal Aspects of Enzyme Uses	12
3.6 Overview of Food Extruders	13
3.7 Extrusion Processing	15
3.7.1 Mixing in extruders	18
3.7.2 Process instability	20
3.7.3 Application of polymer extrusion theory to food extrusion	21
3.8 Rheological Changes During Extrusion	21
3.9 Ideal and Non-ideal Reactors	22
3.9.1 Residence time distribution	23
3.9.2 Extent of chemical reaction	24
3.9.3 Residence time distribution in single and twin screw extruders	25
3.10 Starch Hydrolysis in Twin Screw Extruders	27
3.10.1 Liquefaction	29
3.10.2 Enzyme inactivation in the extruder	29
3.11 Nomenclature	30
3.12 References	32
4 STARCH HYDROLYSIS KINETICS OF THERMOSTABLE ALPHA-AMYLASE	40
4.1 Abstract	40
4.2 Introduction and Background	40
4.3 Theory	43
4.4 Materials and Methods	46
4.4.1 Initial rate study at low starch concentrations	46
4.4.2 Continuous rate study at high starch concentrations	46

4.5 Results	47
4.5.1 Initial rate study at low starch concentrations	47
4.5.2 Continuous rate study at high starch concentration	48
4.6 Discussion	60
4.7 Conclusions	61
4.8 Nomenclature	62
4.9 References	64
5 EFFECT OF SHEAR ON ENZYMATIC ACTIVITY DURING REACTIVE EXTRUSION	67
5.1 Abstract	67
5.2 Introduction and Background	67
5.3 Theory	69
5.4 Materials and Methods	71
5.4.1 Haake viscometer experiments	71
5.4.2 Extruder experiments	72
5.4.3 Determination of the effect of shear in the TSE	74
5.5 Results and Discussion	75
5.5.1 Shear deactivation in the batch system	75
5.5.2 Shear deactivation in twin screw extruders	79
5.6 Conclusions	81
5.7 Nomenclature	82
5.8 References	84
6 EFFECT OF MATERIAL RHEOLOGY ON THE DISPERSION OF FLUIDS IN EXTRUDERS	86
6.1 Abstract	86
6.2 Introduction and Background	86
6.2.1 Diffusion and Dispersion	89
6.3 Theoretical Development	93
6.4 Materials and Methods	96
6.4.1 Rheological behavior	98
6.5 Results and Discussion	98
6.5.1 Rheological data	98
6.5.2 Extrusion data	104
6.6 Conclusions	109
6.7 Nomenclature	110
6.8 References	112
7 A DISPERSION MODEL FOR PREDICTING THE EXTENT OF LIQUEFACTION BY ALPHA-AMYLASE IN REACTIVE EXTRUSION	114
7.1 Abstract	114
7.2 Introduction and Background	114
7.3 Model Development	117
7.4 Materials and Methods	119
7.4.1 Determination of residence time distribution (RTD)	127
7.4.2 Estimation of dispersion coefficients	129
7.4.3 Sample preparation and analysis for reducing sugar	131

7.4.4 Estimation of the apparent viscosity of starch in the extruder	132
7.4.5 Rheological data	134
7.5 Results and Discussion	135
7.5.1 Estimation of dispersion numbers and dispersion coefficients	135
7.5.2 Use of the dispersion model to predict RTD	143
7.5.3 Extent of starch liquefaction in the extruder	147
7.5.4 Relationship between power number and Reynolds number for mixed screws	149
7.5.5 Effect of rheology on extent of reaction	153
7.5.6 Dispersion model for predicting starch hydrolysis in reactive extrusion	154
7.6 Conclusions	160
7.7 Nomenclature	161
7.8 References	164
8 CONCLUSIONS	167
9 RECOMMENDATIONS FOR FURTHER RESEARCH	169
10 APPENDICES	170
Appendix 1. Shear deactivation data from Haake viscometer	170
Appendix 2. Analysis of variance (SAS program) of effect of strain history on % residual enzyme activity from Haake viscometer data	172
Appendix 3. Shear deactivation data from extrusion runs	173
Appendix 4. Analysis of variance (SAS program) of effect of strain history on enzyme activity during extrusion	174
Appendix 5. Analysis of variance (SAS program) of effect of strain history, shear rate and SEC on enzyme activity during extrusion	175
Appendix 6. Extrusion data for corn syrup, 7% SPS in honey and 2.5% Methocel	176
Appendix 7. Paddle configurations in the twin screw extruder	177
Appendix 8. Extrusion data on starch liquefaction (extrusion runs 1-20)	178
Appendix 9. Analysis of variance (SAS program) of mean residence time (RTD) for extrusion runs 1-12	179
Appendix 10. Analysis of variance (SAS program) of dispersion number (DI) for extrusion runs 1-12	180
Appendix 11. Analysis of variance (SAS program) of dispersion number (DI) for extrusion runs 13-20	181
Appendix 12. Percent reducing sugar and DE from extrusion runs 1-20	182
Appendix 13. Analysis of variance (SAS program) of effect of moisture content, screw rpm and enzyme level on % reducing sugar (RS) and % DE for extrusion runs 1-12	185
Appendix 14. Analysis of variance (SAS program) of effect of method of enzyme addition on % reducing sugar (RS) and % DE for extrusion runs 13-20	186

LIST OF TABLES

Table 3.1. Gelatinization temperatures of several native starches.	7
Table 3.2. Profiles of industrial sugar produced from starch.	10
Table 4.1. Relative reducing power of various sugars.	41
Table 4.2. Stability of Termamyl 60L and 120L in terms of enzyme half-life in minutes for DE values in the range of 0-12.	42
Table 4.3. Kinetic models from the literature.	45
Table 4.4. Percent of unreacted starch, reducing sugars DE, and fractional conversion (first replicate of continuous rate study).	50
Table 4.5. Percent of unreacted starch, reducing sugars DE, and fractional conversion (second replicate of continuous rate study).	51
Table 5.1. Experimental conditions used in the Haake viscometer.	72
Table 5.2. Residual enzymatic activity obtained from the Haake viscometer.	76
Table 5.3. Power and Reynolds numbers for 30% SPS in water.	80
Table 5.4. Values of apparent viscosity, shear rate, mean residence time, strain history, specific energy consumption, ratio of mass flow rate to screw rpm and % residual enzyme activity.	80
Table 6.1. Rheological models of the fluids used, derived from steady shear experiments.	99
Table 6.2. Zero shear viscosity and equilibrium creep compliance of corn syrup, 7% SPS in honey and 2.5 % methocel in water.	104
Table 6.3. Apparent viscosity and estimated average shear rate of corn syrup, 7% SPS in honey and 2.5% methocel, at various extrusion conditions.	105
Table 6.4. Dispersion number, dispersion coefficient and molecular diffusion coefficient of corn syrup, 7% SPS in honey and 2.5% methocel.	105
Table 6.5. Axial and radial Peclet number, and dimensionless time of corn syrup, 7% SPS in honey and 2.5% methocel.	109

Table 7.1. Experimental design for extrusion runs 1-12.	123
Table 7.2. Experimental conditions for extrusion runs 13-20.	123
Table 7.3. Mean residence time, dispersion number and dispersion coefficient from extrusion runs 1-12.	135
Table 7.4. Mean residence time, dispersion number and dispersion coefficient from extrusion runs 13-20.	141
Table 7.5. Mean velocity and dispersion coefficient at various zone lengths during extrusion run 20.	142
Table 7.6. Values of "b" (Eq. 7.31) and standard errors for various extrusion runs.	145
Table 7.7. Percent reducing sugar and DE (extrusion runs 1-12).	148
Table 7.8. Percent of un-reacted starch, reducing sugar and DE, and fractional conversion (from extrusion runs 13-20).	148
Table 7.9. Consistency coefficients for corn syrup at various temperatures.	149
Table 7.10. Power and Reynolds numbers for corn syrup.	151
Table 7.11. Normalized viscosity indices of starch extrudates from extrusion runs 1-12.	153
Table 7.12. Normalized viscosity indices of starch extrudates from extrusion runs 13-20.	154
Table 7.13. Observed and predicted fractional conversions (extrusion runs 13-20).	158

LIST OF FIGURES

Figure 4.1 Lineweaver-Burk plot of reciprocal rate of product formation versus reciprocal initial starch concentration.	49
Figure 4.2 Fractional conversion (X) versus residence time.	52
Figure 4.3 Dextrose equivalent (DE) and starch concentration ([S]) versus residence time.	54
Figure 4.4 Rate of starch consumption versus modified starch concentration.	56
Figure 4.5 Rate of product formation versus modified starch concentration.	58
Figure 4.6 Rate of product formation versus rate of starch consumption.	59
Figure 5.1 Percent residual activity of α -amylase versus strain history (data obtained from a mixer viscometer).	77
Figure 5.2 Percent residual activity vs. strain history of rennet, catalase, carboxypeptidase (Charm and Wong, 1970) and α -amylase (this study).	78
Figure 6.1 Contribution of convective transfer and molecular diffusion to dispersion in laminar flow (Butt, 1980).	91
Figure 6.2 Schematic of the setup of the MPF-50D Baker-Perkins twin screw extruder at 15 L/D.	97
Figure 6.3 Storage modulus, loss modulus and complex viscosity versus frequency for corn syrup at 23.4°C.	100
Figure 6.4 Storage modulus, loss modulus and complex viscosity versus frequency for 7% SPS in honey at 24.6°C.	101
Figure 6.5 Storage modulus, loss modulus and complex viscosity versus frequency for 2.5% Methocel at 22.8°C.	102
Figure 6.6 Velocity profile in laminar tube flow of a Newtonian fluid (n=1), non-Newtonian fluid (n<1), and in plug flow (n=0).	106
Figure 6.7 Dispersion coefficient versus mean velocity and molecular diffusion coefficient (based on Eq. 6.13).	108

Figure 7.1 Layout of the Baker-Perkins MPF-50D twin screw extruder.	120
Figure 7.2 Dimensions of screw elements used in the MPF-50D Baker-Perkins twin screw extruder.	121
Figure 7.3 Extruder setup for experiments 1-12 showing entry points of enzyme solution (E) and tracer dyes.	124
Figure 7.4 Extruder setup for experiments 13-16 showing entry points of enzyme solution (E) and tracer dyes.	125
Figure 7.5 Extruder setup for experiments 17-20 showing entry points of enzyme solution (E).	126
Figure 7.6 Extruder setup for experiments 20.1, 20.2 and 20.3 showing entry points of dye solution.	128
Figure 7.7 Schematic setup of the MPF-50D Baker-Perkins twin screw extruder for corn syrup experiments.	133
Figure 7.8 C-curves from experiments 1, 2, 5, 6, 9 and 10 at 60% moisture content.	136
Figure 7.9 C-curves from experiments 3, 4, 7, 8, 11 and 12 at 50% moisture content.	137
Figure 7.10 C-curves (redness versus residence time) from experiments 13-16 (mean residence times: 2.2, 4.7, 7.6 and 10.7 min, respectively).	139
Figure 7.11 C-curves (redness versus residence time) from experiments 17-20 (mean residence times: 4.6, 5.7, 10.3 and 10.4 min, respectively).....	140
Figure 7.12 Experimental and calculated F functions versus time.	146
Figure 7.13 Viscosity versus inverse temperature for corn syrup.	150
Figure 7.14 Power number versus Reynolds number for corn syrup (Newtonian standard).	152
Figure 7.15 Predicted fractional conversion versus normalized length of reactor from experiments 13-16.	156
Figure 7.16 Predicted fractional conversion versus normalized length of reactor from experiments 17-20.	157
Figure 7.17 Predicted and observed fractional conversion versus normalized length of reactor from experiments 13-20.	159

1 INTRODUCTION

Since twin screw extruders provide high productivity and versatility, they have become popular and have replaced the single screw extruder in many processes. The twin screw extruder improves mixing and heat transfer, therefore it is good for high temperature short time (HTST) processes. Use of the twin screw extruder as a bioreactor is a novel approach, and has induced much interest. In the last decade, most of the studies have focused on hydrolysis of starch both with and without enzymes.

Heat and mechanical energy cause degradation of starch, resulting in reduced viscosity and increased solubility. Solubility improves texture and increases digestibility for human nutrition. Without addition of enzymes, solubility is limited and depends highly on extrusion conditions. However, use of an α -amylase accelerates viscosity reduction and increases solubility, preventing the starch from retrogradation. Many investigators have used extrusion for the pretreatment and/or liquefaction of substrates for subsequent saccharification and fermentation. This process converts starch, a cheap material, to more value products such as glucose, maltose and alcohol.

Although α -amylase has been used in liquefaction for many years, the process usually takes place in a batch system where the residence time can be increased to obtain high conversion rates. In contrast, the extrusion process generally occurs over relatively short residence times, therefore a high conversion is difficult to obtain in a single passage. However, the process may be used to partially saccharify starch, and enhance product sweetness without addition of external sugars.

The use of enzymes in twin screw extruders for liquefaction and/or saccharification has a lot of potential. However, its acceptance and utility has been slow because of lack

of understanding of the extrusion process during enzymatic reaction, and lack of information on appropriate quantitative models for predicting the extent of starch conversion.

2 OBJECTIVES

To realize the potential of using twin screw extruders as bioreactors, an accurate model for predicting the extent of reaction is required for process design and control. Because of its versatility and combination of possible operating conditions, a model for enzyme reaction kinetics in the extruder must of necessity be quite general. Unfortunately, such a generalized model would be difficult to develop. However, if the extruder is set up with a screw configuration to induce a flow pattern near plug flow, then a one-dimensional axial dispersion model could be used.

The primary goal of this study was to develop and verify an axial dispersion model for predicting the extent of starch liquefaction by thermostable α -amylase in a co-rotating twin screw extruder. To develop an appropriate model, however, it is necessary to develop an understanding of the interactions between enzyme kinetics, material rheology and flow characteristics in the extruder.

Therefore, to achieve the primary objective above, the following specific activities were undertaken:

1. Determination of the kinetics of starch hydrolysis by α -amylase and the use of the kinetic information for predicting the extent of starch conversion in an extruder being used as a bioreactor;
2. Investigation of the influence of extrusion shear on enzymatic activity during reactive extrusion;
3. Assessment of the effect of material rheological behavior on degree of fluid dispersion, measured in terms of a dispersion coefficient; and
4. Development of a methodology to determine the dispersion coefficient and the use of the coefficients in a model for predicting the extent of starch liquefaction.

3 LITERATURE REVIEW

3.1 The Nature of Starch

3.1.1 Starch components and structure

Starch is a major source of reserved carbohydrate found in plant cells as large granules. These granules are arranged either in concentric layers (as in cereal grains) or in eccentric layers (as in potato tubers). Starch is an α -glucan that consists of two distinct components: amylose and amylopectin.

The structure of amylose is not well defined (Hood, 1982); it was first thought to be a linear glucose polymer linked by α -1,4 linkages until it was proved to be nonlinear, based on chemical evidence reported by Williams (1968), and Wolfrom and Khadem (1965). Banks and Greenwood (1975) concluded that amylose is made up of a mixture of linear molecules with α -1,4 linkages and branched molecules with α -1,6 linkages.

Pure amylose can be separated from amylopectin by two methods (Hood, 1982):

1. Partial gelatinization, which releases low molecular weight linear amylose from the granule.
2. Solubilization of granular starch in dimethylsulfoxide or alkali, followed by adding thymol to form an insoluble complex with amylose.

The purity of the isolated amylose is measured by iodine binding capacity (IBC). The IBC of pure amylose is 20% while that of amylopectin is much smaller. The iodine complex is associated with a helical structure of the starch chains. Dextrins containing less than six D-glucose residues do not produce the characteristic colored complex (Solomon, 1978). Amylose has a molecular weight of $1.5 \times 10^5 - 10^6$, depending on its native source. In the linear chain, the average length is 500-2000 glucose units. Amylose with 250-300 units can form a helix.

Amylose does not easily dissolve in water, or does so only to a limited extent. In the form of its butanol complex, amylose disperses in aqueous solution; its stability depends on pH, concentration, molecular size and the presence of electrolytes (Solomon, 1978). Molecular conformations of concentrated amylose are responsible for retrogradation.

Amylopectin is a branched structure containing 94-96% α -1,4 and 4-6% α -1,6 linkages (Hood, 1982). The average chain length is 20-26 glucose units. Intensive studies on the structure of amylopectin have been conducted using a combination of enzymatic methods and gel permeation chromatographic methods. The molecular arrangement is defined conventionally in terms of the degree of polymerization (DP). The molecular weight of amylopectin is in the 10^7 - 10^8 range. Within the granule, amylose may associate in an orderly manner with the linear portion of amylopectin in the crystalline region of the amylopectin.

Amylopectins dissolve in water, and neutral aqueous solutions are extremely stable, with little tendency towards retrogradation. Amylopectin forms a red color with iodine in contrast to the blue color obtained with amylose. The low binding power as indicated by the red color is due to the branch points which hinder helix formation of amylopectin molecules (Solomon, 1978).

The relative amount of amylose and amylopectin in the starch granule is in the range of one to three. Granules can vary in size and shape depending on their biological origin. Under polarized light, intact granules exhibit a well-defined birefringence pattern with a dark cross which is an indication of the highly organized structure of the granules. The starch molecules are radially oriented within the granule. The highly organized

structure is a result of the double helices formed between the outer chains of amylopectin which contribute to the crystalline properties of starch granules (French, 1982), and are responsible for the birefringent characteristic.

In nature, amylose and amylopectin are combined with other cellular components. Amylose forms a complex with fatty acids, phospholipids and others found in cereal starches. The formation of amylose-lipid complexes in starch alters the gelatinization process. Starches vary in chemical and physical properties depending on their native sources.

3.1.2 Starch gelatinization

The structure of the starch granule is significantly changed when heated in water. In the presence of excess water and at temperatures above the gelatinization threshold, gelatinization occurs and causes an increase in viscosity. Gelatinization causes starch to solubilize in water under applied heat and can be described by non-equilibrium thermodynamics in three processes (Blanshard, 1979):

1. Diffusion: water penetrates into the starch granule and interacts with amylose, primarily in the amorphous region.
2. Swelling: the granule swells and expands its volume.
3. Melting or hydration: with progressive hydration, the granule size increases under restricted movement. This causes the viscosity to increase up to the point where the internal hydrogen bonds break and the granule ruptures. This results in tearing and destruction of the crystalline regions, facilitating enzymatic attack on the unbound starch molecules during starch hydrolysis.

The temperature required to produce complete gelatinization varies, depending on the source of the starch. Using X-ray diffraction and differential scanning calorimetry thermograms, the gelatinization temperature of different native starches can be obtained (Table 3.1).

Table 3.1. Gelatinization temperatures of several native starches.						
Gelatinization temperature (°C)						
Type of starch	Method:DSC			Method:microscope		
	Onset	Peak	End	Onset	Peak	End
Corn	65	71	77	65	69	76
Waxy corn	65	72	80	64	70	78
Wheat	52	59	65	55	61	66
Rye	49	54	61	51	54	58
Oat	52	58	64	54	58	61
Rice	70	76	82	72	75	79
Potato	61	65	71	58	64	68
Tapioca	63	68	79	64	69	80
Arrow root	67	75	85	69	76	84

Source: Reichelt (1983)

3.2 Amylolytic Enzymes

Amylolytic enzymes are used as biocatalysts to convert starches to sweeteners via hydrolysis. These enzymes were originally called diastases but were later renamed amylases. They can be classified into three groups (Norman, 1981): endo-amylases, exo-amylases and debranching enzymes. The specific actions of these enzymes are described by Boyce (1986).

Endo amylases are generally α -amylases which hydrolyze α -1,4 glucosidic bonds in amylose, amylopectin and related polysaccharides, and produce oligosaccharides of varying chain lengths. They hydrolyze the bonds located in the inner region of the substrate, which results in decreasing the viscosity of starch solutions.

✓ α -amylases attack the amylose fraction in two steps. Initially, a completely rapid degradation of amylose occurs and produces maltose and maltotriose by a random attack. The second step is slow hydrolysis of the oligosaccharides to form glucose and maltose as the final products. α -amylases also attack amylopectin and form glucose, maltose and a series of α -limit dextrins (oligosaccharides of DP > 4, containing α -1,6 branch points). Malt α -amylases can act on both insoluble and soluble starch to produce dextrins and maltotrioses (Marc and Engasser, 1983).

✓ α -amylases are derived from animal, plant and microbial sources, and have different action patterns in starch hydrolysis. Microbial α -amylases are thermostable and are used in liquefaction. In contrast, fungal α -amylases are thermolabile and are used during saccharification.

Exo-amylases consist of β -amylases and glucoamylases. These enzymes hydrolyze α -1,4 glycosidic bonds in amylose, amylopectin and related polysaccharides. β -amylases hydrolyze the α -1,4 glycosidic bonds in starch by inverting the configuration at the C-1 position of glucose from α to β , thereby the β -prefix. β -amylases act at the non-reducing ends of the outer chains of starch and gradually remove maltose units. However, they cannot by-pass the α -1,6 glycosidic branch points.

Glucoamylases act in a manner similar to β -amylases, but hydrolyze α -1,6 glycosidic bonds at a slower rate. These enzymes remove glucose from the end of the non-reducing chain in a stepwise manner. The decrease in viscosity induced by exo-amylases is slower than that of endo-amylases.

Debranching enzymes are generally isoamylase and pullulanase. They hydrolyze α -1,6 linkages at branched points and produce glucose and maltose. Pullulanase

hydrolyzes linear and branched substrates when the side chain joined by the $\alpha-1,6$ linkage consists of at least two glucose units in length, but isoamylase requires at least three units (Abdullah et al., 1965). If the branch point joins with one glucose molecule, the branch point cannot be degraded by an enzyme. Amylo-1,6-glucoamylase can hydrolyze the branch points, but only on a premodified substrate.

✓ 3.3 Processes for Producing Sweeteners

In general, sweeteners can be produced from starch through the three processes of gelatinization, liquefaction and saccharification. Starch must first be gelatinized to release amylose and amylopectin from the granule to facilitate enzymatic modification.

Liquefaction dextrinizes starch by thinning or decreasing the viscosity of the starch slurry. The traditional liquefaction agent used to be acid. The starch slurry (industrially, 25-40% dry solid, w/w) was acidified to pH 1.5-2.0 and heated to 140-155°C for 5-10 min to complete gelatinization and to produce a liquefied product. These products were impure because of undesirable compounds and color. Therefore, acid/enzyme and then enzyme systems were introduced. The degree of starch degradation may be quantified in terms of the dextrose equivalent (DE), where the reducing power of the liquefied product is compared with pure dextrose.

α -amylases derived from *Bacillus subtilis* can operate at temperatures of 85-87°C and at 90-95°C for short periods of time. The more heat stable α -amylase derived from *Bacillus licheniformis* was developed and used at temperatures above 95°C and at 105-110°C for a short time. These thermostable enzymes require a cofactor, calcium ion, to maintain their functionality during the process.

The liquefaction process can be carried out in either batch reactors or continuously stirred tank reactors using a single enzyme or dual enzyme. The required final DE in liquefaction is 12-15 and can be up to 40. The residence time for these enzymatic reactions varies, depending on enzyme dosage and starch concentration, but is generally in the range of 1-2 hours. Starch hydrolysates with DE of 3-20 produced by bacterial α -amylases are maltodextrins.

The liquefied products (oligosaccharides) become substrates for enzymatic saccharification and are further hydrolyzed by two enzymes, glucoamylase and fungal α -amylase. These enzymes can be used individually or in combination depending on the sugar profiles required. Some industrial sweeteners are given in Table 3.2.

Product profile	Glucose	Maltose Syrup	High maltose	High glucose + maltose	Iso-glucose
Dextrose equivalent	96-98	40-45	48-55	56-68	98
Glucose	95-97	16-20	2-9	22-35	52
Maltose	1-2	41-44	48-55	40-48	-
Fructose	-	-	-	-	42
Isomaltose	0.5-2	-	-	-	-
Maltotriose	-	-	15-16	-	-

Source: Reichelt (1981)

3.4 Enzyme Kinetics

An enzyme is a biocatalyst used to accelerate the rate of chemical reactions by lowering the required activation energy (barrier) without itself being consumed. Enzymatic reactions are a factor of 10^{15} faster than nonenzymatic reactions (Segel, 1975). The enzyme possesses the active site where a specific substrate can bind. The active site is a specific and precise spatial arrangement of amino acid residues (R-groups) that can

interact with complimentary groups on the substrate. The enzyme-substrate interaction is analogous to a template or a lock-key model, which has successfully been used to explain the majority of specificity patterns exhibited by enzymes (Segel, 1975).

Enzymes are high molecular weight proteins but the active site occupies only a very small fraction. In fact, only few amino acid residues participate in substrate binding or catalysis. The other amino acid residues maintain the protein in its tertiary structure through the forces of electrostatic interactions, hydrogen bonds, disulfide bonds, hydrophobic interactions and dipole-dipole interactions.

The first rate equation for enzymatic reactions was derived in 1903 by Henri (Segel, 1975). The overall reaction was described as:



Henri's equation was based on the following assumptions:

- The enzyme (E) is a catalyst.
- The enzyme reacts rapidly with substrate (S) to form an enzyme-substrate complex (ES) in the transition state.
- Only a single ES is formed and breaks down directly to free enzyme and product (P).
- E, S and ES are at equilibrium, and the reverse reaction is much faster than the rate of product formation.
- [S] is much larger than [E], therefore [ES] does not significantly change.
- The product formation step is the limiting step.
- The rate or velocity is measured during the early stage of the reaction when the reverse reaction is not significant.

Henri's equation can be expressed as:

$$v = K \frac{[S]}{\left(1 + \frac{[S]}{K_s}\right)} \quad (3.2)$$

and was later modified to obtain the Michaelis-Menten (M-M) equation (Segel, 1975):

$$v = \frac{k_p[E]_t[S]}{K_s + [S]} = \frac{V_{\max}[S]}{K_s + [S]} \quad (3.3)$$

This equation was derived using an equilibrium expression for the enzyme and substrate. The rapid equilibrium approach is the simplest and most direct method to derive a kinetic expression without knowledge of the magnitude of the rate constants. In many cases, both the rapid equilibrium and steady state approaches give the same form of kinetic expression but the constants are defined differently. However, the steady state approach can lead to an equation too complicated for practical use.

The rate of reaction of glucoamylase derived from *Schwanniomyces castellii* acting on starch can be modeled by the M-M kinetics based on an initial rate study (Pasari et al., 1988). The M-M equation can be used for malt β -amylases (Marc and Engasser, 1983).

3.5 Legal Aspects of Enzyme Uses

The majority of industrial enzymes are hydrolases and are used as additives or processing aids in the baking (Fox, 1982) and other industries. The Codex Committee of Food Additives has published a list of enzymes derived from plant, animal and microbial sources, limiting their application in food products. In the United States, enzymes are considered secondary direct food additives and are "Generally Recognized As Safe" (GRAS) when manufactured with sound processing practices. A list of enzymes derived from microorganisms is published in the Code of Federal Regulation (CFR). The organisms used for enzymes and applied in the food industry must be known or shown to

be nonpathogenic and not produce toxic substances (Anon., 1987). The amount of enzymes used depends on the type and source of the enzyme. For amyloglucosidase derived from *Rhizopus niveus*, a level not to exceed 0.1% by weight of the gelatinized starch is used. The use of enzymes from other microbial sources is limited by the "Food Additive Amendment" (Anon., 1987).

The amount of residual enzyme allowed in the food product is not mentioned in the GRAS list. However, if the enzyme remains active in the food product, it can cause excessive starch hydrolysis with subsequent deterioration of product quality and a decrease in shelf life.

3.6 Overview of Food Extruders

Extrusion is a widely used thermal process of industrial interest because it provides a combination of three operations in one equipment: transporting, mixing and forming. Food extrusion processes provide many advantages (Harper, 1978), among which are high productivity in a single processing step and versatility to handle a number of food products under processing conditions such as high temperature short time (HTST). A typical HTST extrusion process also occurs at high shear and high pressure (Linko et al., 1980).

Single-screw extruders (SSE) were initially used to provide mixing and pressurization of high moisture dough through a die, to form desired shapes of food products such as macaroni, ready-to-eat (RTE) cereals and puffed snacks (Harper, 1985). When twin screw extruders (TSE) were introduced, they gained a lot of interest due to expanded operational capabilities and broader ranges of application. The TSE improves heat transfer and mixing and its self-wiping design helps eliminate stagnant zones.

A TSE can be differentiated by the direction of screw rotation (co- or counter-rotating). Co-rotating and counter-rotating intermeshing twin screw extruders provide different power consumption, RTD and mixing performances (Rauwendaal, 1981). The specific energy consumption (SEC) of counter-rotating extruders depends on the shear stress while that of co-rotating extruders depends on the shear strain. Co-rotating extruders provide a broad RTD and better distributive mixing capabilities due to the high shear rate. On the other hand, counter-rotating extruders give a narrow RTD and better dispersive mixing due to local, high shear stress in the intermeshing region.

The co-rotating TSE is more popular for food processing than the counter-rotating unit because it provides a larger capacity and better mixing within the chambers, and can be operated at a higher screw speed. In the co-rotating TSE, various screw sections are used to perform different functions during the extrusion process. Screw sections with fully intermeshing and self-wiping screws are desired for sticky or difficult-to-convey materials, to avoid surging. Mechanical energy dissipation and mixing can be increased in TSE by using kneading disks such as two-lobed elements. If the screw section is fully filled, increased mixing, better heat transfer and more viscous dissipation will occur. These conditions allow a TSE to act as a heater rather than a cooler (Harper, 1985). The fully filled condition is obtained by placing restrictions such as reversed pitch screws to build up pressure. The pressure profile in a TSE depends on the screw profile and other process variables (Valle et al., 1987).

Screw elements which are generally used in twin screw food extruders are single-lobe, double-lobe and kneading discs or paddles. A single-lobe screw is used as a discharge screw to build up pressure against back pressure at the die. It also provides conveying, though not as well as the double-lobe screw, which is used as a feed screw.

Kneading discs are used to perform different processing tasks depending on the number of discs and the staggering angle between the discs. They can provide good mixing and generate interparticulate frictional heat to cook the product.

3.7 Extrusion Processing

Although food extrusion has been used to produce a variety of food products, the process has not been well characterized because of complexities resulting from many factors. These include composition of feed ingredients, moisture content, feed rate, screw configuration, screw speed, jacket temperature and die geometry. These factors affect the viscosity of the extruded material, shear rate, throughput, die pressure, power requirements, residence time, total strain, product temperature and product quality (Harper, 1981).

The theory for food extrusion has developed on the basis of polymer extrusion models for fluid and heat transport (Harper, 1981). However, unlike polymers which are relatively homogeneous and singly extruded, food materials are heterogeneous and consist of many ingredients. The interaction between these ingredients and water activity leads to complex reactions such as starch gelatinization and protein denaturation. These reactions cause irreversible changes in extruded materials which are quite opposite to the reversible melting and irreversible polymerization reactions encountered during thermoplastic extrusion.

The extrusion process consists of three basic mechanisms: feed conveying, melting and metering. Although, most of the process models were developed for single screw extruders, their important concepts are applicable to twin screw extruders.

The conveying rate is governed by the dynamic coefficient of friction on the barrel (f_b) and screw (f_s) and local pressure (Rauwendaal, 1986). If f_b increases relative to f_s , the conveying rate will increase because the frictional force on the barrel induces a driving force on the feed bed. If the local pressure increases, the conveying rate will decrease because a positive pressure gradient creates a frictional force on the screw that retracts the feed bed. The maximum forward transport will occur when the frictional force on the screw is zero. If f_b approaches f_s under a relatively small pressure gradient, the retracting force will dominate and there will be no forward movement of material. If there is a positive pressure gradient, the flow backs up toward the feed port. The extruder is unstable when the two frictional coefficients are equivalent or when the frictional coefficients change due to variations in temperature.

In the melting zone, materials are cooked by heat generated from viscous dissipation and heat supplied from the barrel. In a fully-filled TSE, power consumption is proportional to the screw speed raised to an exponent of 2.0; the exponent is 1.9 for partially-filled screws (Secor, 1986). The melting rate can be predicted if the material temperature profile is known.

The metering section acts as a pump to transport the material towards the die. The throughput is governed by drag and pressure flows (Rauwendaal, 1986) and can be described by the expression:

$$\dot{Q} = \dot{Q}_d - \dot{Q}_p \quad (3.4)$$

or

$$\dot{Q} = \frac{pWH(\pi ND \cos \phi)}{2} - \frac{pWH^3 \left(\frac{\partial p}{\partial x} \right)}{12\mu} \quad (3.5)$$

The throughput decreases if pressure flow increases due to positive pressure gradient and when the channel depth (H) increases. The output rate may also decrease due to leakage through clearances between the flight and the barrel. A corrected throughput is obtained when the effect of leakage is included through correction factors.

One-dimensional flow of Newtonian fluids can be determined easily when the operation occurs at steady state under isothermal, fully developed, laminar flow conditions in the absence of slip. In general, the fluids are also assumed to be incompressible and at constant density and viscosity; and gravity and inertial forces are neglected. For one-dimensional flow of a power law fluid under conditions similar to those for Newtonian fluids above, the throughput in dimensionless form (Rauwendaal, 1986) is:

$$\bar{Q} = \frac{\dot{Q}}{\dot{Q}_d} = \frac{2n}{1+2n} \quad (3.6)$$

When cross channel flow occurs, two-dimensional flow results. If the helix angle is zero, there is no cross channel flow and the result of two-dimensional analysis will be equivalent to the one-dimensional analysis (Rauwendaal, 1986). In the presence of cross channel flow, the polymer is subjected to a higher shear rate, which affects the viscosity and, therefore, the flow rate (Rauwendaal, 1986). Two-dimensional analysis shows that throughput-pressure gradient relationships are different from those of one-dimensional analysis when n is less than 0.8. If two-dimensional analysis is required, numerical techniques can be used. However, complicated computation can be avoided by incorporating correction factors for non-Newtonian fluids in the Newtonian model as follows (Rauwendaal, 1986):

$$\dot{Q} = \left(\frac{4+n}{10} \right) \frac{pWH(\pi ND \cos \phi)}{2} - \left(\frac{1}{1+2n} \right) \frac{pWH^3 \left(\frac{\partial p}{\partial x} \right)}{4\mu} \quad (3.7)$$

where $\mu = m \left(\frac{\pi ND \cos \phi}{H} \right)^{n-1}$.

When Eq. 3.7 is used with n in a range of 0.3 to 1.0, the result is less than 10% different from the two-dimensional analysis (Rauwendaal, 1986).

Food doughs are highly pseudoplastic. Therefore, drag and pressure flows become dependent and the predicted flow rate can be under-estimated when the pressure gradient is positive, and over-estimated when it is negative (Harper, 1981). Wyman (1975) developed an axial velocity profile for shallow channels in a TSE in a manner similar to that of a SSE and found that pressure flow induced flow toward the die rather than away from the die as in a SSE. The model did not include leakage between screws.

3.7.1 Mixing in extruders

Mixing is a process that reduces non-uniformity in composition, basically by physical motion of ingredients. Convective motion normally occurs in laminar flow of viscous fluids as a result of shear flow or elongational flow.

The mixing zone in extruders starts from the transition zone and ends at the die. Mixing in the extruder is not uniform for all material elements (Rauwendaal, 1986) because the element with a longer residence time has a greater mixing history. Therefore, the mixing history of the material is difficult to determine. The mixing process is analyzed by determining the velocity profiles in the screw channel, and using these to determine the local deformations in the fluid. However, only the case of simplified flow of isothermal Newtonian fluids is easily solved.

The degree of mixing has been described by using a residence time distribution function. The RTD provides information about mixing in the axial direction but not in the transverse direction which governs laminar mixing of viscous fluids (Bigg, 1975). Dispersion mechanisms were important in single-screw and twin screw compounding

extruders (Eise et al., 1983). Because fluid elements in the extruder are subjected to various amounts of strain which are directly related to mixing, a strain distribution function (SDF) can be calculated in a manner similar to the RTD. The SDF for a continuous mixer, $f(\gamma)d\gamma$, is defined as the fraction of exiting flow that experienced a strain between γ and $\gamma + d\gamma$. This represents the probability that an entering fluid element will exit with that strain. The cumulative SDF is expressed by (Tadmor and Klein, 1970):

$$F(\gamma) = \int_{\gamma_0}^{\gamma} f(\gamma)d\gamma \quad (3.8)$$

The $F(\gamma)$ is the fraction of exiting flow with strain less than or equal to γ . The mean strain of the exiting stream is calculated by (Tadmor and Klein, 1970):

$$\bar{\gamma} = \int_{\gamma_0}^{\infty} \gamma f(\gamma)d\gamma \quad (3.9)$$

Pinto and Tadmor (1970) developed the weighted average total strain (WATS) to describe mixing in non-homogeneous flow fields in single screw extruders. The WATS is expressed as:

$$\bar{\gamma}_t = \int_{\gamma_0}^{\infty} \gamma(t)E(t)dt \quad (3.10)$$

WATS is a theoretical concept that is difficult to measure experimentally. The efficiency of mixing is hard to determine because of the lack of a unifying mixing theory (Ottino and Chella, 1983). The degree of mixing should be determined based on the physical process, the fluid mechanics and the compatibility of the components being mixed (Ottino and Chella, 1983).

It is important to understand how the materials are fed into the extruder and what the mixing mechanisms are. In a SSE, mixing is induced by shear (rotational) flow; in a TSE, the mechanism is elongational (irrotational) flow. Rotational flow causes stretching of materials without breakup while irrotational flow causes breakup of the material matrix, which enhances mixing. The viscosity and elasticity (viscoelasticity) of the components govern the mode of dispersion. The lower viscosity component may encapsulate the higher viscosity component. The degree of mixing also increases with increased interfacial areas. Mohr et al. (1957) reported that interfacial areas increased with increased shear strain. Laminar mixing can be analyzed if the exact flow patterns are known. The velocity profile in the screw mixing zone is normally complex, making quantitative analysis of the mixing section difficult.

3.7.2 Process instability

Process instabilities result from large periodic variations in process and product variables. The extrusion process can undergo stable oscillations for long periods of time, in spite of constant feed rates. The oscillations are of the same order as or longer than the extruder residence time. The oscillations involve the entire extrusion process and are typically caused by a fluctuation in feed moisture content (Roberts and Guy, 1986). As moisture decreases, viscosity increases and the flow through the die decreases while the die pressure increases. The material behind the die is then subjected to shear for a longer period. This results in viscosity reduction, and the material flows through the die quickly while the die pressure decreases. The inconsistent flow through the die, alternately having high and low viscosity, may continue until a stable oscillation is produced or may be damped out to approach a steady state.

Roberts and Guy (1987) have observed that extrusion cooking of expanded wheat flour products exhibited two steady states in processes carried out under the same independent process variables. The two equilibrium states were explained as resulting from moisture movement within the screw system, and were governed by the degree of fill, torque, pressure and mass temperature. The first state occurred at high torque and low die pressure, and with low density products. A good steam barrier was formed under the filled screw in this state. If the steam escaped and backed up to the feed section to moisten the feed, less energy input resulted. The first state was then shifted to the second state, which occurred at low torque and high die pressure, and with high density products.

3.7.3 Application of polymer extrusion theory to food extrusion

The simplified extrusion theory for isothermal, Newtonian flow has been successfully applied to some food systems to measure effects of changing screw geometry and extruder operating conditions (Harper, 1981). Using soy flour data from Mustakas et al. (1970), Fricke et al. (1977) found that the output rate was unaffected by pressure flow because drag flow dominated. The flow was proportional to screw speed at low screw speeds but not at high screw speeds. Jasberg et al. (1979) employed the plug flow model of Darnell and Mol (1956) to predict the output rate of soy dough at low temperatures (30-50°C), and found agreement between predicted and experimental results. The output rate was significantly affected by moisture and screw speed but not by die size. They also reported that increasing flow rate did not affect the back pressure from the die, contradicting the results from plastic extrusion.

3.8 Rheological Changes During Extrusion

Changes in rheological properties of food materials during extrusion has been investigated by Cervone and Harper (1978), Jao et al. (1978), Luxenburg et al. (1985),

Mackey (1989), Morgan et al. (1989) and Remsen and Clark (1978). Jao et al. (1978) reported that the apparent viscosity of defatted soy dough was affected by moisture, shear rate and temperature during extrusion. Luxenburg et al. (1985) used DSC to follow the enthalpy change of soy flour dough during extrusion cooking. They found that the rheological change was due to conformation of protein molecules rather than protein crosslinking.

Most viscosity models for food extrusion have been developed empirically without incorporating temperature-time history and/or strain history effects. Remsen and Clark (1978) combined temperature-time history in a model for soy flour suspensions (70-75% moisture), but the model exponentially approached infinity at large temperature-time histories. In contrast, Morgan et al. (1989) have recently developed a model that approaches a finite value for temperature-time histories and shear rates encountered in extrusion. The model adequately predicted effects of shear rate, moisture content, temperature and temperature-time history on apparent viscosity of defatted soy flour dough undergoing heat induced protein denaturation. The model showed good agreement with experimental data for a wide range of conditions. Mackey (1989) has also shown that the effects of temperature-time and strain histories are important and should be incorporated in models predicting apparent viscosity of starch doughs during extrusion.

3.9 Ideal and Non-ideal Reactors

Ideal reactors consist of batch reactors, continuously-stirred tank reactors (CSTR) and plug flow reactors (PFR). Ideal flow patterns refer to complete backmixing (in batch and CSTR) and zero backmixing (in PFR). In real reactors, flow patterns fall somewhere

between the two ideal flows. The deviation from ideality results from channelling of fluids, recycling of fluids or creation of stagnant regions (Levenspiel, 1972), all of which can occur in food extruders.

Non-ideal flow causes problems in scale-up and design because the magnitude of the nonideality is not always predictable. To predict the flow behavior of fluids in the reactor, it is necessary to determine the length of time an individual element spends while passing through the reactor, resulting in a residence time distribution of the flowing fluid. Fogler (1987) stated that non-ideal reactors can be characterized by residence time distribution (RTD), degree of mixing and the flow model.

3.9.1 Residence time distribution

The RTD provides information on the type of mixing taking place within the reactor. The residence time in batch and plug flow reactors is the same for all fluid elements, while that in a CSTR varies. The RTD can be directly determined by stimulus-response techniques. The stimulus is generally a tracer input into the fluid entering the reactor and the response is a time record of the tracer leaving the reactor. Any material can be used as a tracer if it can be detected and does not disturb the flow of interest. The distribution of the time required by fluids leaving the reactor is called the exit age distribution, E , or the RTD function (Levenspiel, 1972) where E is defined as:

$$E(t) = \frac{C(t)}{\int_0^{\infty} C(t)dt} \quad (3.11)$$

In normalized form,

$$\int_0^{\infty} E(t)dt = 1 \quad (3.12)$$

The C curve is a plot of concentration against the residence time. The F curve is a plot of fraction of tracer concentration against the residence time. The F parameter is defined by:

$$F(t) = \frac{C(t)}{C_o} \quad (3.13)$$

The RTD from different reactors can be compared using three moments: the mean residence time (\bar{t}), the variance (σ^2) and the skewness (s^3), expressed respectively as:

$$\bar{t} = \int_0^{\infty} tE(t)dt \quad (3.14)$$

$$\sigma^2 = \int_0^{\infty} (t-\bar{t})^2 E(t)dt \quad (3.15)$$

and

$$s^3 = \int_0^{\infty} (t-\bar{t})^3 E(t)dt \quad (3.16)$$

3.9.2 Extent of chemical reaction

In a linear system, the stimulus-response experiment at steady state is linear in concentration, and the output tracer concentration is directly proportional to the input tracer concentration. If the reaction is first order, the extent of reaction can be determined directly from the reaction rate expression and tracer information (Fogler, 1987; Levenspiel, 1972) which can be expressed as:

$$\bar{C}_r = \int_0^{\infty} C_r(t)E(t)dt \quad (3.17)$$

For a nonlinear process, where the reaction is not first order, the flow model must be incorporated into the analysis. Models for predicting extent of reaction from RTD data can be developed from a number of adjustable parameters (Fogler, 1987). Segregation and maximum mixedness models are zero adjustable parameters. CSTRs in

series and the dispersion model have one parameter: the number of reactors or the dispersion number. A combination of ideal reactors may involve two or more parameters.

3.9.3 Residence time distribution in single and twin screw extruders

The flow pattern in an extruder has been investigated using RTD data by many researchers (Altomare and Ghossi, 1985; Colonna et al., 1983; Davidson et al., 1983; Valle et al., 1987; Lidor and Tadmor, 1976; Olkku et al., 1979; Todd, 1975; van Zuilichem et al., 1973; Wolf and Resnick, 1963; Wolf and White, 1976; and Wolf et al., 1986). The RTD curve in an extruder has a long tail due to material held in dead spaces.

Wolf and Resnick (1963) proposed an F-function to describe the RTD for real systems:

$$F(t) = 1 - e^{-\delta \left(\frac{t-\epsilon}{\bar{t}} \right)} \quad (3.18)$$

The parameter δ is a measure of mixing efficiency. It is equal to unity for perfect mixing and approaches infinity for pure plug flow. It is greater than unity if the system consists of dead spaces. An error in determining mean residence time can cause δ to be larger or smaller than unity. The parameter ϵ is a measure of the phase shift in the system. Both parameters are determined from a plot of $\ln(1-F)$ against t/\bar{t} which yields a straight line.

Davidson et al. (1983) studied the RTD of wheat starch in a SSE and fitted their data with two flow models developed by Wolf and Resnick (1963) and Levich et al. (1967). They found that the Wolf-Resnick multistage model fit the tail portion well while the Levich model fit the initial portion. The fraction of material held up in the dead space was 5-20%. The remainder passed directly through with an RTD close to plug flow. They found that the dispersion number was larger than 0.01.

Based on the RTD data of PVC polymers, Wolf et al. (1986) reported that the flow pattern in a counter-rotating twin screw extruder was near plug flow. The $F(\theta)$ function was similar to that for solid conveying (plug flow). The normalized θ was defined as:

$$\theta = \frac{t}{\bar{t}} \quad (3.19)$$

The effect of process variables on RTD in a twin screw extruder has been extensively examined by Altomare and Ghossi (1986). The process variables studied were screw profile, feed rate, screw speed, moisture content, barrel temperature and die size. They found that the mean residence time decreased with increased screw speed and feed rate, but decreased with decreased moisture content. The screw inducing higher shear resulted in a broader and longer RTD. Using various die diameters, they found that pressure had little effect on the RTD under a given process condition. A normalized delay time (ratio of time that tracer first appears in the extrudate to average residence time) was about 0.5. Larger values for a single screw extruder were reported by Davidson et al. (1983). The delay time for Newtonian fluids in a SSE was 0.75 (Bigg and Middleman, 1974). Because the dough viscosity is high, flow in the TSE may approach that of laminar pipe flow. Altomare and Ghossi (1986) found that their data correlated well with the model of Wolf and White (1976) which combined complete mixing and plug flow.

The temperature and pressure profiles in a TSE are affected by screw profile, barrel temperature, feed rate, moisture content, screw speed and die size (Valle et al., 1987). Among these variables, moisture content and feed rate have the greatest effect on pressure and temperature profiles. Temperature and pressure decreased with increased moisture content. The ratio of feed rate to screw speed (Q/N) affected the degree of fill in the screw channel. The degree of fill increased with increased feed rate. An increase

in screw speed led to increased shear, decreased viscosity and decreased pressure.

3.10 Starch Hydrolysis in Twin Screw Extruders

The use of an HTST extrusion cooker as a biochemical reactor for enzymatic reactions has been extensively investigated by Linko et al. (1979), Linko et al. (1983a, 1983b), Linko et al. (1984), Reinikainen et al. (1986) and Chouvel et al. (1983).

Thermomechanical modification of starch structure during extrusion cooking has been observed by Christensen (1987), Davidson et al. (1984), Diosady et al. (1985), Linko et al. (1983a), Linko et al. (1980), Linko et al. (1981), Mercier (1979), Mercier and Feillet (1975), Gomez and Aguilera (1983), Colonna et al. (1984), Reinikainen et al. (1986), and Darnoko and Artz (1988). Thermal and mechanical energy input caused cleavages of hydrogen bonds between amylopectins and resulted in reduced viscosity and increased solubility (Mercier and Feillet, 1975). Mercier (1979) found that extrusion cooking solubilizes cereal starches to a certain extent, which increases digestibility for human nutrition. The amount of soluble starch increased with decreased feed moisture contents, but no formation of maltodextrins was observed (Mercier and Feillet, 1975). Christensen (1987) demonstrated that extrusion improved the texture and palatability of an extruded dog food and also increased extruder throughput when α -amylase was used during extrusion of corn grits.

Extrusion of starch is sufficient pretreatment for subsequent enzymatic saccharification to obtain DE values of up to 98 (Linko et al., 1980). Extrusion cooking causes thermomechanical destruction of the starch structure and allows thermostable α -amylase to break down the starch molecules (Linko et al., 1983a). Cassava starch was partially hydrolyzed in the TSE prior to adding saccharifying enzyme to continue

hydrolysis of starch to glucose (Darnoko and Artz, 1988). The degree of starch hydrolysis increased at low pH and high temperature. The glucose concentration in the extruded starch after saccharification was higher than that in the acid-liquified starch.

Pretreatment of substrates can be thermomechanical without addition of enzyme or with enzyme added in a single pass of HTST-extrusion cooking. The combined effect of thermomechanical and enzymatic starch liquefaction in HTST-extrusion was investigated by Linko et al. (1983a) and Chay et al. (1984) who used Termamyl 60L α -amylase, and by Hakulin et al. (1983) who used Termamyl 120L α -amylase. Both enzymes were extremely thermostable under extrusion conditions, but were almost completely inactivated at 160°C (Linko et al., 1983a, 1983b).

Hydrolyzed wheat starch at DE values of 25-30 was obtained using 0.9% w/w Termamyl 120L α -amylase in a twin screw extruder at 120°C, 1500 g/min feed rate and 250 rpm screw speed (Hakulin et al., 1983). It was found that feeding premixed starch-water slurry into the extruder gave higher DE values than feeding starch and water separately. The addition of enzyme to materials in the extruder either before or after starch gelatinization did not significantly affect DE values after the subsequent saccharification process. The addition of both α -amylase and glucoamylase into the extruder accelerated the saccharification process after extrusion.

Both starchy and cellulosic materials can be pregelatinized and preliquefied by HTST-extrusion cooking, which leads to a reduction of reaction time for subsequent saccharification and ethanol fermentation (Linko et al., 1984). Pretreated barley starch was saccharified by glucoamylase at 60°C and a pH of 4.5 (Linko et al., 1979) and was used for ethanol fermentation by yeast at 60°C (Linko et al., 1983b).

3.10.1 Liquefaction

The effect of pH, temperature, moisture content, enzyme to substrate ratio, and calcium ions on extent of enzymatic liquefaction of pregelatinized corn starch in a TSE was investigated by Chouvel et al. (1983). The screw profile consisted of both forwarding and reversing screw elements. *Bacillus licheniformis* Termamyl 60L α -amylase (Novo Industries, France) was used. They observed that the optimum pH was 6.0. The extent of hydrolysis increased with increased moisture content from 40% to 70%, and with increased enzyme to substrate ratio from 5 to 30 ml/kg starch. The addition of calcium ions resulted in a higher heat tolerance of enzymes during a temperature rise from 100 to 145°C.

Continuous liquefaction of pregelatinized starch was carried out at relatively high dry solid contents (up to 60%) in a short period of time, using an α -amylase dosage higher than the usual Novo process (Chouvel et al., 1983). The product profile from the hydrolysis contained less than 1% glucose and relatively high proportions of maltotriose, maltopentaose and maltohexaose. The authors also examined the combination of gelatinization and liquefaction of raw corn starch in the TSE. About 20-30% of glycosidic bonds were hydrolyzed during gelatinization and liquefaction.

3.10.2 Enzyme inactivation in the extruder

Extrusion cooking may be used to inactivate enzymes such as cereal α -amylase, lipase, lipoxidase, peroxidase and urease present in food materials (Linko et al., 1983a). These enzymes interact with food constituents and cause deterioration. However, some residual enzymes such as α -amylase may remain even after extrusion cooking (Linko et al., 1980; Linko et al., 1983a, 1983b; and Chouvel et al., 1983), especially when exposed to short residence times in the extruder (Linko et al., 1980).

The highest residual α -amylase activities in TSE were obtained at short residence times, relatively high moisture content and low temperature (Linko et al., 1980). Residual enzyme activity was small under experimental conditions of moisture contents less than 30%, with relatively complete inactivation at 25% moisture content. Above 125°C, enzyme deactivation was pronounced, however some residual enzyme activity was detected in samples extruded at 140°C (Linko et al., 1980).

3.11 Nomenclature

C_0	Input concentration of tracer, mole/l
$C(t)$	Output concentration of tracer, mole/l
\bar{C}	Mean concentration of reactant in the exit stream, mole/l
C_t	Concentration of reactant at any time, mole/l
D	Barrel diameter, m
$[E]_t$	Total enzyme concentration, ml of enzyme/ml of solution
$E(t)$	Exit age distribution, s^{-1}
f_s	Dynamic coefficient of friction on the screw surface, dimensionless
f_b	Dynamic coefficient of friction on the barrel surface, dimensionless
H	Channel depth, m
k_1, k_{-1}, k_p	Rate constants in Michaelis-Menten model, s^{-1}
K_s	Dissociation constant, $(\text{mole/l})^{-1}$ (Eq. 3.2)
K	Constant for a particular enzyme, s^{-1} (Eq. 3.2)
m	Consistency coefficient, $\text{Pa}\cdot\text{s}^n$
n	Power law index, dimensionless
N	Screw speed, RPS

P	Local pressure, Pa
p	Number of parallel flights, dimensionless
\dot{Q}	Net flow rate, m ³ /h
\dot{Q}_d	Pure drag flow rate, m ³ /h
\dot{Q}_p	Pure pressure flow rate, m ³ /h
\bar{Q}	Dimensionless volumetric flow rate (Eq. 3.6)
[S]	Substrate concentration, mole/l
s^3	Skewness, s ³
t	Residence time, s
\bar{t}	Mean residence time, s
v	Initial velocity (Eq. 3.2), mole/l/s
V_{\max}	Maximum reaction rate, mole/l/s
W	Screw width, m
z	Down channel or axial distance, m
Greek symbols	
δ	Coefficient, dimensionless (Eq. 3.18)
ϵ	System phase shift (Eq. 3.18)
η	Effective viscosity, Pa.s
γ_0	Minimum strain, m/m
$\bar{\gamma}$	Mean strain, m/m
$\gamma(t)$	Strain undergone by a fluid element at time t , m/m
μ	Newtonian viscosity, Pa.s

σ^2	Variance, s^2
ϕ	Screw helix angle, rad.
θ	Normalized time, dimensionless

3.12 References

- Abdullah, M., Cattley, B.J., Lee, E.Y.C., Robyt, J., Wallenfels, K. and Whelan, W.J. 1965. The mechanism of carbohydrase action. XI. pullulanase, an enzyme specific for the hydrolysis of α -1,6 bonds in amylaceous oligo- and polysaccharides. *Cereal Chem.* 43:111.
- Altomare, R.E. and Ghossi, P. 1986. An analysis of residence time distribution patterns in a twin screw cooking extruder. *Biotech. Prog.* 2(3):157.
- Anon. 1987. Enzyme preparations and microorganisms in subpart B, part 173 of Secondary direct food additives permitted in food for human consumption. Food and Drug Administration, HHS, 21 CFR Ch.1 (4-1-1987 edition).
- Banks, W. and Greenwood, C.T. 1975. Starch and Its Components. Halsted Press, New York.
- Bigg, D. 1975. On mixing in polymer flow systems. *Polym. Eng. Sci.* 15(9):684.
- Bigg, D. and Middleman, S. 1974. Mixing in a screw extruder: a model for residence time distribution and strain. *Ind. Eng. Chem. Fund.* 13:66.
- Blanshard, J.M.V. 1979. Physicochemical aspects of starch gelatinization. In: Polysaccharides in Foods. Blanshard, J.M.V. and Mitchell, J.R. (Editors). Butterworth, London.
- Boyce, C.O.L. 1986. *Novo's Handbook of Practical Biotechnology*. A publication of Novo Industries A/S Enzymes Division, Bagsvaerd, Denmark.

- Cervone, N.W. and Harper, J.M. 1978. Viscosity of an intermediate moisture dough. *J. Food Proc. Eng.* 2:83.
- Chay, P.B., Chouvel, H., Cheftel, J.C., Ghommidh, C. and Navarro, J.M. 1984. Extrusion-hydrolyzed starch and flours as fermentation substrates for ethanol production. *Lebensm-Wiss. u.-Technol.* 17:257.
- Chouvel, H., Chay, P.B. and Cheftel, J.C. 1983. Enzymatic hydrolysis of starch and cereal flours at intermediate moisture contents in a continuous extrusion-reactor. *Lebensm-Wiss. u.-Technol.* 16(6):346.
- Christensen, F.M. 1987. Application of enzymes in food extrusion process. Paper presented at the 7th. World congress of Food Science and Technology, Sept 28th - Oct 2nd., Singapore.
- Colonna, P., Doublier, J.L., Melcion, J.P., de Monredon and Mercier, C. 1984. Extrusion cooking and drum drying of wheat starch. I. Physical and macromolecular modifications. *Cereal Chem.* 61(6):538.
- Colonna, P., Melcion, J.P., Vergnes, B. and Mercier, C. 1983. Flow, mixing and residence time distribution of maize starch within a twin-screw extruder with a longitudinally-split barrel. *J. Cereal Sci.* 1:115.
- Darnell, W.H. and Mol, E.A.J. 1956. Solid conveying in extruders. *SPE J.* 12:20.
- Darnoko and Artz, W.E. 1988. Twin-screw extrusion as a continuous pretreatment process for the enzymatic hydrolysis of cassava. *J. Food Sci.* 53(6):1792.
- Davidson, V.J., Paton, D., Diosady, L.L. and Spratt, W.A. 1983. Residence time distribution of wheat starch in a single screw extruder. *J. Food Sci.* 48:1157.
- Davidson, V.J., Paton, D., Diosady, L.L. and Larocque, G. 1984. Degradation of wheat starch in a single screw extruder: characteristics of extruded starch polymers. *J. Food Sci.* 49:454.

- Diosady, L.L., Paton, D., Rosen, N., Rubin, L.J. and Athanassoulis, C. 1985. Degradation of wheat starch in a single screw extruder: Mechano-kinetic breakdown of cooked starch. *J. Food Sci.* 50:1697.
- Eise, K., Curry, J. and Nangeroni, J.F. 1983. Compounding extruders for improved polyblends. *Polym. Eng. Sci.* 23(11):642.
- French, D. 1982. Physical and chemical organization of starch granules. In: Starch Chemistry and Technology, 2nd ed. Whistler, R.L., Paschall, E.F. and BeMiller, J.N. (Editors). Academic Press, New York.
- Fogler, H.S. 1987. Elements of Chemical Reaction Engineering. Prentice-Hall, New jersey.
- Fox, P.F. and Mulvihill, D.M. 1982. Enzyme in wheat, flour, and bread. In Pomeranz: Advances in Cereal Science and Technology. Amer. Assoc. Cereal Chem., St. Paul, Minesota.
- Fricke, A.L., Clark, J.P., and Mason, T.F. 1977. Cooking and drying of fortified cereal foods: Extruder design. *Chem. Eng. Prog. Symp. Ser.* 73(163):134.
- Gomez, M.H. and Aguilera, J.M. 1983. Changes in starch fraction during extrusion cooking of corn. *J. Food Sci.* 48:378.
- Hakulin, S., Linko, Y.Y., Linko, P., Seiler, K., Seibel, W. and Detmold. 1983. Enzymatic conversion of starch in twin-screw HTST-extruder. *Starch/Stärke* 35(12):411.
- Harper, J.M. 1978. Extrusion processing of food. *Food Technol.* 32(7):67.
- Harper, J.M. 1981. Extrusion of Foods. Volume 1. CRC Press, Inc. Boca Raton, Florida.
- Harper, J.M. 1985. Processing characteristics of food extruders. In: Food Engineering and Process Application. Volume 2. Unit Operation. Le Maguer, M. and Jelen, P. (Editors), Elsevier Applied Science Publishers, London and New York.

- Hood, L.F. 1982. Current concepts of starch structure. In: Food Carbohydrates. IFT Basic Symposium Series. Lineback, D.R. and Inglett, G.E. (Editors). AVI Publishing, Connecticut.
- Jao, Y.C., Chen, A.H., Lewandowski, D. and Irwin, W.E. 1978. Engineering analysis of soy dough rheology in extrusion. *J. Food Proc. Eng.* 2:97.
- Jasberg, B.K., Mustakas, G.C. and Bagley, E.B. 1979. Extrusion of defatted soy flakes - model of a plug flow process. *J. Rheology* 23(4):437.
- Levenspiel, O. 1972. Chemical Reaction Engineering. 2nd edition. John Wiley & Sons, New York.
- Levich, V.G., Markin, V.S. and Chismadzhev, V.A. 1967. On hydrodynamic mixing in a model of a porous medium with stagnant zones. *Chem. Eng. Sci.* 22:1367.
- Lidor, G. and Tadmor, Z. 1976. Theoretical analysis of residence time distribution functions and strain distribution functions in plasticating screw extruders. *Polym. Eng. Sci.* 16(6):450.
- Linko, P., Hakulin, S. and Linko, Y.Y. 1984. HTST-extrusion cooking in ethanol production from starchy materials. *Enzyme Microb. Technol.* 6:457.
- Linko, P., Linko, Y.Y. and Olkku, J. 1983a. Extrusion cooking and bioconversions. *J. Food Eng.* 2:243.
- Linko, P., Hakulin, S. and Linko, Y.Y. 1983b. Extrusion cooking of barley starch for the production of glucose syrup and ethanol. *J. Cereal Sci.* 1:275.
- Linko, Y.Y., Lindroos, A. and Linko, P. 1979. Soluble and immobilized enzyme technology in bioconversion of barley starch. *Enzyme Microb. Technol.* 1:273.
- Linko, P., Colonna, P. and Mercier, C. 1981. High temperature short time extrusion cooking. In Pomeranz: Advances in Cereal Science and Technology. Amer. Assoc. Cereal Chem., St. Paul, Minnesota.

- Linko, Y.Y., Vuorinen, H., Olkku, J. and Linko, P. 1980. The effect of HTST-extrusion on retention of cereal α -amylase activity and on enzymatic hydrolysis of barley starch. In: Food Process Engineering, Enzyme Engineering in Food processing. Linko, P. and Larinkari, J. (Editors). Volume 2. Applied Science Publishers, London.
- Luxenburg, L.A., Baird, D.G. and Joseph, E.G. 1985. Background studies in the modeling of extrusion cooking processes for soy flour doughs. *Biotech. Prog.* 1(1):33.
- Marc, A. and Engassar, J.M. 1983. A kinetic model of starch hydrolysis by α - and β -amylases during mashing. *Biotech. Bioeng.* 25:481.
- Mercier, C. and Feillet, P. 1975. Modification of carbohydrate components by extrusion-cooking of cereal products. *Cereal Chem.* 52(1):283.
- Mercier, C. 1979. Structure and digestibility alterations of cereal starches by twin-screw extrusion cooking. *J. Food Proc. Eng.* 1:795.
- Mackey, K.L. 1989. A generalized viscosity model for the cooking extrusion of starch based products. Ph.D. Dissertation, Food Science and Human Nutrition, Michigan State University, East Lansing, Michigan.
- Mohr, W.D., Saxton, R.L. and Jeepon, C.H. 1957. Theory of mixing in the single screw extruders. *Ind. Eng. Chem.* 49:1857.
- Morgan, R.G., Steffe, J.F. and Ofoli, R.Y. 1989. A generalized viscosity model for extrusion of protein doughs. *J. Food Proc. Eng.* 11:55.
- Mustakas, G.C., Albrecht, W.J., Bookwalter, G.N., McGhee, J.E., Kwolek, W.F., and Griffin, E.L. 1970. Extruder-processing to improve nutritional quality, flavor and keeping quality of full-fat soy flour. *Food Technol.* 24:1290.

- Norman, B.E. 1981. New developments in starch technology. In: Enzymes and Food Processing. Birch, G.G., Blakebrough, N. and Parker, K.J. (Editors). Applied Science Publishers, London.
- Olkku, J., Antila, J., Heikkinen, J. and Linko, P. 1979. Residence time distribution in a twin screw extruder. In: Food Process Engineering. Linko, P., Malkki, Y., Olkku, J. and Larinkari, J. (Editors). Volume 1. Applied Science Publishers, London.
- Ottino, J.M. and Chella, R. 1983. Laminar mixing of polymeric liquids: a brief review and recent theoretical developments. *Polym. Eng. Sci.* 23(7):357.
- Pasari, A.B., Korus, R.A. and Heimsch, R.C. 1988. Kinetics of the amylase system of *schwanniomyces castellii*. *Enzyme Microb. Technol.* 10:156.
- Pinto, G. and Tadmor, Z. 1970. Mixing and residence time distribution in melt screw extruders. *Polym. Eng. Sci.* 10:270.
- Rauwendaal, C.J. 1981. Analysis and experimental evaluation of twin screw extruders. *Polym. Eng. Sci.* 21(16):1092.
- Rauwendaal, C.J. 1986. Polymer Extrusion. Hanser Publishers, New York.
- Reichelt, J.R. 1983. Starch. In: Industrial Enzymology, The Application of Enzymes in Industry. Godfrey, T. and Reichelt, J. (Editors), Nature Press, New York.
- Reinikainen, P., Suortti, T., Olkku, J., Malkki, Y. and Linko, P. 1986. Extrusion cooking in enzymatic liquefaction of wheat starch. *Starch* 38:20.
- Remsen, C.H. and Clark, J.P. 1978. A viscosity model for a cooking dough. *J. Food Proc. Eng.* 2:39.
- Roberts, S.A. and Guy, R.C.E. 1986. Instabilities in an extrusion-cooker: a simple model. *J. Food Eng.* 5:7.
- Roberts, S.A. and Guy, R.C.E. 1987. Metastable states in a food extrusion cooker. *J. Food Eng.* 6:103.

- Secor, R.M. 1986. Power consumption of partially filled twin screw extruders. *Polym. Eng. Sci.* 26(14):969.
- Segel, I.H. 1975. Enzyme Kinetics. Behavior and Analysis of Rapid Equilibrium and Steady State Enzyme Systems. John Wiley & Sons, New York.
- Solomon, B. 1978. Starch hydrolysis by immobilized enzymes, industrial applications. In: Advances in Biochemical Engineering. Ghose, T.K., Fiechter, A. and Blakebrough, N. (Editors). Springer-Verlag, New York.
- Tadmor, Z. and Klein, I. 1970. Engineering Principles of Plasticating Extrusion. Van Nostrand Reinhold, New York.
- Todd, D.B. 1975. Residence time distribution in twin-screw extruders. *Polym. Eng. Sci.* 15(6):437.
- Valle, D.G., Tayeb, J. and Melcion, J.P. 1987. Relationship of extrusion variables with pressure and temperature during twin screw extrusion cooking of starch. *J. Food Eng.* 6:423.
- van Zuilichem, D.J., de Swart, J.G. and Buisman, G. 1973. Residence time distributions in an extruder. *Lebensm-Wiss. u. Technol.* 6(5):184.
- Williams, J.M. 1968. The chemical evidence for the structure of starch. In: Starch and Its Derivatives, 4th ed. Radley, J.A. (Editor), Chapman and Hall, London.
- Wolf, D. and White, D.H. 1976. Experimental study of the residence time distribution in plasticating screw extruders. *AIChE J.* 22:122.
- Wolf, D. and Resnick, W. 1963. Residence time distribution in real systems. *Ind. Eng. Chem. Fund.* 2:287.
- Wolf, D., Holin, N. and White, D.H. 1986. Residence time distribution in a commercial twin-screw extruder. *Polym. Eng. Sci.* 26(9):640.

Wolfrom, M.L. and Khadem, H.E. 1965. Chemical evidence for the structure of starch.

In: Starch: Chemistry and Technology. Whistler, R.L. and Paschall, E.F. (Editors).

Volume 1. Academic Press, New York.

Wyman, C.E. 1975. Theoretical model for intermeshing twin screw extruders: axial

velocity profile for shallow channels. *Polym. Eng. Sci.* 15(8):606.

4 STARCH HYDROLYSIS KINETICS OF THERMOSTABLE ALPHA-AMYLASE

4.1 Abstract

Reaction kinetics for thermostable α -amylase were determined by two experiments: an initial rate study at low starch concentrations (1-8% w/w), and a continuous rate study at a high starch concentration of 40%. The Michaelis-Menten model was used to describe the kinetics at low starch concentrations, and a modified first order model was used at high concentration. There appeared to be no substrate inhibition at the high starch concentration. The rate of product formation (in terms of DE values) was found to be proportional to the square root of the rate of starch consumption.

4.2 Introduction and Background

Reaction kinetics are important in reactor design and analyses. They are used to predict the extent of substrate conversion under a given set of conditions and can be used to evaluate reactor performance. Reaction kinetics can be determined from experiments using a batch or continuous system.

Theoretically, the activity of α -amylase could be characterized by the number of bonds broken in a D-glucan per unit time. Since this is difficult to measure experimentally, lumped methods for determining the number of reducing groups are used instead. However, these lumped methods are not related to stoichiometry (Greenwood and Milne, 1986). Equimolar quantities of maltodextrins do not have equal reducing power to an alkaline 3,5 dinitrosalicylate reagent (DNS), which is widely used to track the rate of reaction. Also, there is a problem with thermal degradation of the alkaline reagents which contain ferricyanide or copper. Therefore, the lumped methods cannot be

used to determine absolute values of maximum velocities or kinetic constants. Iodine stain-ability of whole starch and viscometric methods cannot be used to estimate the rate of bond scission, either. It appears that no suitable methods for the absolute determination of maximum velocity or kinetic constants has been found for α -amylase (Greenwood and Milne, 1968).

The relative reducing power of low molecular weight sugars is presented in Table 4.1.

Table 4.1. Relative reducing power of various sugars.		
Type of sugar	Theoretical	Observed
Monosaccharide	100.0	100.0
Disaccharide	52.6	58.0
Trisaccharide	35.7	39.5
Tetrasaccharide	27.0	29.8
Pentasaccharide	21.7	24.2
Hexasaccharide	18.2	20.8

Source: Anon., 1984.

There are many factors which influence the activity of α -amylase. In extrusion, effects of high temperature, pressure and shear on enzyme activity are of primary concern, besides pH and the presence of Ca ions. For example, the optimum temperature for α -amylase varies depending on the source. The optimum temperature for *B. licheniformis* is 92°C (110°C maximum) whereas that for *B. amyloliquefaciens* is 70°C (85-90°C maximum).

Optimum pH for α -amylase also varies with enzyme sources. The optimum pH ranges are 6.0-7.0 for mammalian enzymes, 5.9-6.0 for *B. subtilis*, 4.8-5.8 for *A. oryzae* and 4.7-5.4 for barley-malt. *B. licheniformis* α -amylase is active over a much wider pH range than *B. amyloliquefaciens* (Norman, 1981).

α -amylase requires calcium ion to stabilize its activity. The enzyme from *B. licheniformis* at 70°C requires about 3-4 ppm (Norman, 1981). The saturation level of calcium for this enzyme is about 150 ppm. In a starch slurry, Termamyl α -amylase is stabilized in the presence of 50-70 ppm of Ca^{++} (Anon., 1985a). Table 4.2 shows the stability of Termamyl 60L and 120L at different Ca^{++} levels, pH and temperatures.

Table 4.2. Stability of Termamyl 60L and 120L in terms of enzyme half life in minutes for DE values in the range of 0-12.				
	93°C	98°C	103°C	107°C
Ca⁺⁺ 70 ppm				
pH 6.5	1500	400	100	40
pH 6.0	600	200	75	20
pH 5.5	300	75	25	10
Ca⁺⁺ 20 ppm				
pH 6.5	450	125	40	10
pH 6.0	250	75	20	5
pH 5.5	100	25	5	2
Ca⁺⁺ 5 ppm				
pH 6.5	150	40	10	4
pH 6.0	75	20	5	2

Source: Anon., 1985a.

The objectives of this study were to determine the kinetics of α -amylase and to develop a kinetic model to predict the extent of starch conversion in an extruder used as a bioreactor.

4.3 Theory

Using electron microscopy, particle size analysis, DSC, and x-ray diffractometry, Colonna et al. (1988) found that *Bacillus subtilis* α -amylase attacked starch from one granule to another, while acid hydrolysis occurs at all granules simultaneously. The enzyme attacks amylose and amylopectin equally. The mechanism of starch hydrolysis is a two-stage process:

Stage one



Stage two



The reaction was assumed to be quasi-steady-state, leading to the expression:

$$-\frac{dS}{dt} = \frac{dSS}{dt} = k_2ES = \frac{k_2ES \cdot S_o}{\frac{k_{-1}}{k_1} + E_o} \quad (4.3)$$

This rate expression is applicable to short term hydrolysis only, because of product inhibition during long term processes.

The kinetics of α -amylase from different sources have been studied by several researchers (Hakkarainen and Linko, 1985; Henriksnäs and Lövgren, 1978; Marc and Engasser, 1983; Pasari et al., 1988; Reinikainen et al., 1986; Rollings and Thompson, 1984; Steverson et al., 1984; and Yankov et al., 1986). The results of their studies are

summarized in Table 4.3. The reaction kinetics of α -amylase depends on the source of the enzyme and the chain length of the starch. Enzymes from different sources have different optimum reaction conditions (temperature, pH and cofactor levels).

Using gel chromatography, Henriksnäs and Lövgren (1978) found that dextrans were formed within four ranges of molecular weights (MW): $<5 \times 10^4$, $5 \times 10^4 - 10^5$, $10^5 - 5 \times 10^5$ and $>5 \times 10^5$. Most high molecular weight products were obtained at short reaction times. The authors used a lumped first order reaction for the dextrinization. The lumped first order model provides good simulation of the experimental results but does not intrinsically describe the enzyme kinetics. Marc and Engasser (1983), and Rollings and Thompson (1984) developed the kinetics of α -amylase on the basis of resultant product profiles. Incorporating the effects of starch dissolubility and thermal deactivation of enzymes, Marc and Engasser (1983) showed that the theoretical results agreed with experimental data.

Using an aqueous size exclusion chromatographic (SEC) method, Rollings and Thompson (1984) found that the reaction products consisted of four MW groups: 1.5×10^3 , 2×10^4 , 5×10^5 and 10^7 . Their results were consistent with those reported by Henriksnäs and Lövgren (1978). Rollings and Thompson (1984) derived the rate of formation for each constituent based on the molecular weight of the possible transformation between groups using a pseudo kinetic constant, and enzyme and constituent concentrations. The results showed good agreement between predictions and experimental data because the SEC analysis is more sensitive than reducing sugar measurement.

Table 4.3. Kinetic models from the literature.			
Source of α -amylase	Experimental conditions	Kinetic model	Reference
<i>Schwannio-myces castellii</i>	1% starch at 32°C, pH 5.0	Michaelis-Menten with product inhibition: $v = \frac{d[P]}{dt} = \frac{v_{max}[S]}{[S] + K_m \left(1 + \frac{[P]}{K_i}\right)}$	Pasari et al. (1988)
<i>Saccharo-mycopsis fibuliger</i>	0.1-0.9% starch at 32°C, pH 4.8	Michaelis-Menten with product inhibition.	Steverson et al. (1984)
Malt α -amylase	malt starch at 40-70°C	First order reaction for each product component. First order enzyme deactivation.	Marc and Engasser (1983)
Termamyl 60L	35-55% wheat starch at 80°C, in a batch system	Non-linear model: $r = f(C_s, C_w, C_e)$	Reinikainen et al. (1986)
Termamyl 60L	30-50% wheat starch at 90-120°C in a batch system	Irreversible first order reaction.	Hakkarainen & Linko (1985)
Thermo-stable Termamyl	1% corn starch at 60-65°C, pH 6.0, batch process	$\frac{dm}{dt} = f(k, [E_t], \alpha, m)$	Rollings & Thompson (1984)
<i>Bacillus subtilis</i>	1% wheat flour	Consecutive first order reaction	Henriksnäs & Lövgren (1978)
<i>Bacillus licheniformis</i>	6.6-40% starch at 100°C and pH 7.0	Michaelis-Menten	Yankov et al. (1986)

4.4 Materials and Methods

Pre-gelatinized corn starch (23% amylose and 77% amylopectin) (American Maize, Indiana) was used to study the kinetics of Termamyl 120L and 240L α -amylase (Novo Industries, Connecticut). The reaction kinetics of the enzyme were investigated by an initial rate approach at dilute starch concentrations and by a continuous rate at high starch concentrations. The activity of Termamyl 120L (30,000 units/ml) and 240L (80,000 units/ml) were determined by the methods described by Saha et al. (1987).

4.4.1 Initial rate study at low starch concentrations

The initial rate of starch hydrolysis by Termamyl 120 L α -amylase was determined in a test tube used as a batch reactor. Pre-gelatinized corn starch at concentrations of 1%, 2%, 4% and 8% (w/w) in 50 mM acetate buffer at a pH of 6.0 were prepared and placed in test tubes. An enzyme solution containing 18 units of Termamyl 120L per ml was prepared using the same buffer. A reaction mixture containing 1 g starch solution and 0.1 ml of the enzyme solution was incubated in an ethylene glycol bath at 100°C for 5 min. The reaction was stopped by adding 0.3 ml of 0.1 M NaOH and cooled to room temperature. The sample was diluted to 10 g using distilled water and centrifuged at 15,000 rpm for 10 min. The supernatant was analyzed for total reducing sugar, using the DNS method (Saha et al., 1987).

4.4.2 Continuous rate study at high starch concentrations

An MPF-50D Baker-Perkins twin screw food extruder was used to carry out starch liquefaction by α -amylase. Two replicate experiments were conducted at 60% (w/w) moisture, 95°C and a pH of 6.0, using 45 units (activity/g starch) of enzymes. Termamyl 240L α -amylase was diluted in a 30 mM acetate buffer solution (pH 6.0) before mixing with starch in the extruder. After the system reached steady state, the residence time was

measured using a tracer method. About 0.3-0.5 g of a dye ball containing starch and an erythrosine solution in water was dropped through the feed opening. Extrudate collection began when a slight change in color was observed, and continued at intervals of 15s until the dye was no longer visible. The intensity of dye in each sample was measured against a base containing no dye using a CR-200 Chroma Meter (Minolta Camera, Japan). The mean residence time was calculated to be about 10 min by the first moment formulation.

After RTD measurement, six extrudates were collected in liquid nitrogen to freeze the reaction, and then placed in a freezer at -17°C for subsequent sugar and starch analyses. To obtain the complete reaction profile, about 400 g of extrudate was collected in a PE-laminated fibrous sausage casing (Union Carbide, OH) 5.08 cm in diameter. The casing was sealed and immediately immersed in a circulating water bath which was maintained at 95°C to continue the reaction. Periodically, the casing was opened and stirred before approximately 6-10 g of liquefied product was withdrawn and dipped in liquid nitrogen. This was continued for 25-30 hours until the reaction reached equilibrium.

Reducing sugars were analyzed using DNS and DE methods. The DNS procedure used was developed by Bernfeld (1955) and modified by Saha et al. (1987). The DE method used was developed by Dygert et al. (1965). The amount of unreacted starch was analyzed by the UV method as described by Boehringer (Anon. 1987).

4.5 Results

4.5.1 Initial rate study at low starch concentrations

Results from the initial rate experiments showed that the Michaelis-Menten kinetic model could be used for data analysis. Using the Lineweaver-Burk plot (Figure 4.1) and regression analysis (R^2 of 0.986 at $P < .05$), V_{\max} (1.1334 mg/g of extrudate/min) and K_m

(17.34 mg/g of extrudate) were calculated.

4.5.2 Continuous rate study at high starch concentration

Tables 4.4 and 4.5 show experimental data obtained from two extrusion runs and the fractional conversion (X) at each residence time, calculated by:

$$X = 1 - \frac{[S]}{[S]_0} \quad (4.4)$$

Results at reaction times less than 10 minutes were obtained from separate experiments (discussed in Chapter 7) which were conducted under identical conditions of moisture content, temperature, pH and enzyme level.

Results from the DNS and DE methods were different in magnitude, although both increased with increasing reaction times. Between %RS and %DE, %DE values were more consistent with respect to fractional conversion. In fact, the DE method is more accurate since it can be used to measure the amount of reducing sugars in a very narrow range of 0-150 micrograms. Since the results from the two experiments were fairly consistent (Figure 4.2), they were pooled together and analyzed to formulate a rate expression.

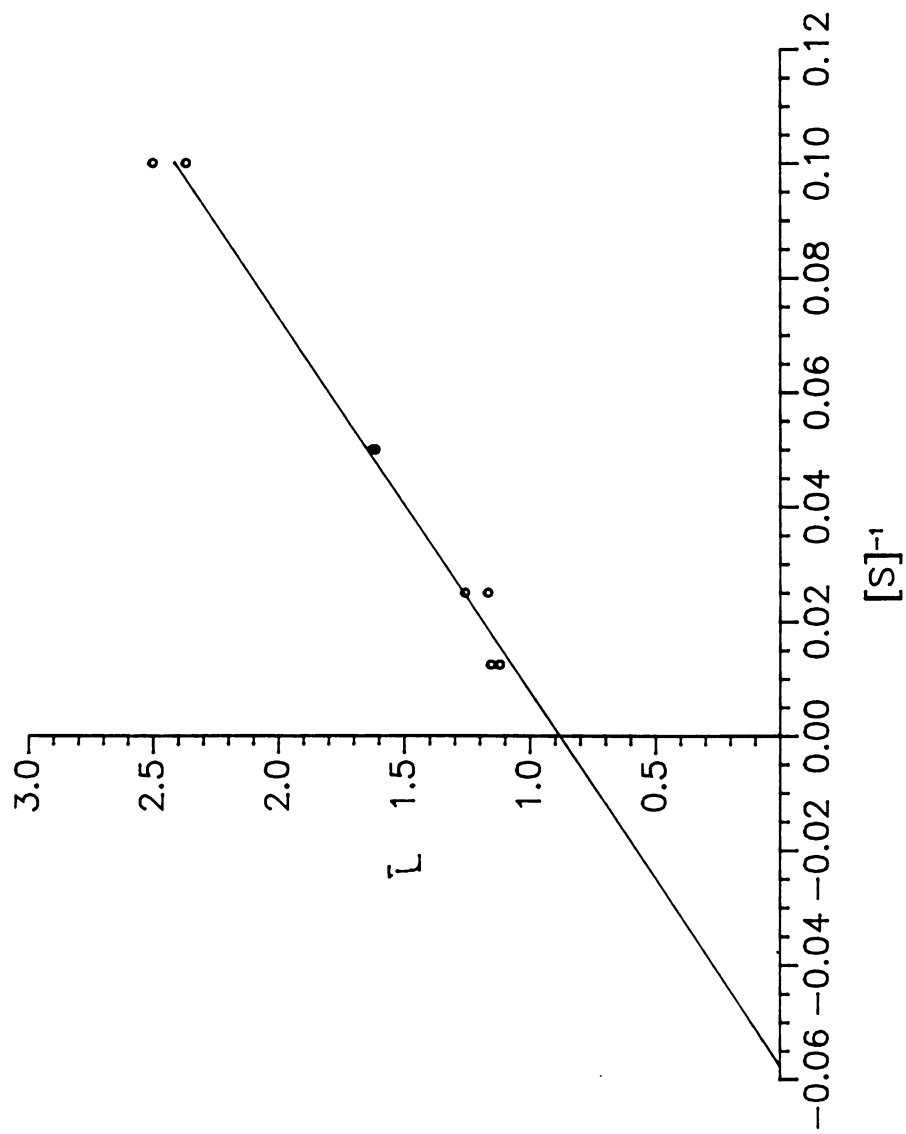


Figure 4.1 Lineweaver-Burk plot of reciprocal rate of product formation versus reciprocal initial starch concentration.

Table 4.4. Percent of unreacted starch, reducing sugars, DE, and fractional conversion (first replicate of continuous rate study).

Residence time (min)	% Unreacted starch	% Total reducing sugar (RS)	%DE	Fractional conversion
0.0	38.8	0.0	0.0	0.00
2.2	34.3	8.5	3.3	0.12
4.7	34.4	10.0	3.4	0.11
7.5	30.8	12.3	4.7	0.21
10.7	27.6	15.1	6.3	0.29
43.9	9.3	32.4	15.6	0.76
48.9	9.1	33.0	17.1	0.77
61.9	8.1	36.8	19.5	0.79
65.9	7.1	36.9	19.5	0.82
73.9	5.9	41.5	22.0	0.85
78.9	5.2	39.8	21.6	0.87
86.9	5.1	41.0	23.0	0.87
102.9	4.4	44.0	24.9	0.89
116.9	4.1	44.3	26.3	0.90
132.9	3.2	46.4	28.0	0.92
161.9	3.3	48.9	30.7	0.92
190.9	2.8	50.7	32.0	0.93
1500.0	2.3	53.1	41.8	0.94

Table 4.5. Percent of unreacted starch, reducing sugars, DE, and fractional conversion (second replicate of continuous rate study).				
Residence time (min)	% Unreacted starch	% Total reducing sugar (RS)	% DE	Fractional conversion
0.0	42.8	0.0	0.0	0.00
10.4	31.4	20.4	7.1	0.27
20.4	24.3	23.4	9.3	0.43
27.9	19.5	25.0	9.1	0.54
31.4	17.4	25.1	10.2	0.59
37.9	13.2	28.9	12.5	0.69
41.4	11.7	28.3	12.4	0.73
48.9	7.5	32.5	13.3	0.83
57.9	5.8	34.1	15.4	0.87
68.4	5.0	36.6	17.7	0.88
77.4	4.9	38.0	18.9	0.89
82.9	4.7	38.4	20.6	0.89
91.9	4.4	38.8	20.6	0.90
110.9	4.1	41.8	21.5	0.90
141.9	3.6	45.3	26.0	0.92
171.9	3.8	47.3	28.0	0.91
299.9	3.5	54.3	32.6	0.92
401.9	3.2	54.9	35.4	0.93
586.9	3.0	54.9	37.4	0.93
1201.9	3.3	57.1	39.7	0.92
1333.4	2.8	63.4	41.0	0.94
1880.9	2.7	64.0	42.0	0.94

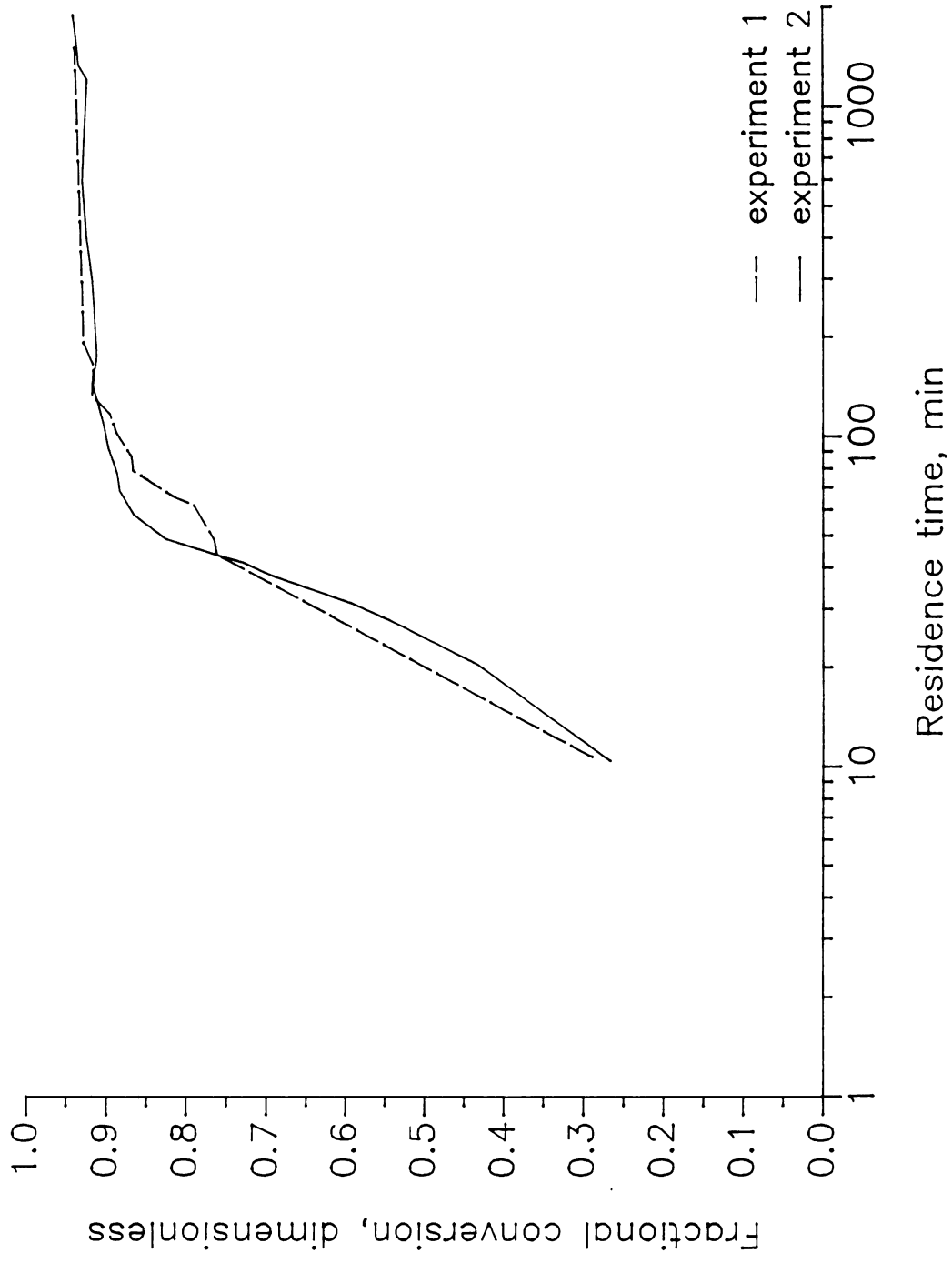


Figure 4.2 Fractional conversion (X) versus residence time.

Since the SEC method was used in this study, the liquefied product profile could not be determined. Therefore, the rigorous approach which uses the probability of producing products by starch hydrolysis could not be used to derive the intrinsic kinetics for Termamyl α -amylase. However, if the rate expression is used as a tool to predict the extent of starch hydrolysis in the extruder at a given condition, then the kinetics can be empirically developed.

A plot of starch concentration and DE values versus residence time shows that a rapid reduction in starch concentration and a rapid increase in DE values occurred within the first 2 hours, at similar but inverse rates (Figure 4.3). However, the DE values increased at a higher rate than the reduction of starch concentration after 2 hours. This is due to the action of the enzymes which randomly attack starch molecules rapidly in the early stages to produce oligosaccharides ($DP > 3$). As the reaction continues, the enzymes attack the oligosaccharides to produce shorter chain molecules which have higher reducing power. When the reaction is complete ($X = 1$), only glucose is obtained. However, this condition never occurs because starch molecules contain branched chains which α -amylase cannot break down. When the reaction reaches equilibrium, the products are a mixture of low DP molecules and dextrans. From the experimental results, the equilibrium DE was estimated at 42, which is consistent with what has been reported in the literature.

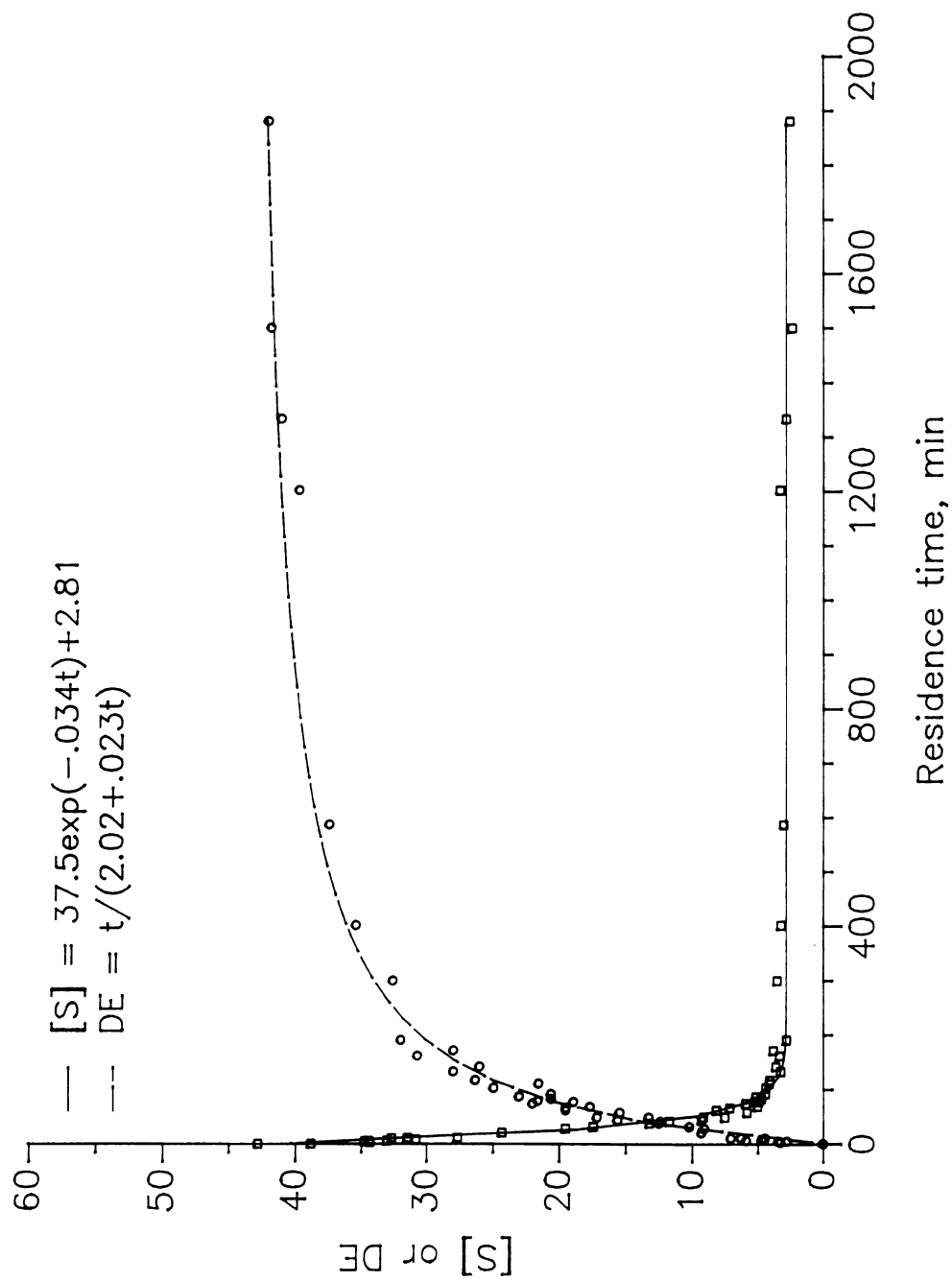


Figure 4.3 Dextrose equivalent (DE) and starch concentration ([S]) versus residence time.

Empirical relationships for starch concentration and the DE value as a function of reaction time were developed using regression analyses ($R^2 = 0.99$). They are, respectively:

$$[S] = 37.5 \exp(-0.034t) + 2.81 \quad (4.5)$$

$$DE = \frac{t}{(2.02 + 0.023t)} \quad (4.6)$$

By taking the derivative of Eq. 4.6, the rate of starch consumption was calculated and plotted against starch concentration. The rate decreased with decreased starch concentration; however, this behavior did not follow the Michaelis-Menten model. Instead, the profile approached a first order reaction for most starch concentrations except those lower than 3%, where the rate was close to zero. Therefore, the rate of consumption was plotted against a modified starch concentration (Figure 4.4), $[S]'$, defined by:

$$[S]' = [S] - 0.06[S]_0 \quad (4.7)$$

where 0.06 is the fractional conversion of unreacted starch at equilibrium. This definition allowed the plot to be extended through the origin.

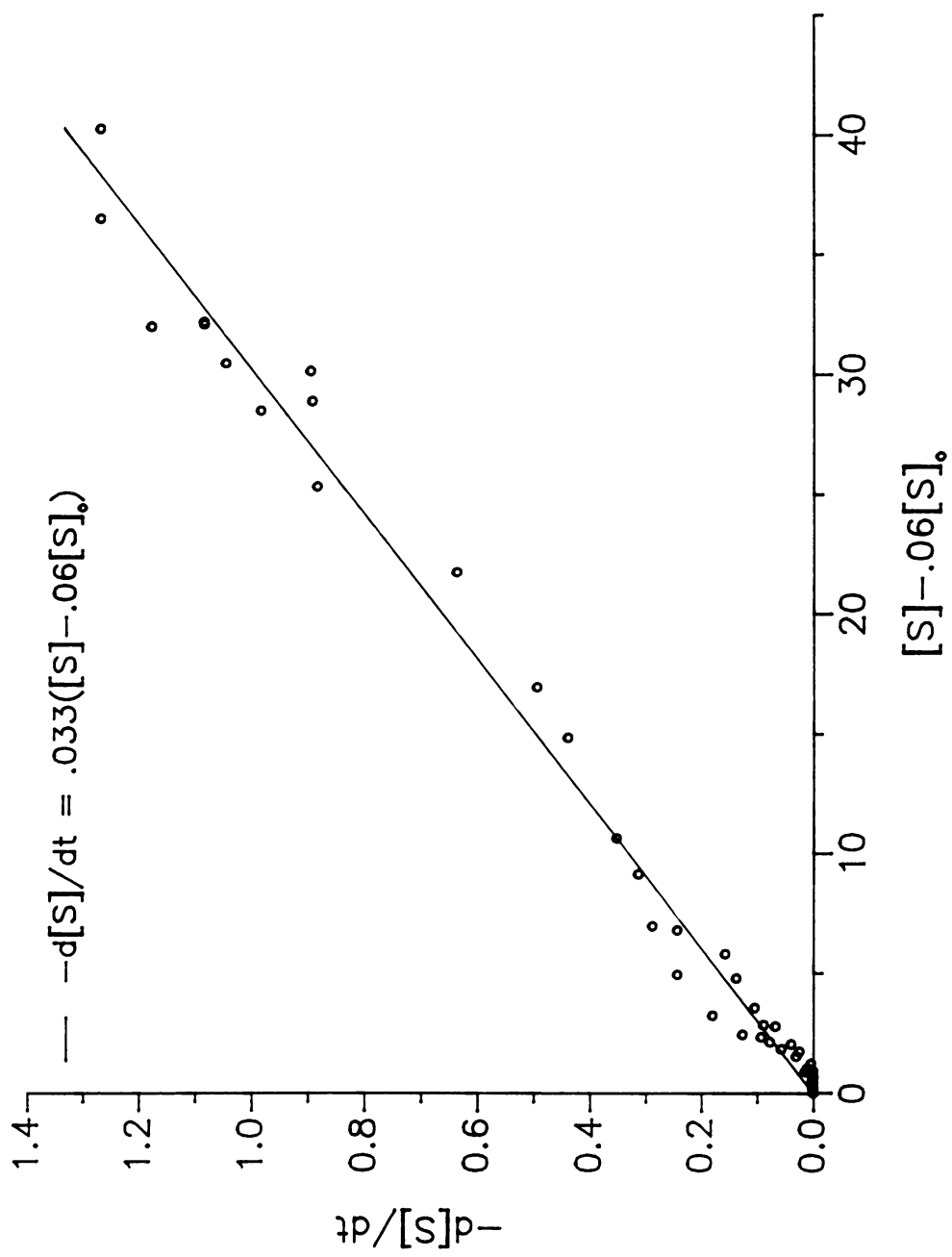


Figure 4.4 Rate of starch consumption versus modified starch concentration.

An empirical first order model was developed using regression analysis ($R^2 = 0.99$) and can be expressed by the equation:

$$-r_s = -\frac{d[S]}{dt} = 0.033[S] \quad (4.8)$$

The rate constant was 0.033 g/g/min. The rate of product formation in terms of DE values was calculated in the same manner and is plotted against the modified starch concentration (Figure 4.5). Using regression analysis ($R^2 = 0.99$), the rate of product formation was developed and may be expressed by:

$$r_p = \frac{d[DE]}{dt} = 0.191 \exp(0.026[S]) - 0.206 \exp(-0.415[S]) \quad (4.9)$$

Since Figures 4.4 and 4.5 could not be superimposed, the rate of product formation was not equal to the rate of starch consumption. Figure 4.6 shows a plot between the two rates. The relationship between the two was developed using regression analysis ($R^2 = 0.99$) and may be expressed by:

$$r_p = 0.425(-r_s)^{0.467} \quad (4.10)$$

On the whole, the rate of product formation is proportional to the square root of the rate of starch consumption.

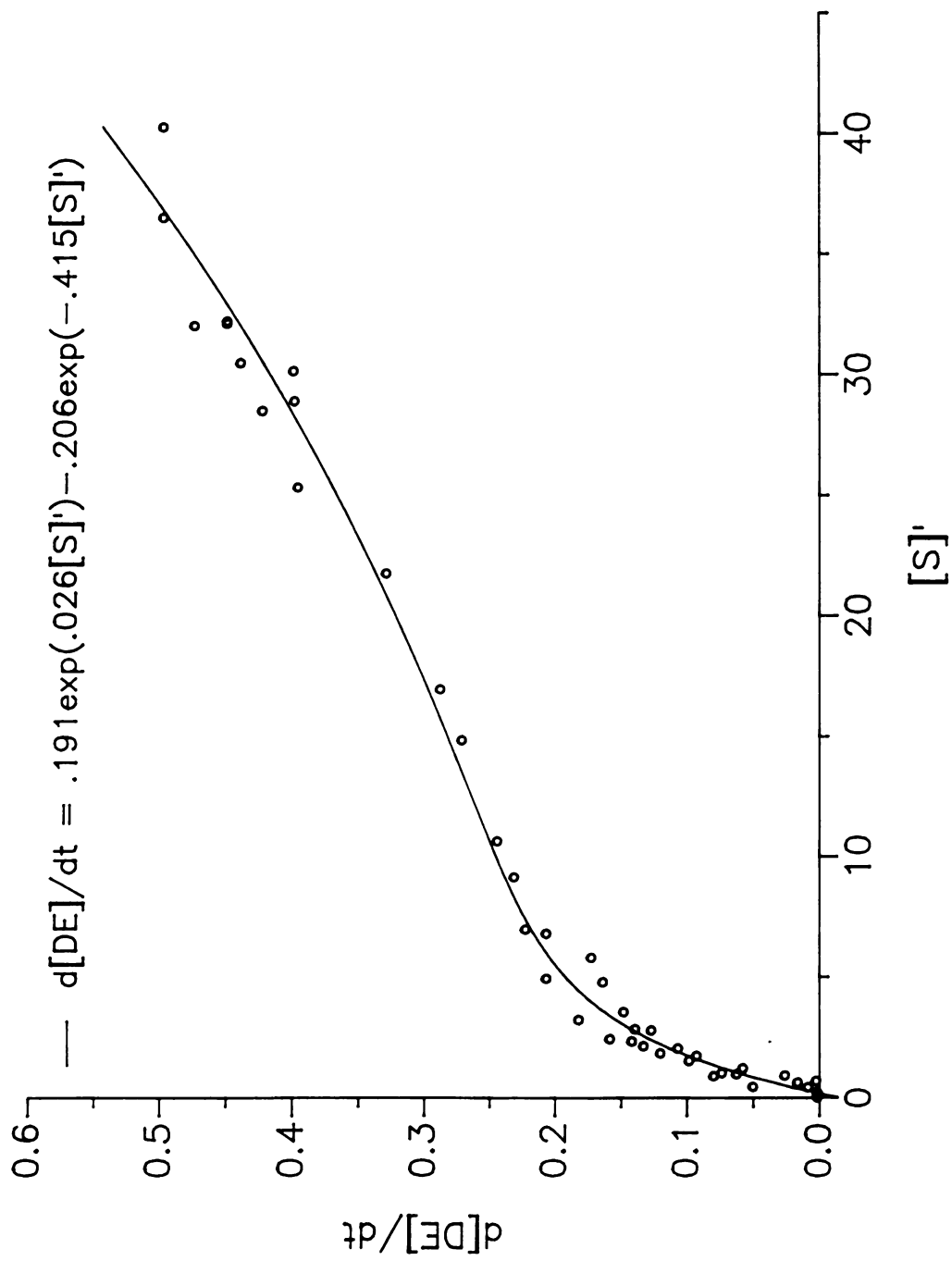


Figure 4.5 Rate of product formation versus modified starch concentration.

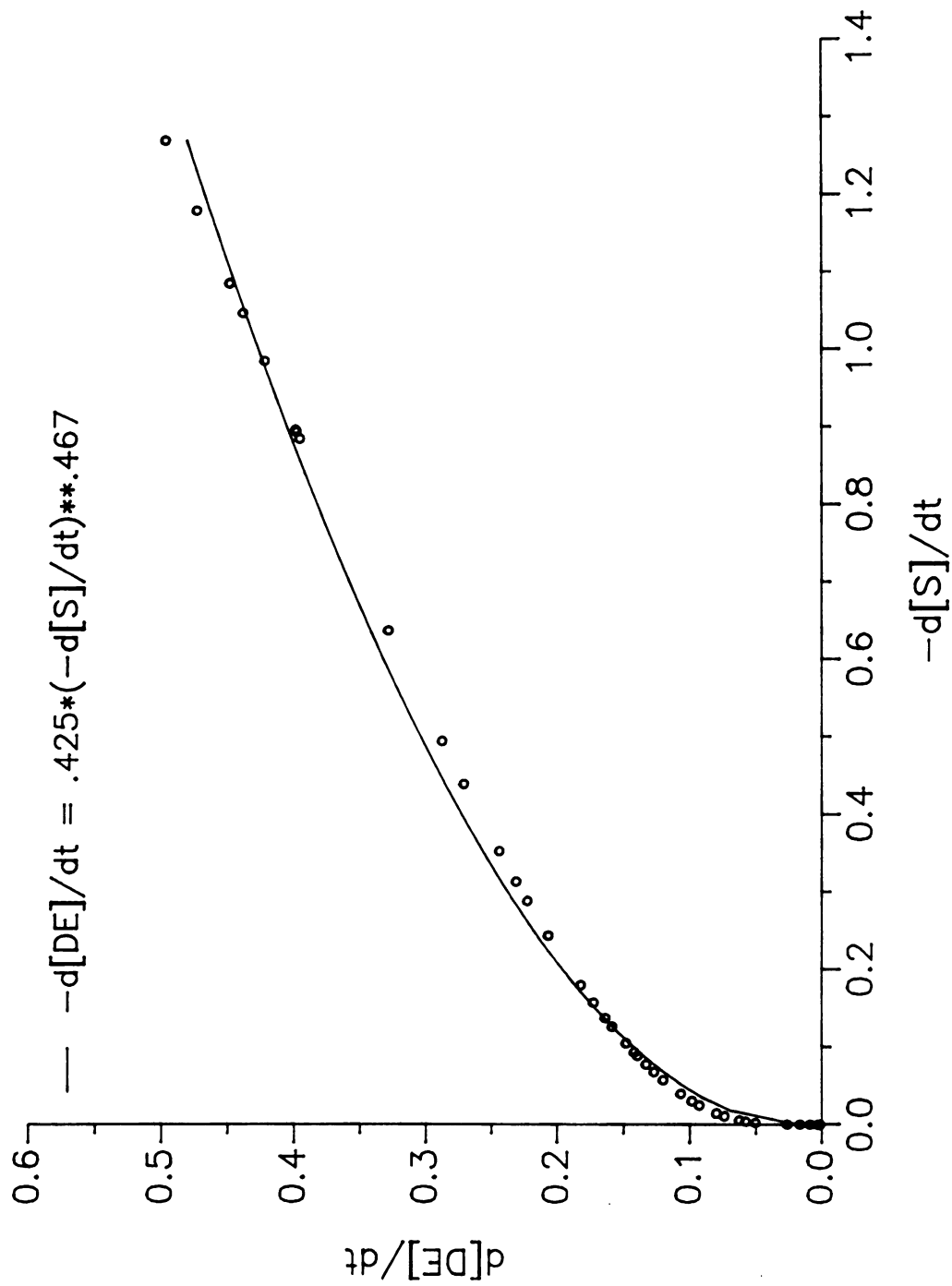


Figure 4.6 Rate of product formation versus rate of starch consumption.

4.6 Discussion

Within the range of low starch concentrations (up to 8%), the rate expression for starch hydrolysis by thermostable Termamyl α -amylase can be represented by the classical Michaelis-Menten model. These results are in agreement with those reported by Yankov et al. (1986), who found that the model was valid for up to about 25% starch concentration. In this study, viscosity increased with increased pre-gelatinized starch concentration, therefore experiments at the high concentrations were difficult to conduct.

At high starch concentration, the reaction has been known to become substrate inhibited (Yankov et al., 1986). This may be due to network formation by starch molecules which inhibited attack by enzymes. Macroscopically, a system containing soluble enzyme in a starch-water mixture is homogeneous, but microscopically it may be considered as segregated where enzyme molecules are dispersed in the starch-water matrix. At low starch concentrations, starch and enzyme molecules move freely to contact each other, therefore reaction takes place. On the other hand, at high starch concentrations, the molecules cannot move freely due to viscous effects, therefore the rate of reaction decreases.

This viscous effect is analogous to the effect of mass transfer, which may be described in terms of the mass transfer coefficient. In suspensions of small particles, the mass transfer coefficient can be determined (Geankoplis, 1983) by:

$$k_L = \frac{2D_{12}}{d_p} + \frac{0.31}{Sc^{0.667}} \left[\frac{(\rho_c - \rho_p)\mu_c g}{\rho_c^2} \right]^{0.333} \quad (4.11)$$

where

$$Sc = \frac{\mu_c}{\rho_c D_{12}} \quad (4.12)$$

$$D_{12} = \frac{9.96 \times 10^{-16} T}{\mu V_1^{0.333}} \quad (4.13)$$

It is obvious that increasing viscosity results in decreasing k_L and, therefore, the rate of mass transfer. However, the rate of mass transfer may be improved if convection compensates for the effect of limited mass diffusion.

The rate of reaction in this study, however, did not decrease at high starch concentrations (Figure 4.4). Therefore, it appears that substrate inhibition was negligible, and that the results can be used to represent the real reaction rates.

The data in Table 4.2 suggests that thermal inactivation of the enzyme should be considered. However, one must note that data in Table 4.2 are based on DE values of 0-12. For example, the half-life of Termamyl 60 L and 120 L is 1500 min at 93°C, Ca^{++} of 70 ppm and pH 6.5. By contrast, DE values of 40 were obtained in this study after a reaction time of only 1500 min. This is probably because the enzyme levels used in this study are much greater than the levels used to obtain the results in Table 4.2. Therefore, it is hypothesized that the rate of reaction was so fast that the percent of un-reacted starch decreased rapidly before thermal inactivation could become a factor.

4.7 Conclusions

The reaction kinetics of thermostable α -amylase was determined by two experimental methods. The first, an initial rate experiment, was carried out at low concentrations of pre-gelatinized starch. The second, a continuous rate experiment, was conducted at a starch concentration of 40% in a twin screw extruder. To obtain a complete product profile, the extrudate was collected and put in a batch system to allow the enzymatic reaction to continue to equilibrium.

Because the two methods were different, it was difficult to compare one to the other. At low starch concentrations, the Michaelis-Menten model is applicable. But at high starch concentrations, an empirical first order model was more suitable for describing the reaction profile for starch hydrolysis by α -amylase. Substrate and product inhibition, which are mechanistically analogous to mass transfer limitation, have been observed and reported in the technical literature. However, in this study no effects of product inhibition were observed.

At high starch concentrations, the relationship between the rate of product formation (r_p) in terms of DE values and the rate of starch consumption ($-r_s$) was not linear. Instead, r_p was found to be proportional to the square root of $-r_s$. It must be noted, however, that DE values are indices used only to indicate the extent of reaction and cannot be used to describe the intrinsic reaction kinetics.

Initial rate studies at various high starch concentrations in the twin screw extruder needs to be further investigated. Because the extruder provides excellent mixing and resolves the mass transfer limitation problem, a more generalized rate expression can be derived by this method. The initial rate studies also eliminate the effect of thermal inactivation of the enzyme, which can occur during a continuous rate study. The reaction kinetics should be studied at various temperatures, to account for temperature variation during extrusion.

4.8 Nomenclature

A	High MW concentration, g/l
A_i	Initial activity at time 0, activity unit
A_t	Residual activity at time t, activity unit
B	Dextrin concentration, g/l

C	Low MW concentration, g/l
C_s	Normalized starch fraction, dimensionless
C_w	Actual water fraction in extrudate, dimensionless
C_e	Enzyme concentration, ml of enzyme per 100 g dry starch
d_p	Diameter of small solid particle, m
D₁₂	Mass diffusivity of solute 1 in solution 2, m²/s
E	α-amylase
[E]	Total enzyme concentration, g/l
E-S, E-LS	Enzyme-substrate intermediates, g/l
g	gravitational acceleration, m/s²
K_m	Michaelis-Menten constant, mg/ml
K_i	Inhibitor constant, mg/ml
k_L	Mass transfer coefficient for liquid suspension, m/s
k₁ and k₃	Rate constants, g/l/min
k, k₁, k₂ and k₄	Rate constants, min⁻¹
LS	Large oligosaccharides
P	Product
m	Mass fraction of each constituent (Table 4.2), dimensionless
Sc	Schmidt number, dimensionless
S, [S]	Substrate or starch concentration, g/g
S_o, [S]_o	Original substrate concentration, g/g
SS	Small oligosaccharides
T	Temperature, K
t	Reaction time, min

$t^{1/2}$	Enzyme half life, $\text{min}^{1/2}$
V_{\max}	Maximum enzymatic rate, mg/g/min
V_1	Molar volume of liquid, $\text{m}^3/\text{kg mol}$

Greek symbols

α	Molar ratio of species i to j, dimensionless
μ, μ_c	Viscosity of solution or continuous phase, kg/m/s
ρ_c	Density of the continuous phase, kg/m^3
ρ_p	Density of solid particles, kg/m^3
v	Reaction rate, mg/ml/min

4.9 References

- Anon. 1984. Nutritive sweetness from corn. Corn Refiners Association. Washington D.C.
- Anon. 1985a. Termamyl. Novo brochure B 204, Novo Industries Inc. Denmark.
- Anon. 1985b. Use of Termamyl for starch liquefaction, Novo brochure, Novo Industries Inc. Denmark.
- Anon. 1987. Methods of Biochemical Analysis and Food Analysis: Using Test-Combinations. Boehringer Mannheim GmbH Biochemica. W. Germany.
- Bernfeld, P. 1955. Amylases α and β . Methods Enzymol. 1:149.
- Colonna, P., Buleon, A. and Lemarie, F. 1988. Action of Bacillus subtilis α -amylase on native wheat starch. Biotech. Bioeng. 31:895.
- Dygart, S., Li, L.H., Florida, D. and Thoma, J. 1965. Determination of reducing sugar with improved precision. Anal. Chem. 13:367.

- Geankoplis, C.J. 1983. Transport Processes and Unit Operations. 2nd ed. Allyn and Bacon, Boston.
- Greenwood, C.T. and Milne, E.A. 1968. III Theories of the Stepwise Degradation of Linear Polysaccharides In: Advances in Carbohydrate Chemistry. Wolfson, M.L. and Tipson, R.S. (Editors). Academic Press, New York. 23:299.
- Hakkarainen, L. and Linko, P. 1985. State vector model for contherm scraped surface heat exchanger used as an enzyme reactor in wheat starch conversion. *J. Food Eng.* 4:135.
- Henriksnäs, H. And Lövgren, T. 1978. Chain-length distribution of starch hydrolyzed with α - and β -amylase action. *Biotech. Bioeng.* 20:1303.
- Marc, A. and Engasser, J.M. 1983. A kinetic model of starch hydrolysis by α - and β -amylases during mashing. *Biotech. Bioeng.* 25:481.
- Norman, B.E. 1981. New developments in starch syrup technology. In: Enzymes and Food Processing. Birch, G.G., Blakebrough, N. and Parker, K.J. (Editors) Applied Sci. Publ., London.
- Pasari, A.B., Korus, R.A. and Heimsch, R.C. 1988. Kinetics of the amylase system of *Schwanniomyces castellii*. *Enzyme Micro. Technol.* 10:156.
- Richardson, T. and Hyslop, D.B. 1985. Enzymes. In: Food Chemistry. Fennema, O.R. (Editor). 2nd ed., Marcel Dekker Inc., New York.
- Reinikainen, P., Suortti, T., Olkku, J., Malkki, Y. and Linko, P. 1986. Extrusion cooking in enzymatic liquefaction of wheat starch. *Starch* 38:20.
- Rollings, J.E. and Thompson, R.W. 1984. Kinetics of enzymatic starch liquefaction: simulation of the high-molecular weight product distribution. *Biotech. Bioeng.* 26:1475.

- Saha, B.C., Shen, G.J. and Zeikus, J.G. 1987. Behavior of a novel thermostable β -amylase on raw starch. *Enzyme Microb. Technol.* 9:598.
- Steverson, E.M., Korus, R.A., Admassu, W. and Heimsch, R.C. 1984. Kinetics of the amylase system of *Saccharomycopsis fibuliger*. *Enzyme Micro. Technol.* 6:549.
- Yankov, D., Dobreva, E., Beschkov, V. and Emanuilova, E. 1986. Study of optimum conditions and kinetics of starch hydrolysis by means of thermostable α -amylase. *Enzyme Microb. Technol.* 8:665.



5 EFFECT OF SHEAR ON ENZYMATIC ACTIVITY DURING REACTIVE EXTRUSION

5.1 Abstract

The effect of shear on the activity of Termamyl 120L α -amylase was studied in a batch reactor and in a twin screw extruder. In the batch experiment conducted at room temperature, strain histories above 4×10^4 produced a significant reduction in enzymatic activity. On the other hand, strain history by itself did not appear to cause significant loss of activity in extrusion runs conducted at flow rates of 10-40 kg/hr and screw speeds of 60-400 rpm. Statistically, the combination of shear rate, strain history and specific energy consumption (SEC) was significant in the reduction of enzymatic activity in the extruder.

5.2 Introduction and Background

The effect of shear on enzyme activity has been studied by several researchers (Charm and Wong, 1970; Charm and Lai, 1971; Tirrell and Middleman, 1975; and Thomas and Dunnill, 1979). Charm and Wong (1970) examined the loss of activity of catalase, rennet and carboxypeptidase in solutions at 4°C, using a coaxial viscometer and a capillary rheometer, and found similar results in both systems. The effect of shear was reported over a strain history (integral of the product of shear rate and exposure time) range of 5×10^3 - 16×10^6 . Enzyme activity decreased significantly with increasing strain histories beyond 10^4 . The shear-induced deactivation was postulated to be caused by the breaking up of tertiary structure due to molecular reorientation in the shear field.

A similar study was carried out by Tirrell and Middleman (1975). They used a coaxial cylinder viscometer to examine the shearing effect on urease during urea hydrolysis at a pH of 6.75 and a controlled temperature of 23°C. They found that there was a continuous decrease in urea hydrolysis due to loss of enzyme activity with increased strain histories beyond 10^4 , in agreement with the results of Charm and Wong (1970). Both irreversible and reversible enzyme deactivation occurred under shear. Tirrell and Middleman (1975) postulated that the conformation of protein caused dislocation of active sites which led to loss of enzyme activity. As the shearing force was removed, some enzyme activity was recovered as a result of molecular relaxation of the enzyme or the reformation of the broken tertiary structure (Charm and Lai, 1971). The shear effect on enzyme activity depends on the size and shape of the enzyme (Tirrell and Middleman, 1975).

The effect of shear on activity also depends on the source of the enzyme and the equipment used. Thomas and Dunnill (1979) found that the effect of shear on the loss of catalase activity in a closed coaxial concentric viscometer at 20-60°C was less than what would be expected based on the results of Charm and Wong (1970). The difference was due to the source of the enzyme and the system used. Charm and Wong (1970) used an open system. Above 50°C, shearing reduces thermal deactivation of catalase by interfering with protein precipitation. Thomas and Dunnill (1979) proposed that activity can be lost by other means during processing, such as pressure and oxidation.

A search of the technical literature did not yield any information on the effect of shear on α -amylase activity. The loss of enzymatic activity can be significant, however, especially when the enzymes are exposed to the high shear rates encountered during extrusion. The objective of this study was to investigate the influence of high shear on the activity of α -amylase during reactive extrusion.

5.3 Theory

Because material is sheared in four regions inside the extruder (Martelli, 1983), an accurate estimation of shear rate is difficult to obtain, especially with non-Newtonian fluids. However, since twin screw extruders are good mixers, the average shear rate can be estimated using an approach analogous to that used with mixers: the average shear rate of a non-Newtonian fluid is estimated on the basis of power consumption during mixing, using a relationship between the power number (Po) and the Reynolds number (Re) developed in the same equipment for a Newtonian fluid. This method was developed by Metzner and Otto (1957), and used successfully by Rao and Cooley (1984), and Mohamed (1988). The approach is valid when both fluids are operated in an identical mixing system with identical impeller speeds in the laminar region.

The power number for Newtonian fluids in a twin screw extruder is (Mohamed, 1988):

$$Po = \frac{E_v}{\rho N^3 D_h^5} \quad (5.1)$$

where

$$E_v = P_w - \Delta P Q_n \quad (5.2)$$

and P_w is computed from the manufacturer's relationship:

$$P_w = 0.354(\%Torque)N \quad (5.3)$$

The Reynolds number for Newtonian fluids is:

$$Re = \frac{D_h^2 N \rho}{\mu} \quad (5.4)$$

where the hydraulic diameter (D_h) is defined as:

$$D_h = \frac{4V_w}{A_w} \quad (5.5)$$

The hydraulic diameter is generally used to characterize complex geometries in fluid mechanics. In the extruder, it can be reliably determined only for screws in fully-filled zones. The hydraulic diameters for different screw types have been calculated by Mohamed (1988): 0.75 cm for single lead screws, 1.01 cm for feed screws and 1.22 cm for 30° forwarding paddles. Using the same approach, D_h for any mixed screws can be calculated by:

$$D_h = \frac{4 \sum V_{wi}}{\sum A_{wi}} \quad (5.6)$$

The power number versus Reynolds number for a Newtonian fluid is used to determine the corresponding Reynolds number (Re') for the non-Newtonian fluid during extrusion at the calculated power number. The apparent viscosity (η_a) for the non-Newtonian fluid can then be calculated by:

$$\eta_a = \frac{\rho D_h^2 N}{Re'} \quad (5.7)$$

If the fluid is described by a power law model, its average shear rate ($\dot{\gamma}_a$) can be obtained from the viscosity calculated in Eq. 5.7 by:

$$\dot{\gamma}_a = \left[\frac{\eta_a}{k_o e^{\left(\frac{\Delta E}{RT}\right)}} \right]^{\frac{1}{n-1}} \quad (5.8)$$

5.4 Materials and Methods

The effect of shear forces on the activity of thermostable Termamyl 120L α -amylase (Novo Laboratories, Connecticut) was investigated in a Haake viscometer and in a Baker-Perkins MPF 50D twin screw extruder. Enzymatic activity, determined by the DNS method developed by Bernfeld (1955) and modified by Saha et al. (1987), was 30,000 units/ml.

5.4.1 Haake viscometer experiments

The enzyme solution, containing three activity units per ml, was prepared in distilled water prior to testing. Batch experiments were carried out in a Haake RV-12 viscometer consisting of an MV paddle sensor attached to an M-500 viscometer drive head. Fifty grams of the diluted enzyme solution (pH 5.6) was loaded into an MV cup. The F3-C water circulator maintained the enzyme solution at a constant temperature of 25°C. The viscometer behaves as a mixer, with a well defined shear rate (Steffe and Ford, 1985):

$$\dot{\gamma} = k' \omega \quad (5.9)$$

where k' is the paddle constant and ω is the rotational speed of the paddle in rad/s. The paddle constant of 4.46 was determined by Steffe and Ford (1985).

The experiment was conducted over four different reaction times at each of six rotational speeds (Table 5.1). At the end of each reaction time, the paddle was stopped for 15s, and 0.1 ml of the enzyme solution was pipetted to a 15 ml test tube. Duplicates were prepared at each time step.

Residual enzyme activity was determined immediately by the following process. One ml of 2% soluble starch was added to the tube and the mixture was immersed in a water bath controlled at 60°C for 30 min. The reaction was stopped by adding two ml of

DNS reagent. The mixture was heated in an ethylene glycol bath maintained at 100°C for 10 min and then cooled to room temperature. The dark brown color developed was then measured with a spectrophotometer at 640 nm against a blank containing distilled water, prepared in exactly the same way as the samples. The absorbance was converted to glucose equivalence using the standard curve established from several known glucose concentrations. One unit of enzyme activity is defined as 1 micromole of glucose liberated per ml of enzyme per minute.

RPM	Residence time (min)
100	10, 20, 35 and 70
150	10, 20, 35 and 60
350	10, 20, 35 and 60
400	10, 20, 35 and 65
500	10, 35, 60 and 90
550	10, 20, 35 and 60

The depletion of the enzyme solution due to sampling over the second, third and fourth steps was insignificant, and should not alter the shear rate in the flow field. Therefore, the shear rate was assumed to be relatively constant at each rotational speed.

5.4.2 Extruder experiments

Soy polysaccharide (SPS) (Fibrim 2000, supplied by Ralston Purina Co., MO) was used as a starch-free, inert material to carry α -amylase through the extruder. The SPS was fed via a K-tron feeder and mixed with deionized water in the extruder. Termamyl 120L α -amylase (Novo Industries, Connecticut) was diluted and fed through another injection port. The enzyme constituted 0.0003 ml per g of the feed mixture. With a screw profile of 90° paddles, the mixture was too dry to be properly conveyed, and the

extrudate became cooked and discolored due to viscous heat dissipation. Although the barrel was chilled, the rate of cooling could not keep up with the rate of heat generation. Therefore, product temperatures in the paddle zone reached or exceeded 95°C, the optimum temperature of the enzyme. A higher SPS moisture content might have solved the problem but this was not investigated. Instead, 30° forwarding paddles were used, to reduce the rate of viscous dissipation. The Po-Re relationship for this configuration had previously been developed by Mohamed (1988).

During the experiment, the mass flow rate was increased with increasing screw rpm to maintain the die pressure within as narrow a range as possible. The extruder was operated at flow rates of 10-40 kg/hr and screw speeds of 60-400 rpm. Under these conditions, the screws were partially filled and product temperatures remained below 55°C with chilled water circulation. Therefore, protein denaturation and thermal deactivation of enzymes were avoided. After the extruder reached steady state, five extrudates were collected for analysis on the same day.

RTD measurements were made for all extrusion runs. About 0.5 g of dye ball (mixture of starch and erythrosine solution) was dropped through the feed port. Extrudate samples were collected at the first sign of a color, and at intervals of 15s until the color was no longer visible. The intensity of red (Δa) in the extrudates was measured against a base extrudate containing no dye, using a CR-200 Chroma Meter (Minolta Camera Co., Japan). The mean residence time was calculated by:

$$\bar{t} = \frac{\sum_{i=0}^m \Delta a_i \Delta t}{\sum_{i=0}^m a_i} \quad (5.10)$$

where Δa_i is the redness value at any discrete time t_i and Δt is the time interval, equal to 15s.

Use of SPS was advantageous since it does not contain any soluble starch and, therefore, does not interfere with the determination of residual enzymatic activity. The procedure used was as follows: One tenth of a gram of SPS extrudate was placed in a 15 ml test tube and mixed with one ml of 2% soluble starch in a 50 mM acetate buffer (pH 6.0). The mixture was incubated in a water bath maintained at 60°C for 30 min. One half ml of 0.2 M sodium hydroxide was then added and the test tube was immediately immersed in an ice bath for 10 min. An additional 5 ml of water was added to the test tube which was then heated in an ethylene glycol bath at 100°C for 10 min to complete enzyme deactivation and also to extract all soluble constituents including reducing sugars. The mixture was brought up to 15 g by adding water and then centrifuged at 15,000 rpm for 10 min. The supernatant was subsequently measured for the amount of glucose equivalence by the DNS method. The enzyme activity was then calculated.

5.4.3 Determination of the effect of shear in the TSE

An average shear rate for 30° forwarding paddles was estimated by the Power number and Reynolds number relationship developed by Mohamed (1988):

$$P_o = 6.9 \times 10^5 Re^{-1.34} \quad (5.11)$$

The rheological model for 30% SPS in water was obtained from Howkins (1987):

$$\tau = 2.85e \left(\frac{4520}{RT} \right) \dot{\gamma}^{0.25} \quad (5.12)$$

An alternative approach is to determine the shear effect by using the specific energy consumption (SEC) or the ratio of mass flow rate to screw rpm $\left(\frac{\dot{m}}{N} \right)$. The SEC is

defined as the ratio of power input to the mass flow rate, and is directly proportional to the shear strain and shear stress during extrusion (Rauwendaal, 1981). In this study, the SEC was expressed as:

$$\text{SEC} = \frac{E_v}{\dot{m}} \quad (5.13)$$

The ratio of mass flow rate to screw speed is generally used as an indicator of the degree of fill in an extruder.

5.5 Results and Discussion

5.5.1 Shear deactivation in the batch system

The residual activity of α -amylase and the associated strain histories were calculated (Appendix 1), and are summarized in Table 5.2 and plotted in Figure 5.1. The effect of strain history on enzyme activity was significant at $P < .05$ (Appendix 2). A marked reduction in enzymatic activity was observed at strain histories above 4×10^4 , in agreement with what has been reported in the technical literature (Figure 5.2).

Table 5.2. Residual enzymatic activity obtained from the Haake viscometer.				
Screw speed, rpm	Shear rate, s⁻¹	Residence time, min	Strain history x10⁻⁴	% Average residual activity
100	46.7	10	2.8	99.0
		20	5.6	99.8
		35	9.8	92.7
		70	19.6	88.3
150	70.0	10	4.2	100.0
		20	8.4	94.6
		35	14.7	95.3
		60	25.2	95.8
350	163.4	10	9.8	95.3
		20	19.6	99.5
		35	34.3	92.0
		60	58.8	87.5
400	186.7	10	11.2	93.2
		20	22.4	90.0
		35	39.2	84.7
		65	72.8	82.4
500	233.4	10	14.0	97.6
		35	49.0	83.4
		60	84.0	76.2
		90	126.0	65.0
550	256.7	10	15.4	91.7
		20	30.8	93.0
		35	53.9	77.5
		60	92.4	68.5

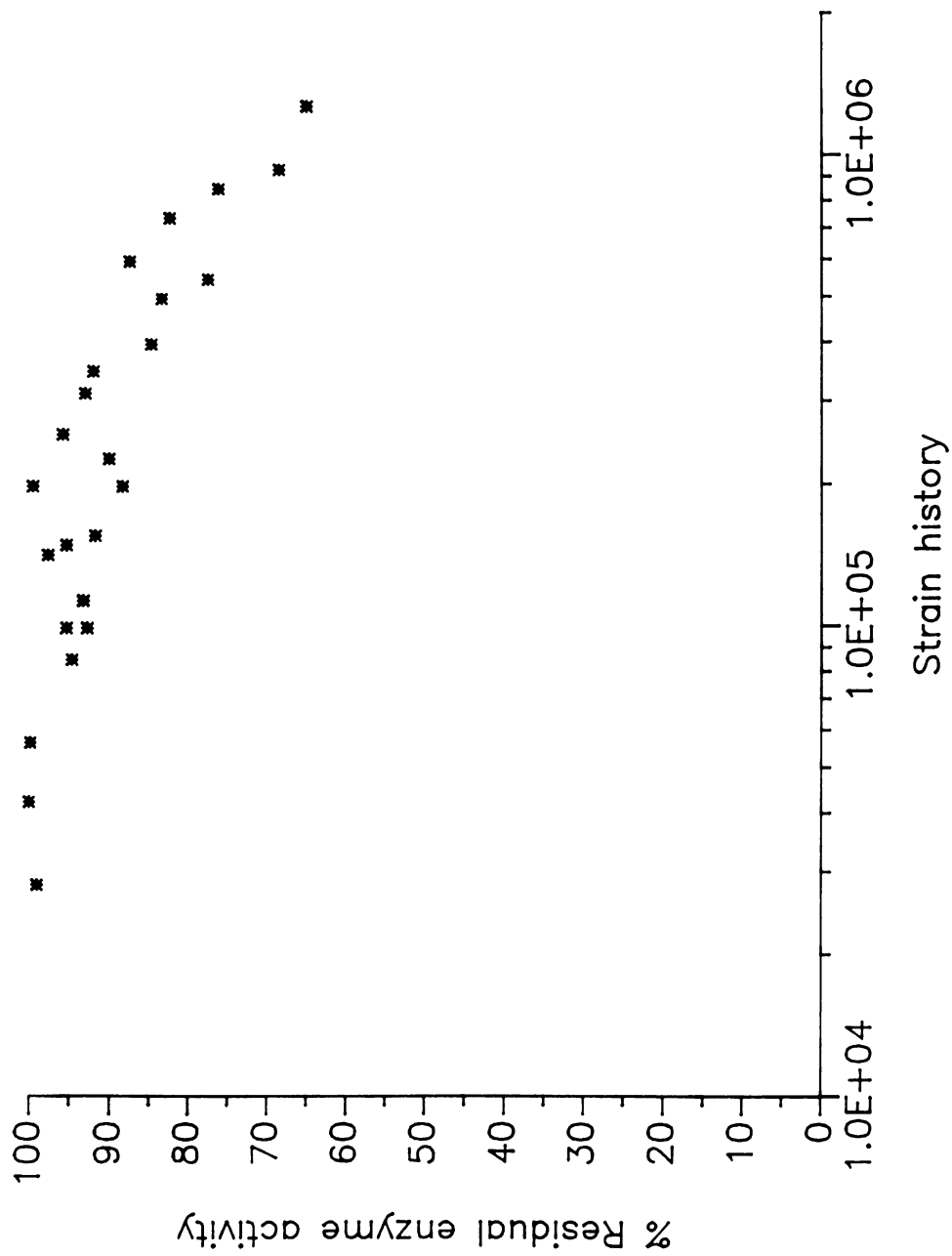


Figure 5.1 Percent residual activity of α -amylase versus strain history (data obtained from a mixer viscometer).

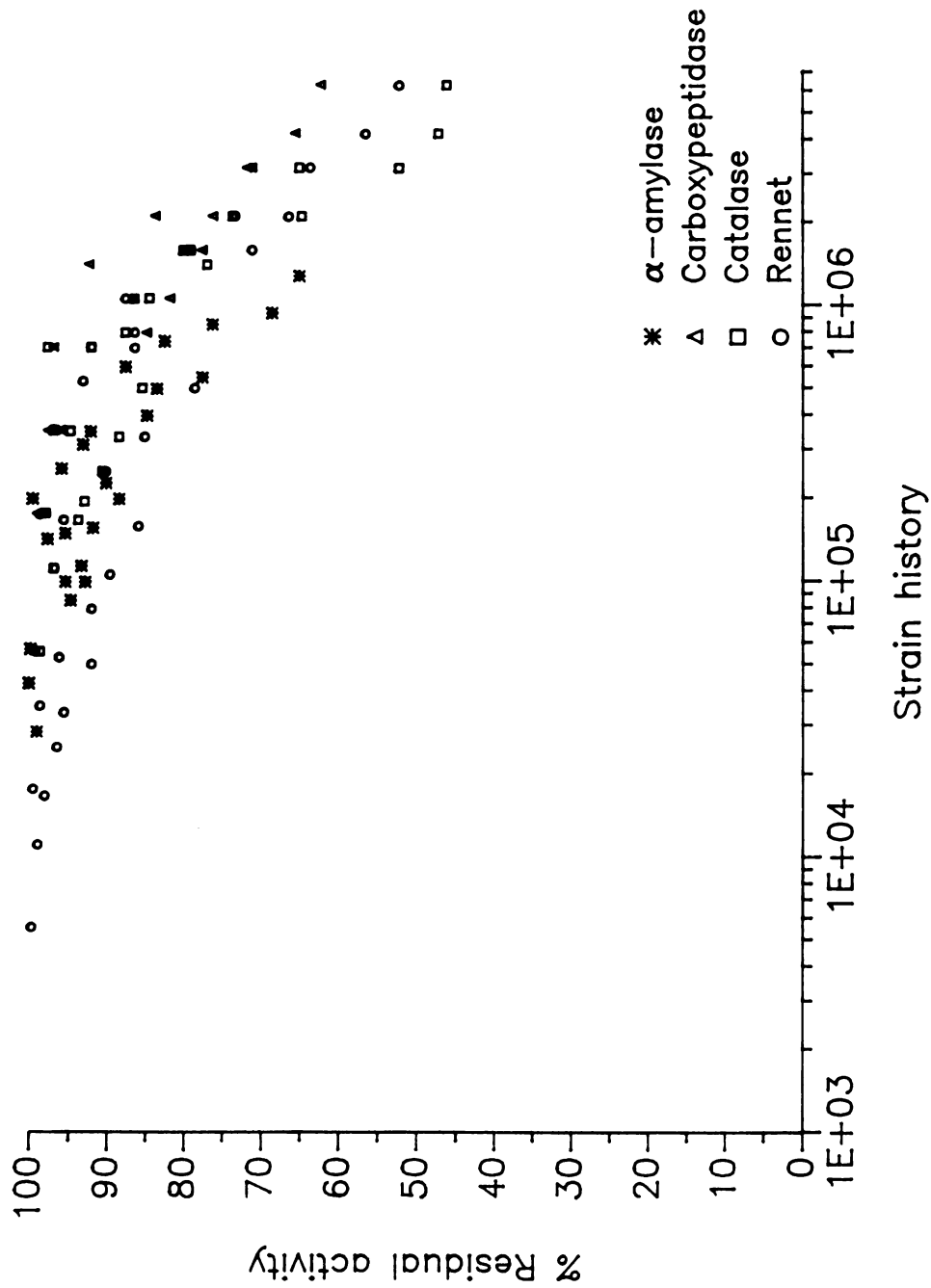


Figure 5.2 Percent residual activity vs. strain history for rennet, catalase, carboxypeptidase (Charm and Wong, 1970) and α -amylase (this study).

5.5.2 Shear deactivation in twin screw extruders

Extrusion data was used to calculate Po for 30% SPS in water. Eq. 5.11 was then used to calculate the corresponding Reynolds numbers (Table 5.3).

The Reynolds numbers and Eqs. 5.6, 5.7 and 5.8 were used to estimate the average shear rates (Table 5.4). The corresponding mean residence time, strain history, SEC, and ratio of mass flow rate to screw rpm ($\frac{\dot{m}}{N}$) and % average residual enzyme activity are also summarized in Table 5.4.

Since SEC and $\frac{\dot{m}}{N}$ were found to be highly correlated ($R^2 = 0.97$) in this study, either parameter may be used in the analysis.

Using the enzyme activity data from extrusion runs (Appendix 3), analysis of variance (Appendix 4) was performed and results showed that none of the three variables (strain history, shear rate or SEC) individually significantly affected the residual enzyme activity, at the 0.05 probability level. Over the range of strain histories in this study, less than a 20% loss in activity was observed. An important reason for this is that the $Po-Re$ relationship was developed for fully-filled screws, and may not be valid for the partially-filled screw application in this study. If used for partially-filled zones, the method would result in over-estimation of the shear rate, leading to strain histories higher than actual.

Cond. no.	RPM	% Torque	Pressure drop, kPa	Avg. Temp (°C)	Mass flow rate, kg/hr	Po	Re
1	60	36.5	1758	27.1	10.0	3.0×10^7	0.06
2	80	36.5	1862	28.6	15.2	1.0×10^7	0.10
3	100	35.5	1896	31.0	14.7	1.0×10^7	0.13
4	150	33.5	1965	34.7	15.1	5.0×10^6	0.22
5	200	29.5	1931	37.3	15.0	3.0×10^6	0.36
6	300	32.5	1896	44.6	24.6	1.0×10^6	0.61
7	400	35.5	1965	51.1	38.7	8.0×10^5	0.90

Run no.	η_a	$\dot{\gamma} \times 10^{-3}$	\bar{t}	$\gamma \times 10^{-7}$	SEC	$\frac{m}{N}$	% Avg. residual activity
1	2.4	30.5	6.6	1.2	0.8	0.167	94.5
2	1.9	40.5	4.2	1.0	0.6	0.190	100.0
3	1.9	38.0	4.0	0.9	0.9	0.147	88.4
4	1.6	40.5	3.8	0.9	1.4	0.101	91.8
5	1.3	47.9	3.7	1.1	1.8	0.075	83.0
6	1.2	45.1	2.2	0.6	1.8	0.085	92.4
7	1.1	42.6	1.5	0.4	1.6	0.097	91.0

Strain is the product of the average shear rate and the mean residence time.

Mohamed (1988) found that the average shear rate in the extruder is a power function of the screw rpm. As screw rpm increased, shear rate increased but residence time decreased. This indirect relationship may mask the effect of strain history on activity. In this study, the estimated shear rates were in a narrow range of 3×10^4 - 5×10^4 , while the corresponding mean residence times were in a relatively broad range of 1.5-6.6 min.

Based on ANOVA results (Appendix 4), each variable was significant at a low probability level of 0.15. If strain history, shear rate and SEC were considered simultaneously, however, results from analysis of variance (Appendix 5) showed that they contributed a significant effect to the reduction of enzyme activity at a probability level of 0.05.

5.6 Conclusions

The effect of shear on the activity of α -amylase was determined in a mixer viscometer and a twin screw extruder. Results from the mixer viscometer showed that loss of enzymatic activity was pronounced at strain histories above 4×10^4 , in agreement with what has been reported for other enzymes in the literature. The loss of enzyme activity in the extruder did not depend significantly on strain history, shear rate or SEC alone at a probability of $P < 0.05$, although each of the three was significant at $P = .15$ and their combined effect was significant at $P < .05$. Among these parameters, the SEC seemed to be the best parameter to describe the effect of shear on enzyme activity because it was quantitatively determined rather than estimated. In this study, only a 20% loss of the original activity was observed. Additional studies of the three variables when a higher loss of activity occurs will help clarify their respective effects.

It is worth noting that the loss of activity due to shear depends on the test system used. In a batch system where the flow field is well defined, the shear rate can be accurately determined. However, it is difficult to obtain it in a complex flow field such as occurs in an extruder. The rheology of the fluid containing the enzyme is also critical, since viscosity plays an important role in the degree of mixing. In a batch system, complete mixing is obtained; however, depending on screw configuration, this may not be necessarily true in the extruder.

Enzymes in the SPS mixture formed a dispersed phase which can be protected from exposure to high shear in the extruder. Therefore, the effect of shear may not be as pronounced as in the batch system. This is in agreement with Thomas and Dunnill (1979) who found that increasing viscosity enhanced the resistance of enzymes.

It is also possible that the enzyme may be undergoing reversible rather than irreversible shear deactivation, making immediate assays on enzyme activity necessary. This is not practical, however, when the recovery time for the enzyme is shorter than the time required by the assay procedure. All these make the effect of shear on enzyme activity in the extruder relatively hard to determine. Another factor that can influence activity loss during shearing is calcium ion, which acts as a co-factor to protect the enzyme from structural deformation.

5.7 Nomenclature

A_w, A_{wi}	Wetted area for one screw type (i refers to each screw in mixed screws), cm^2
D_b	Hydraulic diameter, cm
E_v	Viscous dissipation of mechanical energy, W
k'	Paddle constant for mixer viscometer, dimensionless

K	Consistency coefficient, Pa.s ⁿ
K₀	Consistency coefficient at a reference temperature, Pa.s
<i>m</i>	Mass flow rate, kg/s
n	Flow behavior index, dimensionless
N	Screw speed, rps
Po	Power number, dimensionless
R	Gas constant, cal/mole/K
Re, Re'	Reynolds number, dimensionless
T	Absolute temperature, K
V_w, V_{wi}	Wetted volume for one screw type (i refers to each screw in mixed screws), cm ³

Greek symbols

Δa_i	Redness value for a sample relative to a base color at discrete time t_i
ΔE	Activation energy, cal/mole
ΔP	Pressure drop, Pa
δt	discrete time interval, s
η_a	Non-Newtonian apparent viscosity, Pa.s ⁿ
η_i	Non-Newtonian viscosity index, Pa.s ⁿ
γ	Strain history, dimensionless
$\dot{\gamma}$	Shear rate, s ⁻¹
μ	Newtonian viscosity, Pa.s

ω	Rotational speed of paddle, rad/s
ρ	Fluid density, kg/m ³
τ	Shear stress, Pa

5.8 References

- Bernfeld, P. 1955. Amylases, α and β . *Methods Enzymol.* 1:149.
- Charm, S.E. and Wong, B.L. 1970. Enzyme inactivation with shearing. *Biotech. Bioeng.* 12:1103.
- Charm, S.E. and Lai, C.J. 1971. Comparison of ultrafiltration systems for concentration of biologicals. *Biotech. Bioeng.* 13:185.
- Howkins, M.D. 1987. A predictive model for pressure drop in food extruder dies. M.S. Thesis. Dept. Agr. Engr., Michigan State University.
- Martelli, F.G. 1983. Twin Screw Extruders: A Basic Understanding. Van Nostrand Reinhold Compence, New York.
- Metzner, A.B. and Otto, R.E. 1957. Agitation of non-Newtonian fluids. *AIChE. J.* 3(1):3.
- Mohamed, I.O. 1988. Modeling shear rate and heat transfer in a twin screw co-rotating food extruder. Ph.D Dissertation. Dept. Agr. Engr., Michigan State University.
- Rao, M.A. and Cooley, H.J. 1984. Determination of effective shear rates in rotating viscometers with complex geometry. *J. Texture Studies* 15:327.
- Rauwendaal, C.J. 1981. Analysis and experimental evaluation of twin screw extruders. *Polym. Eng. Sci.* 21(16):1092.
- Saha, B.C., Shen, G.J. and Zeikus, J.G. 1987. Behavior of a novel thermostable β -amylase on raw starch. *Enzyme Microb. Technol.* 9:598.

Steffe, J.F. and Ford, E.W. 1985. Rheological techniques to evaluate the shelf-stability of starch-thickened, strained apricots. J. Texture Studies 16:179.

Thomas, C.R. and Dunnill, P. 1979. Action of shear on enzymes: studies with catalase and urease. Biotech. Bioeng. 21:2279.

Tirrell, M. and Middleman, S. 1975. Shear modification of enzyme kinetics. Biotech. Bioeng. 17:299.

6 EFFECT OF MATERIAL RHEOLOGY ON THE DISPERSION OF FLUIDS IN EXTRUDERS

6.1 Abstract

The effect of rheological properties on dispersion coefficients in a twin screw extruder was investigated, using corn syrup, 7% soy polysaccharide (SPS) in honey and 2.5% methocel in water. Material rheological behavior was characterized by steady shear and dynamic experiments. It was shown that the extruder could be characterized as a tube, with the hydraulic diameter providing a characteristic dimension. Using the Taylor-Aris model, the effective dispersion coefficient was found to be affected more by convective diffusion than molecular diffusion, with the mean velocity exerting the greatest effect on the dispersion of fluids in the extruder. Due to equipment limitations, no reliable relationships could be developed to link viscoelastic behavior, expressed in terms of equilibrium creep compliance, to the degree of dispersion.

6.2 Introduction and Background

In a twin screw extruder, the extrudate is subjected to both shear and elongational forces. Shear flow occurs between the rotating screw and the stationary barrel, while elongational flow occurs in the inter-meshing region. At steady state, elongational flow causes an exponential rate of separation of fluid elements, in comparison to the linear rate caused by shear flow (Bird et al., 1987). Both flows increase the degree of mixing and dispersion.

Mohamed (1988) has recently demonstrated that the average shear rate in a twin screw extruder can be estimated by an empirical correlation between the power number and the Reynolds number. Mohamed (1988) lumped the effects of shear and elongational flows, describing them in terms of an average shear rate.

The degree of mixing and dispersion in the extruder is expected to be influenced by the rheological behavior of the extruded materials. The rheology may be described in terms of the linear viscoelastic behavior of materials, which is characterized by the stress relaxation modulus, $G(t)$, and the creep compliance, $J(t)$. $G(t)$ is the ratio of time-dependent stress to strain at constant deformation, while $J(t)$ is the ratio of time-dependent strain to stress at constant stress. $G(t)$ and $J(t)$ are correlated by:

$$G(t) = \frac{1}{J(t)} \quad (6.1)$$

Instead of using transient experiments to characterize $G(t)$ and $J(t)$, a periodic experiment is commonly used. In the periodic experiment, the fluid undergoes small amplitude sinusoidal oscillatory shear, and the in-phase and out-of-phase components on the stress at steady state are measured as a function of frequency. The experiment at frequency ω is qualitatively equivalent to the transient experiment at time $t = 1/\omega$. The oscillatory data are presented in terms of complex modulus (G^*) and complex viscosity (η^*) by the expressions (Ferry, 1980):

$$G^* = G' + iG'' \quad (6.2)$$

$$\eta^* = \eta' + i\eta'' \quad (6.3)$$

where

$$\eta' = \frac{G''}{\omega} \quad (6.4)$$

and

$$\eta'' = \frac{G'}{\omega} \quad (6.5)$$

The complex modulus is related to the complex creep compliance (J^*) by:

$$J^* = \frac{1}{G^*} \quad (6.6)$$

$G'(\omega)$ is the storage modulus (stress in phase with the strain divided by the strain), and measures the elastic energy stored. Its magnitude is related to the conformation and rearrangement of the material during oscillatory deformation. At $t = 1/\omega$, $G(t)$ is approximately equivalent to $G'(\omega)$. $G''(\omega)$ is the loss modulus (stress 90° out of phase with the strain divided by the strain), and measures energy dissipated or lost.

Since the frequency is equal to the shear rate, the Cox-Merz rule (Bird et al. 1987) is valid, and the complex viscosity (η^*) and the steady shear viscosity (η) are equivalent. This rule produces accurate results, especially at low frequencies where the dynamic viscosity (η') is much larger than the imaginary part of the complex viscosity (η''). Therefore, η' is approximately equal to η^* and also equal to the zero shear viscosity (η_0). $J'(\omega)$ is the storage creep compliance; its value approaches the equilibrium creep compliance (J_e^0) at low frequency.

Viscoelastic properties depend on molecular weight, molecular weight distribution, temperature, concentration and chemical structure, among other variables (Ferry, 1980). Zero shear viscosity and equilibrium creep compliance are used to characterize the terminal zone behavior of the material during extrusion (Ferry, 1980). In the terminal zone where the material has been sheared for a long period of time, the viscoelastic properties are pronounced.

The zero shear viscosity is a measure of the energy consumed in the flow while the equilibrium creep compliance is a measure of the energy stored during the flow. The zero shear viscosity is relatively temperature dependent, but the equilibrium creep compliance is not. Both are expected to play an important role in dispersion during extrusion. The zero shear viscosity and equilibrium creep compliance can be calculated by (Graessley, 1984):

$$\eta_0 = \lim_{\omega \rightarrow 0} \eta^* = \lim_{\omega \rightarrow 0} \eta' \quad (6.7)$$

$$J_c^0 = \frac{1}{\eta_0^2} \lim_{\omega \rightarrow 0} \frac{G''(\omega)}{\omega^2} \quad (6.8)$$

6.2.1 Diffusion and Dispersion

Diffusion is a slow process, caused by a concentration gradient. On the other hand, dispersion is a fast process, caused by micromolecular diffusion and convective flow (Cussler, 1984). Dispersion and diffusion are, however, described by similar mathematical expressions. The dispersion coefficient is not highly dependent on molecular weight or structure but strongly dependent on position and flow direction (Cussler, 1984).

In laminar flow, a one-dimensional dispersion model is commonly used. The model is a modification of the plug flow model, which incorporates a dispersion coefficient (D_d) to describe the overall effect of different phenomena in the system. Taylor (1953) observed that the residence time distribution for laminar flow through a tube is influenced by the velocity profile as well as molecular diffusion, as depicted in Figure 6.1. At moderate flow velocities, the dispersion of a tracer occurs by axial and

radial diffusion from the flow front via a molecular diffusion mechanism (Taylor, 1953); however, axial diffusion is small compared to axial convective flow. Therefore, dispersion leads to two-dimensional flow, expressed by (Butt, 1980):

$$\frac{\partial C}{\partial t} = D_m \left(\frac{\partial^2 C}{\partial r^2} + \frac{1}{r} \frac{\partial C}{\partial r} \right) - u(r) \frac{\partial C}{\partial z} \quad (6.9)$$

where D_m is the molecular diffusion coefficient for the tracer, and $u(r)$ is the laminar flow velocity profile.

For one-dimensional flow, Eq. 6.9 may be simplified to (Butt, 1980):

$$\frac{\partial C_m}{\partial t} = D_e \frac{\partial^2 C_m}{\partial z^2} - \bar{u} \frac{\partial C_m}{\partial z} \quad (6.10)$$

where C_m is a mean concentration, \bar{u} is the average axial velocity and D_e is an effective dispersion coefficient, defined as:

$$D_e = \frac{R^2 \bar{u}^2}{48 D_m} \quad (6.11)$$

where R is the radius of the tube.

The expression in Eq. 6.11 indicates that the dispersion coefficient decreases with increased radial molecular diffusion. If the radial molecular diffusion is large, material in the center diffuses outward while the material near the tube walls diffuse inward, inhibiting dispersion (Cussler, 1984).

Eq. 6.9 is valid only if (Taylor, 1954):

$$\frac{4L}{R} \gg \frac{\bar{u}R}{D_m} \gg 6.9 \quad (6.12)$$

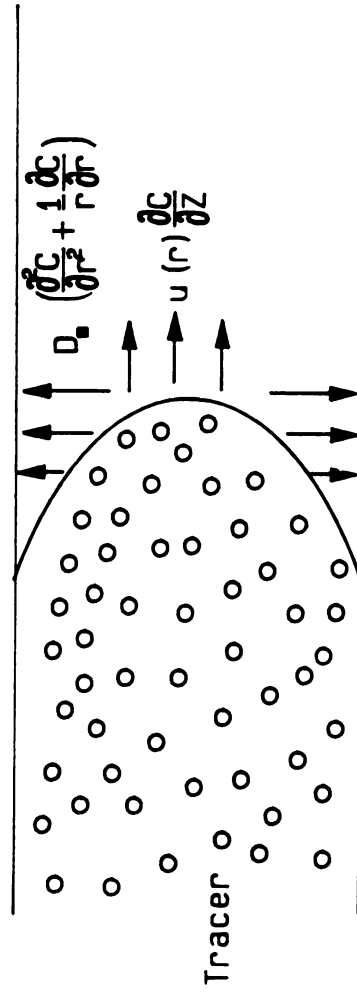


Figure 6.1 Contribution of convective transfer and molecular diffusion to dispersion in laminar flow (Butt, 1980).

where $\frac{\bar{u}R}{D_m}$ is a radial Peclet number. However, Ananthakrishnan et al. (1965) proposed that the radial Peclet number should be larger than 50 for application of the one-dimensional dispersion model. In practice, axial molecular diffusion is neglected when the radial Peclet number is equal to or larger than 100 (Subramanian and Gill, 1976).

The dispersion coefficient in Eq. 6.11 was modified by Aris (1956) to provide a generalized expression valid for all velocity profiles in flow vessels of any geometry, regardless of the value of the radial Peclet number. In terms of the tube diameter (d), the expression is:

$$D_e = D_m + \frac{d^2 \overline{u^2}}{192 D_m} \quad (6.13)$$

Ananthakrishnan et al. (1965) demonstrated that the Taylor-Aris dispersion model applies to Newtonian fluids at steady state only, or for values of the dimensionless time parameter τ ($D_m t/R^2$) ranging from 0.8 at $Pe=500$ to 20 at $Pe=1$. Later, unsteady-state convection-diffusion in Newtonian fluids at small values of τ was analyzed by Gill (1967), and Gill and Sankarasubramanian (1970, 1971). Gill and Sankarasubramanian (1971), and Sankarasubramanian and Gill (1972, 1973) subsequently developed a generalized dispersion model applicable to many flow problems.

Booras and Krantz (1976) applied the generalized dispersion model of Gill and co-workers to describe the effect of the velocity profile on dispersion in power law fluids. They reported that at small dimensionless times, the generalized dispersion coefficient for all power law fluids ($0.25 < n < 2.0$) were identical. As the dimensionless time increased, the dispersion coefficient increased at the same rate towards an asymptotic value. They showed that the asymptotic dispersion coefficient decreased with decreased flow

behavior index (n), in agreement with the results of Subramanian and Gill (1976). The result was due to the flatter velocity profiles of pseudoplastic fluids, which tended to decrease axial dispersion.

The effect of molecular diffusion on dispersion of non-Newtonian fluids is significant (Booras and Krantz, 1976). For large Peclet numbers, the Taylor-Aris model can be used for non-Newtonian fluids at dimensionless times above 0.60 (Booras and Krantz, 1976).

The objective of this study was to determine the effect of rheological behavior on the dispersion of fluids during extrusion, using the dispersion coefficient as a characteristic indicator of dispersion.

6.3 Theoretical Development

An expression for the dispersion coefficient was developed on the basis of the Taylor-Aris model (Eq. 6.13). The model was modified by incorporating the following rheological properties: apparent viscosity (η), consistency coefficient (K) and flow behavior index (n).

The molecular diffusion coefficient (D_m) of a solution is expressed as a function of temperature and viscosity via an empirical correlation, developed on the basis of the Stokes-Einstein equation. The correlation is applied to a dilute solution, containing large spherical solutes (A) in small molecules of solvent (B). The empirical correlation can be expressed (Geankoplis, 1983) as:

$$D_{AB} = \frac{9.96 \times 10^{-16} T}{\mu V_A^{0.333}} \quad (6.14)$$

For an isothermal system at temperature T_o , the molecular diffusion coefficient is a function of the inverse of the viscosity of the solution only; therefore Eq. 6.14 may be rewritten as:

$$D_{AB} = \frac{k}{\mu} \quad (6.15)$$

where k is a constant defined by:

$$k = \frac{9.96 \times 10^{-16} T_o}{V_A^{0.333}} \quad (6.16)$$

This correlation may be used for a power law fluid by replacing the Newtonian viscosity (μ) by the apparent viscosity (η), given by:

$$\eta = K \dot{\gamma}^{n-1} \quad (6.17)$$

Incorporating Eqs. 6.15 and 6.17, Eq. 6.13 becomes:

$$D_e = \left(\frac{k}{K \dot{\gamma}^{n-1}} \right) + \left(\frac{d^2 \bar{u}^2}{192} \right) \left(\frac{K \dot{\gamma}^{n-1}}{k} \right) \quad (6.18)$$

The mean velocity (\bar{u}) of a power law fluid can be calculated by (Bird et al., 1960):

$$\bar{u} = \left(\frac{\tau_w}{K} \right)^{\frac{1}{n}} \frac{nR}{1+3n} \quad (6.19)$$

Substituting Eq. 6.19 into Eq. 6.18, the dispersion coefficient can be expressed as a function of K and n , both measurable rheological properties of the fluid.

The geometry of an extruder is more complex than that of a tube. However, to provide simplicity, the hydraulic diameter may be used to characterize the extruder as an equivalent tube. If the configuration consists of more than one screw in the fully filled zone, the average hydraulic diameter of the screw combination may be calculated by:

$$d_h = \frac{4 \sum_i^p V_{wi}}{\sum_i^p A_{wi}} \quad (6.20)$$

The equivalent length of the configuration in terms of the above characterization may then be calculated by:

$$L_e = \sum_i^p \frac{V_{wi}}{A_{ci}} \quad (6.22)$$

The mean velocity in the extruder then becomes:

$$\bar{u} = \frac{L_e}{\bar{t}_c} \quad (6.22)$$

An average shear rate in the extruder can be calculated on the basis of a power number versus Reynolds number relationship (the development is given in Chapter 7) and is expressed as:

$$Po = 9.12 \times 10^3 Re^{-1.26} \quad (6.23)$$

where

$$Po = \frac{E_v}{\rho N^3 d_h^5} \quad (6.24)$$

and

$$Re = \frac{d_h^2 N \rho}{\eta} \quad (6.25)$$

The dispersion coefficient for an extrusion process can be estimated from Eq. 6.18 by appropriate substitution of d_h , $\dot{\gamma}$ and \bar{u} , all of which are obtained from experiment. Also, the molecular diffusion coefficient (D_m) can be calculated by Eq. 6.13. if D_e is known.

6.4 Materials and Methods

The effect of rheology on dispersion in an MPF-50D Baker-Perkins twin screw extruder was investigated using corn syrup (type C, Cleveland Syrup, OH), 2.5% (w/w) Methocel (K4M, Dow Corning, MI) and a mixture of 7% (w/w) soy polysaccharide (SPS) (Fibrim 2000 soy fiber, Ralston Purina, MO) in honey. The extruder was operated at 15 L/D, using a combination of feed screws (FS), single lead (SL) screws and 90° forwarding paddles (90 F). The schematic of the extruder setup is shown in Figure 6.2. Two circular full flange dies, 3.2 mm in diameter and 25.4 mm in length, were used. The barrel temperature was maintained at 10°C with chilled water. The material was fed at a fixed rate of 10 kg/hr. The extruder was operated at screw speeds of 100 and 150 rpm, with fully-filled screws. The methocel solution could not be run at 100 rpm because it tended to back up toward the feed port and entrap air bubbles.

RTD measurements were performed when steady state conditions were reached. A tracer ball containing 0.1-0.2 ml of 4% erythrosine and 0.2-0.3 g of the feed material was dropped in the feed port. The extrudate was collected when a slight color was observed and continued at intervals of 15 s until the tracer color was no longer visible. The intensity of dye in each extrudate was measured using a CR-200 Chroma Meter (Minolta Camera Co., Japan) against a base extrudate. The mean residence time and variance were then calculated by using the first and second moment formulations. The results were used to estimate the dispersion number and dispersion coefficient.

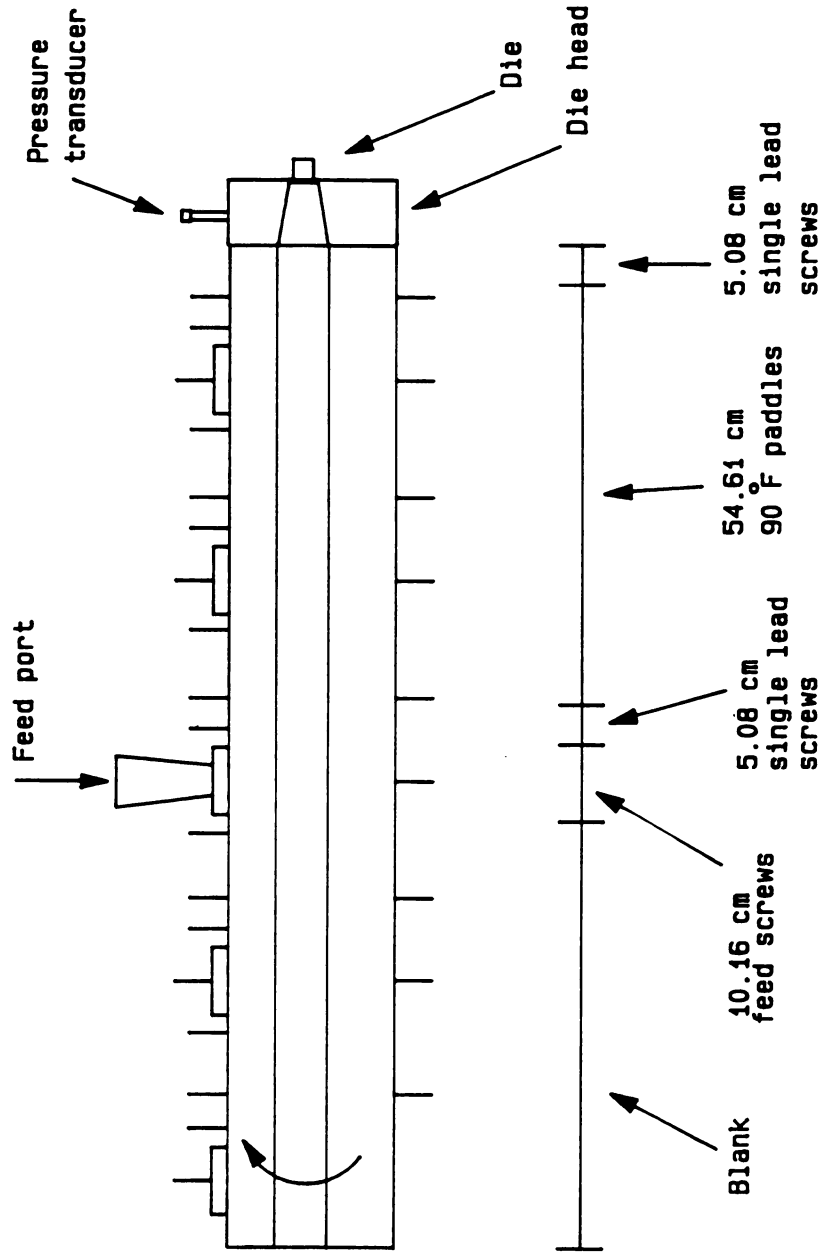


Figure 6.2 Schematic of the setup of the MPF-500 Baker-Perkins twin screw extruder at 15 L/D.

6.4.1 Rheological behavior

The rheological behavior of corn syrup, 7% SPS in honey and 2.5 % methocel were characterized by steady shear and dynamic experiments. The steady shear experiments were carried out in a Haake concentric cylinder viscometer; the dynamic experiments were done in a Rheometric Fluids Spectrometer. Steady shear data were collected via a computer interface with the VI sensor of the Haake RV-12 system. The experiments were conducted at temperatures of 20-50°C within as wide a shear rate range as possible.

The dynamic experiments were done on the Rheometric Fluids Spectrometer in oscillatory mode, using a disk-plate system. The disk was 25 mm in diameter, and was set at a gap of 1.0-1.4 mm. All experiments were performed at a fixed strain rate of 1%, in a frequency range of 0.1 to 100 rad/s. The viscoelastic properties of the fluids were recorded, using the RECAP2 software via a computer interface. For each fluid, two replicates were performed at or near room temperature.

All samples were withdrawn from the same batch used for extrusion runs.

6.5 Results and Discussion

6.5.1 Rheological data

Results from the steady shear experiments are presented in Table 6.1. As expected, the corn syrup was found to be Newtonian, while 2.5% methocel in water and 7% SPS in honey were non-Newtonian fluids.

Table 6.1. Rheological models of the fluids used, derived from steady shear experiments.		
Fluid	Test condition	Rheological model
Corn syrup	T range: 23-65°C $\dot{\gamma}$ range: 0-270 s ⁻¹	$\tau = \mu \dot{\gamma}$ where $\mu = 2.73 \times 10^{-14} \exp\left(\frac{10480}{T}\right)$
7% SPS in honey	T range: 40-80°C $\dot{\gamma}$ range: 0-180 s ⁻¹	$\tau = \eta \dot{\gamma}^{0.416}$ where $\eta = 5.92 \times 10^{-14} \exp\left(\frac{3978}{T}\right)$
2.5% Methocel	T range: 23-35°C $\dot{\gamma}$ range: 0-240 s ⁻¹	$\tau = \eta \dot{\gamma}^{0.30}$ where $\eta = 5.14 \exp\left(\frac{866}{T}\right)$

Results from oscillatory tests are shown in Figure 6.3 for corn syrup, Figure 6.4 for 7% SPS in honey and Figure 6.5 for 2.5% methocel in water. The curves of G^* , G' , G'' and η^* were different for each material. Since corn syrup is a pure liquid, G'' dominated and its complex viscosity was frequency-independent and was constant (100 Pa.s) at 23.4°C. The slope of the G'' curve was unity, indicating Newtonian behavior. The G' of corn syrup was zero at low frequencies and generally increased with increased frequency, although this increase was inconsistent. There is no clear explanation for the shape of the G' curve. Theoretically, G' should be zero for Newtonian fluids. While this is not the case, the contribution of G' to G^* was small.

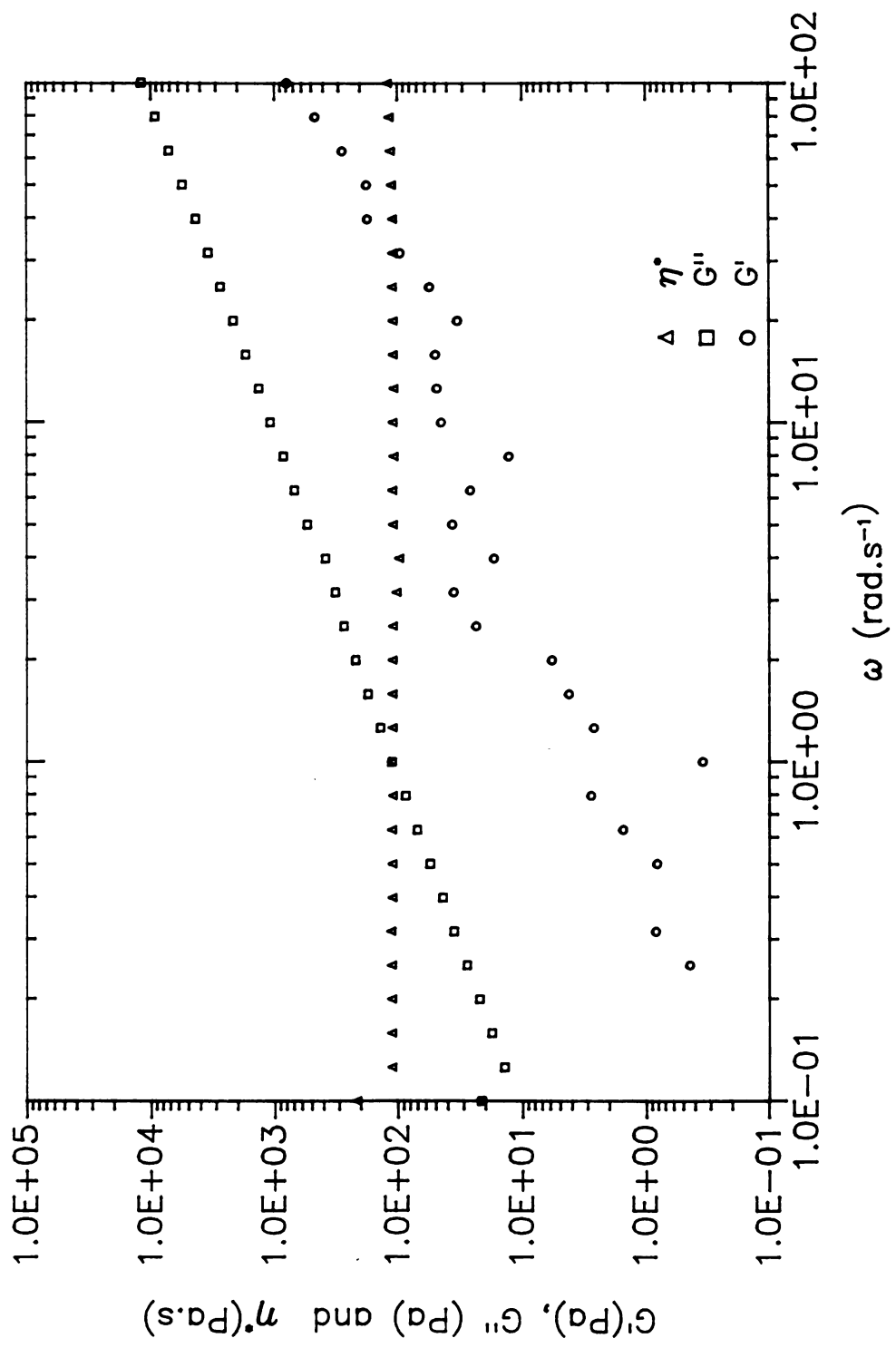


Figure 6.3 Storage modulus (G'), loss modulus (G'') and complex viscosity (η^*) versus frequency (ω) for corn syrup at 23.4° C.

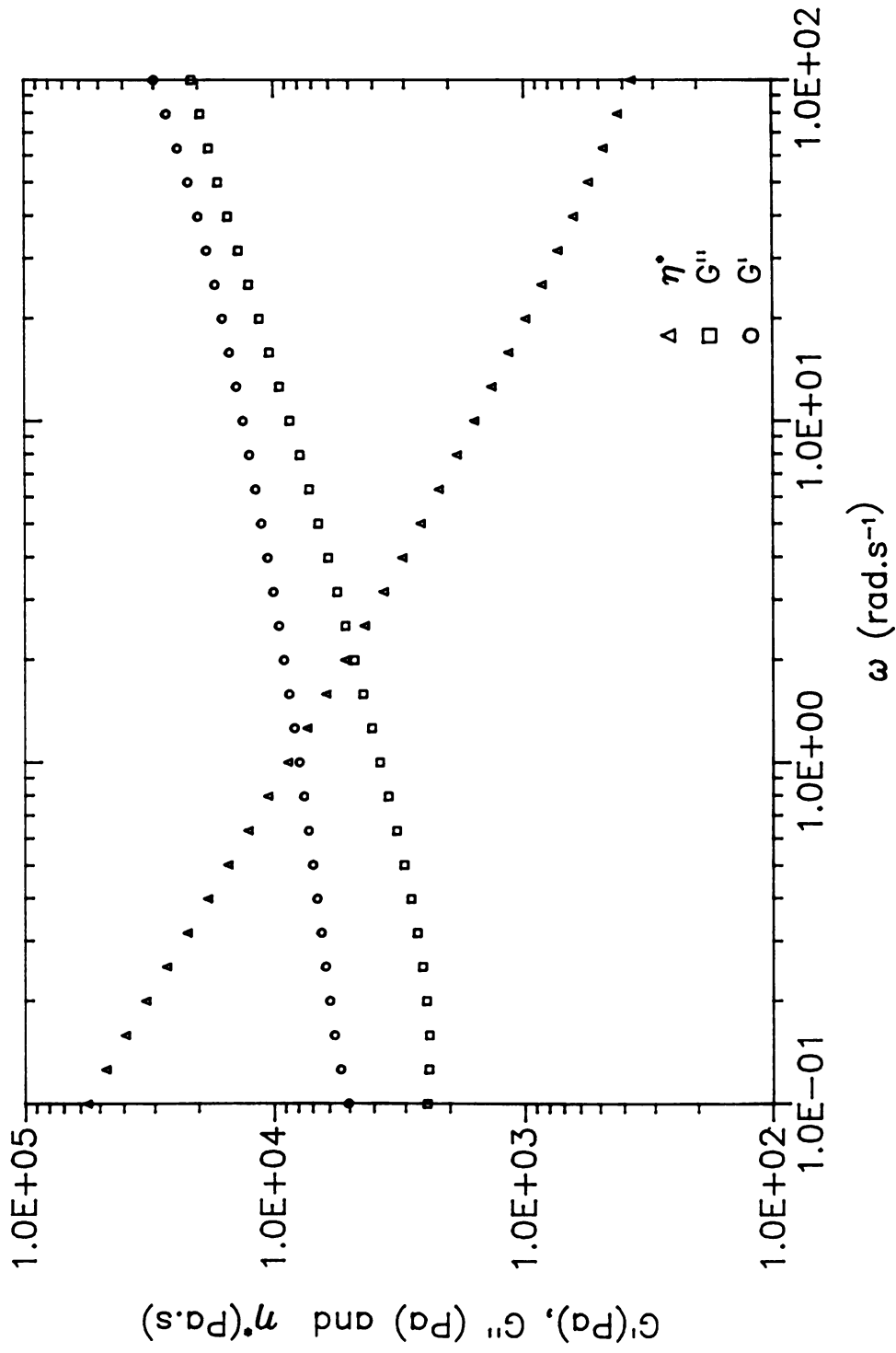


Figure 6.4 Storage modulus (G'), loss modulus (G'') and complex viscosity (η^*) versus frequency (ω) for 7% SPS in honey at 24.6°C.

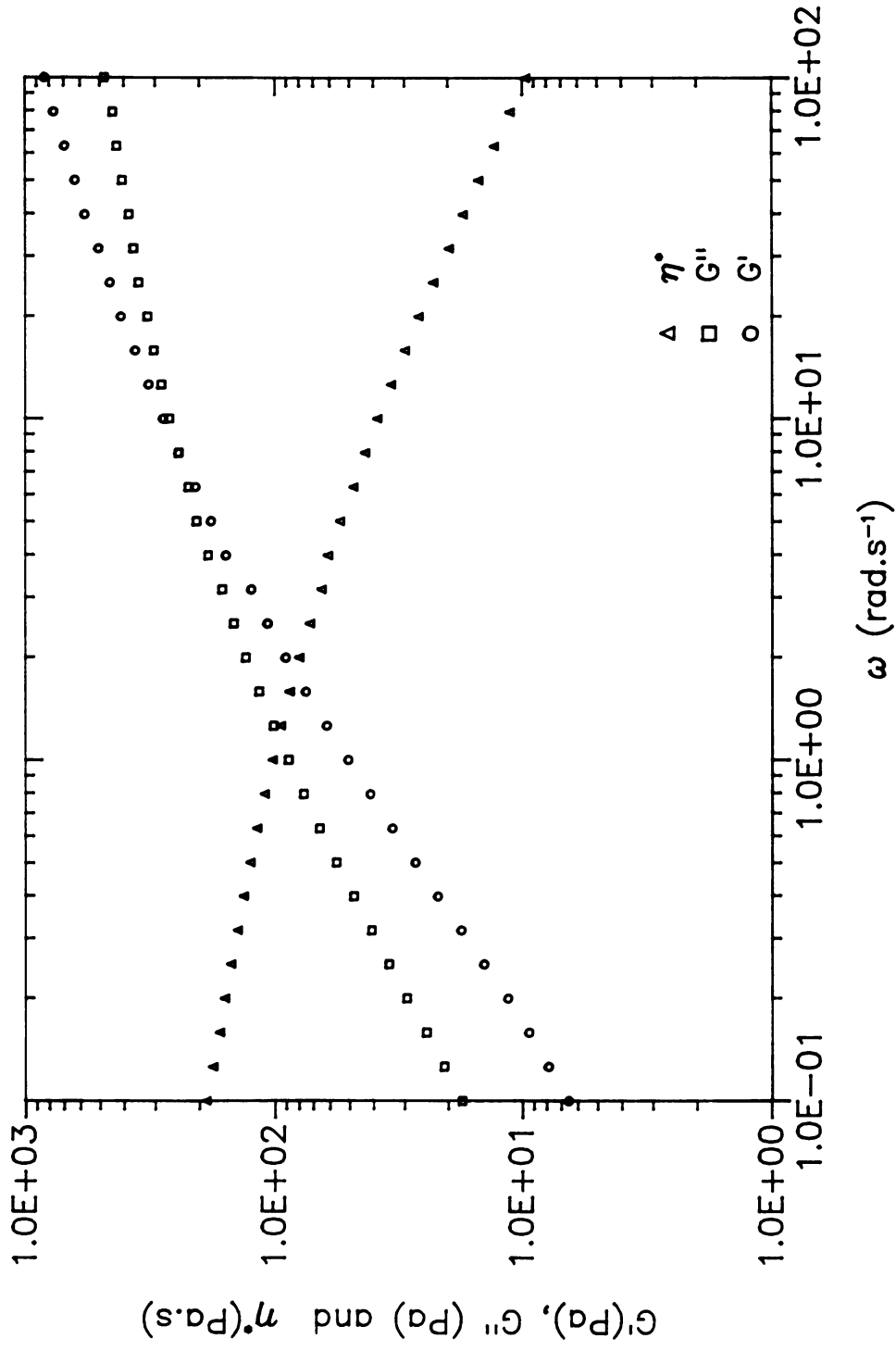


Figure 6.5 Storage modulus (G'), loss modulus (G'') and complex viscosity (η^*) versus frequency (ω) for 2.5% Methocel at 22.8° C.

On the other hand, the SPS-honey and methocel mixtures exhibited purely viscoelastic properties. For the SPS-honey mixture, G' was greater than G'' in the range of frequencies studied, indicating elastic behavior in the transition or rubbery state. However, the terminal state of the SPS-honey mixture could not be determined because the fluids spectrometer could not be operated at frequencies lower than 0.01. Increasing the temperature up to 50°C did not significantly change the viscoelastic data. No experiments were conducted above 50°C.

In contrast to the SPS-honey mixture, methocel behaved as a viscous liquid at low frequencies: G'' was larger than G' . The complex viscosity decreased with increased frequency, exhibiting shear thinning behavior.

Zero shear viscosity (η_0) and equilibrium creep compliance (J_e^0) of corn syrup, SPS-honey and methocel were determined by Eqs. 6.7 and 6.8. For the SPS-honey mixture, the values could not be obtained because no data was available at frequencies below 0.1 rad/s. For purposes of comparison, however, η_0 and J_e^0 were calculated at 0.1 rad/s (reference frequency) for all three materials (Table 6.2).

J_e^0 is a measure of the energy stored in the molecules during flow. The smaller the value, the higher the energy stored and recovered. The more elastic the fluid, the less molecular rearrangements or molecular deformation occurs during flow, and possibly the smaller the degree of mixing or dispersion. Among the three fluids, methocel produced the greatest dispersion.

Table 6.2. Zero shear viscosity and equilibrium creep compliance of corn syrup, 7% SPS in honey and 2.5% methocel in water.

Material	Temperature, C	Reference frequency, rad/s	η_0 , Pa.s	J_e^0 , Pa ⁻¹
Corn syrup	23.4	.1	100	.0
7% SPS in honey	24.6	.1	5.5×10^4	.00016
2.5% methocel	22.8	.1	170	.021

6.5.2 Extrusion data

Using extrusion data (Appendix 6), Eqs. 6.23-6.25 and the rheological models of the fluids in Table 6.1, the average shear rates were calculated (Table 6.3). It is clear from the Reynolds numbers in this table that the flow was laminar. Since the viscosity of a Newtonian fluid is shear-independent, the average shear rate in the extruder could not be estimated for corn syrup.

Using RTD data, the dispersion number, mean velocity and dispersion coefficient were calculated (Table 6.4). The dispersion coefficient of corn syrup ($n = 1$) was larger than that of SPS-honey ($n = 0.416$). This is in agreement with the results of Booras and Krantz (1976), and Subramanian and Gill (1976): the dispersion coefficient of the Newtonian fluid is larger than that of the non-Newtonian fluid, due to differences in the velocity profiles (Figure 6.6). However, the dispersion of methocel ($n = 0.3$) was larger than that of corn syrup, contradicting what was expected. It is clear, therefore, that factors other than the flow behavior index (n) may also be involved. Eqs. 6.18 shows that the dispersion coefficient depends on rheological behavior (K and n), shear rate and the mean velocity, all of which are related in a complex fashion. Therefore, the effect of each factor is not easy to isolate.

Table 6.3. Apparent viscosity and estimated average shear rate of corn syrup, 7% SPS in honey and 2.5% methocel, at various extrusion conditions.

Material	RPM	Feed rate (kg/hr)	Avg. temp., C (s.v.)	Mass density, g/ml	Re	η , Pa.s	$\dot{\gamma}_a$, s ⁻¹
Corn syrup	100	9.4	23.5(0.8)	1.41	.0031	72.7	NA
			22.1(0.9)		.0029	76.5	
	150	9.6	23.2(1.1)	1.41	.0053	63.4	NA
					.0053	63.3	
7% SPS, 93%honey	100	9.2	26.6(0.9)	1.24	.0027	74.0	19.9
			23.7(0.6)		.0027	74.0	19.9
	150	9.6	24.0(0.7)	1.24	.0049	60.0	24.7
			23.8(2.0)		.0049	60.0	24.7
2.5% Methocel	150	8.4	18.3(0.7)	1.10	.0081	32.2	5.1
		9.2	22.3(0.4)		.0081	32.1	4.8

NA = Not applicable

Table 6.4. Dispersion number, dispersion coefficient and molecular diffusion coefficient of corn syrup, 7% SPS in honey and 2.5% methocel.

Material	RPM	\bar{t} (min)	σ^2 , min ²	$\frac{D_e}{\bar{u}L}$	\bar{u} , cm/s	D_e , cm ² /s	$D_m \times 10^4$, cm ² /s
Corn syrup	100	11.6	5.34	.0202	2.22	69.3	3.6
		11.7	5.59	.0207	2.19	70.2	3.4
	150	11.4	5.42	.0212	2.26	73.9	3.5
		11.4	5.44	.0213	2.26	74.3	3.4
7% SPS, 93%honey	100	13.6	6.41	.0176	1.89	51.3	5.1
		12.6	4.52	.0144	2.04	45.2	4.0
	150	11.4	4.00	.0156	2.26	54.2	3.2
		11.2	3.79	.0174	2.19	59.0	4.9
2.5% Methocel	150	9.7	4.09	.0222	2.65	91.0	3.9
		8.7	2.68	.0180	2.96	82.0	5.3

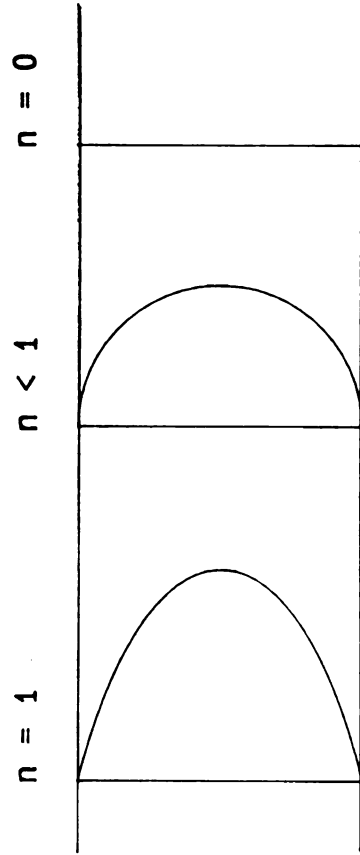


Figure 6.6 Velocity profile in laminar tube flow of a Newtonian fluid ($n=1$), non-Newtonian fluid ($n<1$), and in plug flow ($n=0$).

Using Eq. 6.13, the effect of d_h , D_m and \bar{u} on dispersion coefficient can be easily determined. For a constant hydraulic diameter, the effect of velocity and the molecular diffusion coefficient on the dispersion coefficient is plotted in Figure 6.7. It is apparent that velocity is the dominant variable, causing a large change in the dispersion coefficient in comparison to the molecular diffusion coefficient. Clearly, the dispersion of methocel was larger than that of corn syrup because the average velocity of the methocel was large. If the mean velocity could be maintained constant for all fluids, the dispersion of methocel would be smallest. The effect of viscosity on the molecular diffusion coefficient (Eq. 6.15) appeared to be insignificant.

Having obtained D_e from Eq. 6.18, the molecular diffusion coefficient (D_m) was calculated from Eq. 6.13, using a hydraulic diameter of 0.98 cm for mixed screws (Table 6.4). Since Eq. 6.13 is quadratic, two values of D_m were obtained. The smaller value was chosen, based on physical considerations. On the basis of these results, the Taylor model (Eq. 6.11) which ignores axial molecular diffusion could be used with resulting errors of less than 1%.

The axial and radial Peclet numbers, and dimensionless time were calculated and are summarized in Table 6.5. Axial Peclet number is in a range of 45-69. The radial Peclet numbers were larger than 1000, therefore, the one-dimensional dispersion model can be used. The dimensionless times were in a range of 0.94-1.36; therefore, the Taylor-Aris dispersion model is applicable.

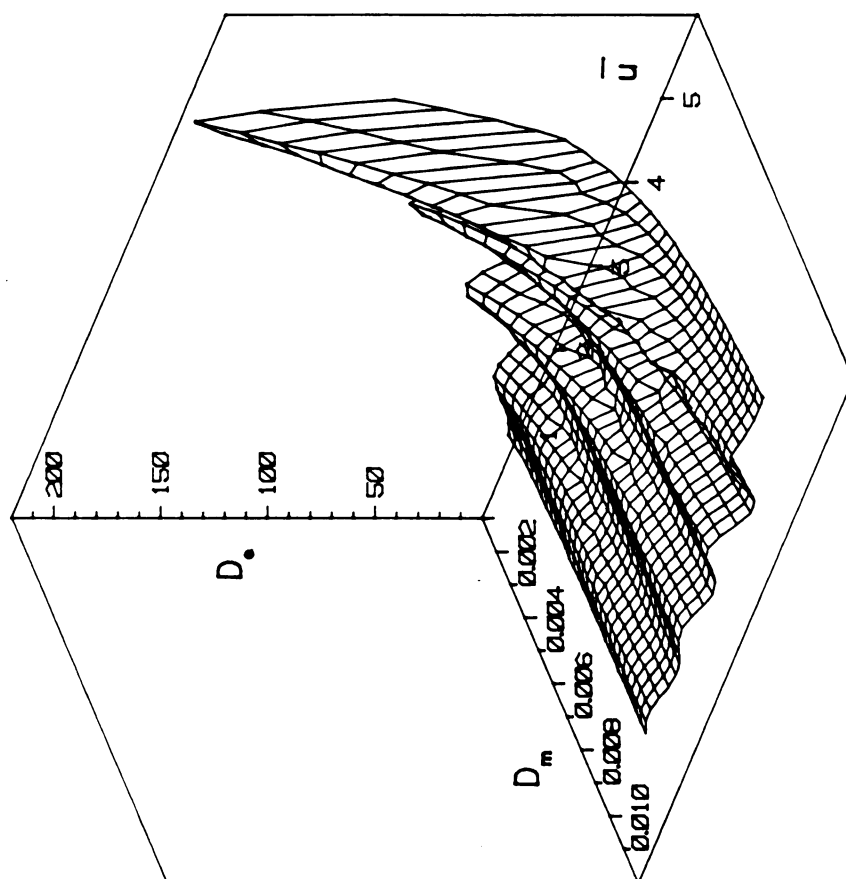


Figure 6.7 Dispersion coefficient (D_d) versus mean velocity (\bar{u}) and molecular diffusion coefficient (D_m) (based on Eq. 6.13).

Table 6.5. Axial and radial Peclet number, and dimensionless time of corn syrup, 7% SPS in honey and 2.5% methocel.

Material	RPM	$\frac{\bar{u}L_e}{D_e}$	$\frac{\bar{u}R_h}{D_m}$	$\frac{D_m t}{R_h^2}$
Corn syrup	100	49.5	3056	1.03
		48.3	3138	1.00
	150	47.2	3200	0.99
		46.9	3219	0.98
7% SPS in honey	100	56.8	1819	1.73
		69.4	2518	1.25
	150	64.1	3516	0.90
		57.5	2208	1.36
2.5% methocel	150	45.1	3364	0.94
		55.6	2737	1.15

6.6 Conclusions

The effect of rheology on the dispersion coefficient was investigated using corn syrup, 7% SPS in honey and 2.5% methocel in water. The rheological behavior of the fluids was characterized by steady shear and dynamic experiments. Corn syrup was confirmed to be Newtonian, while SPS-honey ($n = 0.416$) and methocel ($n = 0.3$) were non-Newtonian. The dispersion coefficient of corn syrup was found to be higher than that of SPS-honey. This is in general agreement with results from laminar tube flow, where the effect of velocity profiles on dispersion is more pronounced with Newtonian fluids than with non-Newtonian fluids. Contrary to expectation, methocel produced more dispersion than corn syrup.

The results showed that the extruder may be characterized as a tube if an appropriate hydraulic diameter is used. The effect of rheological behavior on the dispersion coefficient can be described by the Taylor-Aris model, as supported by the

experimental results of this study. Viscoelastic properties in terms of the equilibrium creep compliance may be related to the dispersion of non-Newtonian fluids: the higher the equilibrium creep compliance, the greater the dispersion. However, additional study is required to verify this relationship.

6.7 Nomenclature

A	Solute molecule
A_{ci}	Cross-sectional area of screw type i, treated as a circular tube, cm^2
A_{wi}	Wetted area of screw i, cm^2
B	Solvent molecule
C	Concentration of tracer, g/l
D_e	Effective dispersion coefficient, cm^2/s
D_m	Molecular diffusion coefficient, cm^2/s
D_{AB}	Mass diffusion of solute A in solvent B, m^2/s
d	Tube diameter, cm
d_h	Hydraulic diameter of extruder, cm
G	Transient relaxation modulus, Pa
G^*	Complex modulus, Pa
G'	Storage modulus, Pa
G''	Loss modulus, Pa
J	Transient creep compliance, Pa^{-1}
J^*	Complex creep compliance, Pa^{-1}
k	Constant for a given solution under isothermal conditions

K	Consistency coefficient, Pa.s ⁿ
L_e	Equivalent length of the extruder, cm
n	Flow behavior index, dimensionless
p	Number of screw types
R	Tube radius, cm
R_h	Hydraulic radius, cm
T	Temperature, K
T_0	Isothermal temperature, K
t	time, s
\bar{t}	Residence time, s
$u(r)$	Velocity at any r , cm/s
\bar{u}	Mean velocity in the tube or extruder, cm/s
V_{wi}	Wetted volume of screw type i , cm ³
V_A	Molar volume of solute A at boiling point, m ³ /kg mole
z	Axial length, cm

Greek symbols

δ	Phase angle between stress and strain, radian
η	Apparent viscosity, Pa.s
η_0	Zero shear viscosity, Pa.s
η'	Dynamic viscosity, Pa.s
η''	Imaginary part of complex viscosity, Pa.s
η^*	Complex viscosity, Pa.s
$\dot{\gamma}$	Steady shear rate, s ⁻¹

ω	Frequency, rad/s
ρ	Mass density, g/ml
τ	Dimensionless time
τ_w	Wall shear stress, Pa

6.8 References

- Ananthkrishnan, V., Gill, W.N. and Barduhn, A.J. 1965. Laminar dispersion in capillaries: Part 1. Mathematical analysis. *AICHE J.* 11:1063.
- Aris, R. 1956. On the dispersion of a solute in a fluid flowing through a tube. *Proceed. Roy. Soc. London, Series A.* 235:67.
- Bird, R.B., Armstrong, R.C. and Hassager, O. 1987. Dynamics of Polymeric Liquids. Wiley Interscience. New York.
- Bird, R.B., Stewart, W.E., and Lightfoot, E.N. 1960. Transport Phenomena. John Wiley & Sons. New York.
- Booras, G.S. and Krantz, W.B. 1976. Dispersion in the laminar flow of power-law fluids through straight tubes. *Ind. Eng. Chem. Fundam.* 15(4):249.
- Butt, J.B. 1980. Reaction Kinetics and Reactor Design. Prentice-Hall, New Jersey.
- Cussler, E.L. 1984. Diffusion: mass transfer in fluid systems. Cambridge University Press. New York.
- Ferry, J.D. 1980. Viscoelastic Properties of Polymers. 3rd ed. Wiley Interscience. New York.
- Geankoplis, C.J. 1983. Transport Processes and Unit Operations. 2nd ed. Allyn and Bacon, Boston.

- Gill, W.N. 1967. A note on the solution of transient dispersion problems. Proc. Roy. Soc. London, Series A. 298:335.
- Gill, W.N. and Sankarasubramanian, R. 1970. Exact analysis of unsteady convective diffusion. Proc. Roy. Soc. London, Series A. 316:341.
- Gill, W.N. and Sankarasubramanian, R. 1971. Dispersion of a non-uniform slug in time-dependent flow. Proc. Roy. Soc. London, Series A. 322:101.
- Graessley, W.W. 1984. Viscoelasticity and flow in polymer melts and concentrated Solutions. In: Physical Properties of Polymers. Mark, J.E., Eisenberg, A., Graessley, W.W., Mandelkern, L. and Koenig, J.L. (Editors) American Chemical Society, Washington D.C.
- Mohamed, I.O. 1988. Modeling shear rate and heat transfer in a twin screw co-rotating food extruder. Ph.D. Dissertation. Michigan State University. Lansing, MI.
- Sankarasubramanian, R. and Gill, W.N. 1972. Dispersion from a prescribed concentration distribution in time variable flow. Proc. Roy. Soc. London, Series A. 329:479.
- Sankarasubramanian, R. and Gill, W.N. 1973. Unsteady convective diffusion with interphase mass transfer. Proc. Roy. Soc. London, Series A. 333:115.
- Subramanian, R.S. and Gill, W.N. 1976. Unsteady convection diffusion in non-Newtonian flows. Can. J. Chem. Eng. 54:121.
- Taylor, G. 1953. Dispersion of soluble matter in solvent flowing through a tube. Proceed. Roy. Soc. London, Series A. 219:186.
- Taylor, G. 1954. Conditions under which dispersion of a solute in a stream of solvent can be used to measure molecular diffusion. Proceed. Roy. Soc. London, Series A. 225:473.

7 A DISPERSION MODEL FOR PREDICTING THE EXTENT OF LIQUEFACTION BY ALPHA-AMYLASE IN REACTIVE EXTRUSION

7.1 Abstract

A Baker-Perkins co-rotating twin screw extruder was used as a bioreactor for hydrolysis of pre-gelatinized corn starch, using thermophilic α -amylase. The extruder was modeled as a tube, and characterized as a closed system. This characterization is not in terms of thermodynamics, but rather relates to the nature of the tracer fluid upon entry into and exit from the reaction zone. The reaction kinetics were modeled by a modified first order equation, which allowed the dispersion equation to be solved analytically with the Danckwerts boundary condition. Data from several extrusion runs were super-imposed to obtain a profile to evaluate the model. The dispersion number, determined from the first and second moments of the RTD curve was primarily a function of the length of the reaction zone. Results showed good agreement between predictions and experimental data, especially at low dispersion numbers. In general, the axial dispersion model is suitable for analysis of enzymatic reactions up to 30% conversion. At a fixed flow rate and constant temperature, the extent of starch conversion significantly depended on moisture content, residence time and enzyme dosage, but not on screw speed.

7.2 Introduction and Background

The use of an HTST extruder as a biochemical reactor for enzymatic reactions is a new application which has been extensively investigated by several researchers (Linko et al., 1983; and Linko et al., 1984; Reinikainen et al., 1986; Komolprasert and Ofoli, 1989;

and Ofoli et al., 1989). Thermostable α -amylase can be used to partially hydrolyze starch during extrusion to prepare pre-gelatinized and pre-liquefied starch for subsequent syrup manufacture (Linko and Linko, 1983). Although starch can be gelatinized and liquefied thermomechanically during extrusion, use of α -amylase provides advantages in decreasing product viscosity and reducing or eliminating starch retrogradation.

The flow behavior of the TSE is not well characterized, but generally falls between the CSTR (complete mixing) and PFR (no mixing). Based on RTD measurements, several models have been proposed to describe the flow pattern in single screw extruders (SSE). These include such configurations as PFR, CSTR, PFR+CSTR, CSTR in series and PFR+CSTR in series. Few models have been proposed for the TSE because its flow patterns are more complex than those in the SSE. Bounie (1988) used Fourier functions and multivariable optimization techniques to predict a pulse response from several flow models. He found that the model of PFR+nCSTR gave the best fit to the experimental data. Among the flow models developed, the one-dimensional axial dispersion model is used most frequently for polymer processes.

The dispersion model for laminar flow in a tube was developed by Taylor and Aris (Taylor, 1953; Aris, 1956) to describe laminar flow of a solute as a combined action of molecular diffusion and a non-uniform velocity profile (Butt, 1980):

$$D_e = D_m + \frac{D_m \bar{u}^2}{192 D_m} \quad (7.1)$$

Bischoff (1968); and Bischoff and Levenspiel (1962) used the Taylor-Aris dispersion model to characterize a two-dimensional system, using a first-order reaction equation. They found that the model produced accurate results if the reaction was slow.

In general, the dispersion model seems to be valid for a system where the residence time is long enough to enable the process to be represented by the one-dimensional dispersion model (Bischoff, 1968).

The boundary conditions used with the dispersion model depend on whether the system is open or closed. This characterization is not in the thermodynamic sense. A closed system has a flat velocity profile, with no diffusion at the boundaries; an open system involves molecular diffusion and axial dispersion at the boundaries (Nauman, 1981). For a long tube where end effects can be ignored, the Peclet number is large and the difference between open and closed systems is less critical. If an open system is described by the dispersion model, the impulse response method can be used to approximate the RTD function in exactly the same manner as a closed system (Gibilaro, 1978). The solution from RTD measurement depends on the injection and detection modes (Kreft and Zuber, 1978).

The classical Taylor-Aris dispersion model was primarily used for Newtonian and non-Newtonian fluids at steady state. However, the model was modified during the 1970's by Gill and co-workers (Gill, 1967; Gill and Sankarasubramanian, 1970; and Sankarasubramanian and Gill, 1972) to provide a wider range of applications, including unsteady state cases. Booras and Krantz (1976), and Subramanian and Gill (1976) applied the general dispersion model to non-Newtonian fluids for laminar flow in tubes under unsteady state conditions. They found that the dispersion coefficients increased with time and approached a steady state value. Between pseudoplastic and dilatant fluids, the former caused more dispersion (Booras and Krantz, 1976).

Using RTD data and the moment method introduced by Levenspiel and Smith (1957), Parimi and Harris (1957) found that results from a reactive tracer under unsteady state conditions could be used to select, among model candidates, the most appropriate model for describing a system of interest.

In general, the one-dimensional axial dispersion model is suitable for real systems such as fixed beds and flow in tubes (Froment and Bischoff, 1979). The dispersion number is normally determined from RTD data through various techniques (Froment and Bischoff, 1979), including direct nonlinear regression, time moments (which can be improved by incorporating a weighting factor (e^{-t}) or weighted moments (Michelsen, 1972)), fitting RTD data by Laplace transform functions (Michelsen and Ostergaard, 1970, Pham and Keey 1977 and Van der Laan, 1958) and fitting RTD data by Fourier transform (Subramanian, 1977).

No investigation of biochemical reactions using the dispersion model was found in the technical literature. Therefore, the goals of this study were 1) to determine the dispersion coefficients under several extrusion conditions, and 2) to use the dispersion coefficients in an axial dispersion model for predicting the extent of starch liquefaction by α -amylase in a twin screw extruder.

7.3 Model Development

The dispersion equation derives from Fick's law of molecular diffusion:

$$\frac{\partial C}{\partial t} = D_m \frac{\partial^2 C}{\partial x^2} \quad (7.2)$$

Since the extruder is modeled as a tube, the axial one-dimensional dispersion equation may be written on the basis of the mass balance for starch. In terms of mass flow by convection, diffusion and reaction, the mass balance gives

$$C_{s,x}\bar{u}A_c - C_{s,x+\Delta x}\bar{u}A_c + \left(-D_s A_c \frac{dC_s}{dx} \Big|_x + D_s A_c \frac{dC_s}{dx} \Big|_{x+\Delta x} \right) - (-r_s)A_c\Delta x = 0 \quad (7.3)$$

If Eq. 7.3 is divided by $A_c\Delta x$, then in the limit as Δx approaches zero, it becomes:

$$D_s \frac{d^2 C_s}{dx^2} - \bar{u} \frac{dC_s}{dx} - (-r_s) = 0 \quad (7.4)$$

At a starch concentration of 40% at 95°C, the rate of starch conversion ($-r_s$) may be modeled by a modified first order reaction (Chapter 4):

$$-r_s = -\frac{dC_s}{dt} = 0.033C_s' \quad (7.5)$$

where

$$C_s' = C_s - 0.06C_o \quad (7.6)$$

If the extruder is treated as a closed system, then Danckwerts boundary condition may be used:

$$\bar{u}C_o = \bar{u}C_{o^+} - D_s \left(\frac{dC}{dx} \right)_{o^+} \quad \text{at } x = 0 \quad (7.7)$$

$$\frac{dC}{dx} = 0 \quad \text{at } x = L \quad (7.8)$$

Eq. 7.4 may be written in a non-dimensional format as:

$$\left(\frac{1}{Pe} \right) \frac{d^2 \bar{C}}{dz^2} - \frac{d\bar{C}}{dz} - k\bar{C} = 0 \quad (7.9)$$

where

$$\bar{C} = \frac{C_s}{C_o} \quad (7.10)$$

$$Pe = \frac{\bar{u}L}{D_s} \quad (7.11)$$

and

$$z = \frac{x}{L} \quad (7.12)$$

The analytical solution of Eq. 7.9, in terms of \bar{C} as a function of the normalized length of the extruder (z), is (Danckwerts, 1953):

$$\bar{C}(z) = \exp\left(\frac{Pe}{2}z\right) \left[\frac{2(1+\zeta)\exp\left[\frac{Pe\zeta}{2}(1-z)\right] - 2(1-\zeta)\exp\left[\frac{Pe\zeta}{2}(z-1)\right]}{(1+\zeta)^2\exp\left(\frac{Pe\zeta}{2}\right) - (1-\zeta)^2\exp\left(\frac{-Pe\zeta}{2}\right)} \right] \quad (7.13)$$

where

$$\zeta = \sqrt{1 + \frac{4k\bar{t}}{Pe}} \quad (7.14)$$

Having obtained \bar{C} , the fractional conversion, $X(z)$, can be calculated by:

$$X(z) = 1 - \bar{C}(z) \quad (7.15)$$

Eq. 7.15 then allows the extent of starch hydrolysis to be determined along the barrel.

7.4 Materials and Methods

A Baker-Perkins MPF-50D co-rotating twin screw food extruder (APV Baker, Grand Rapids, MI) was used for all runs. Its barrel is 50 mm in diameter and 125 cm long. The relevant dimensions of the extruder are given in Figure 7.1. The screw configuration in the TSE consisted of feed screws and single lead screws, followed by a reaction zone of 90° paddles (Appendix 7) to promote mixing. The size and shape of all screw elements used in the TSE are given in Figure 7.2.

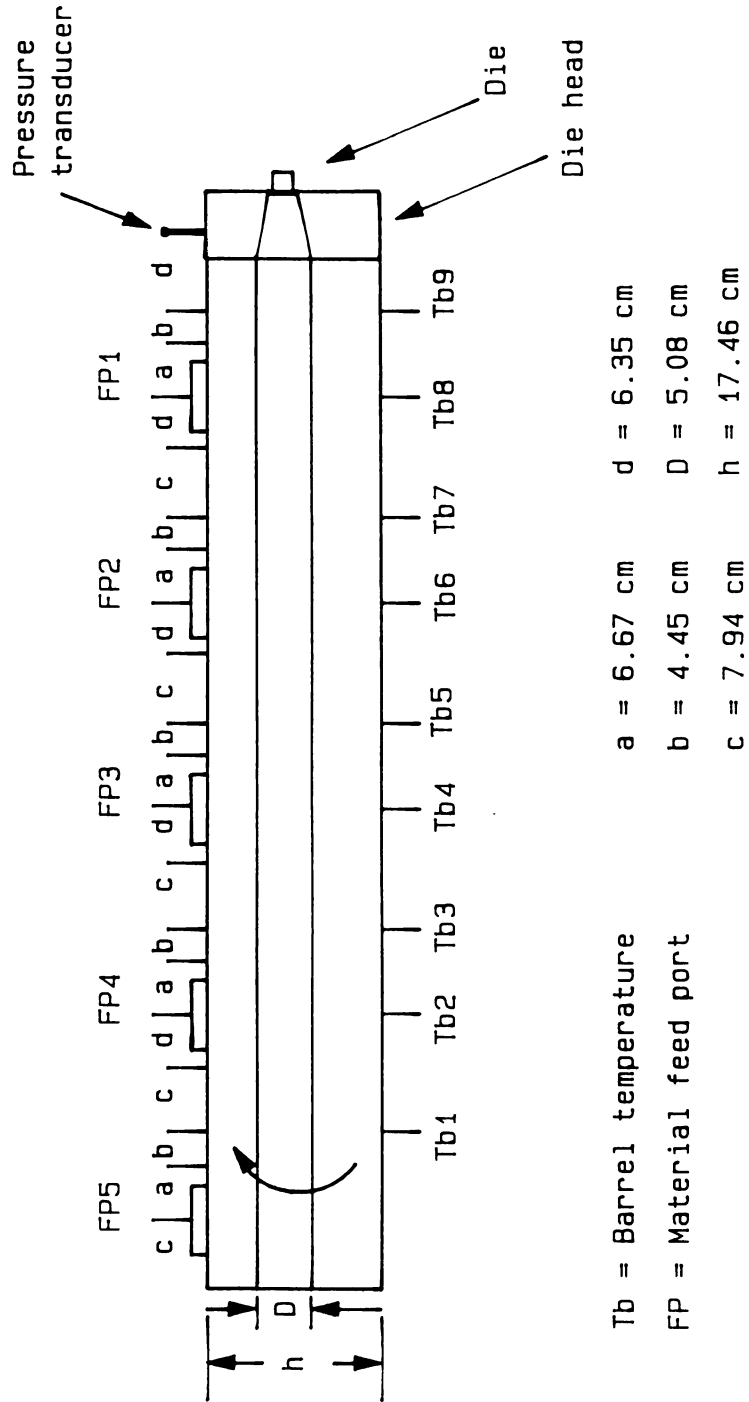


Figure 7.1 Layout of the Baker-Perkins MPF-500 twin screw extruder.

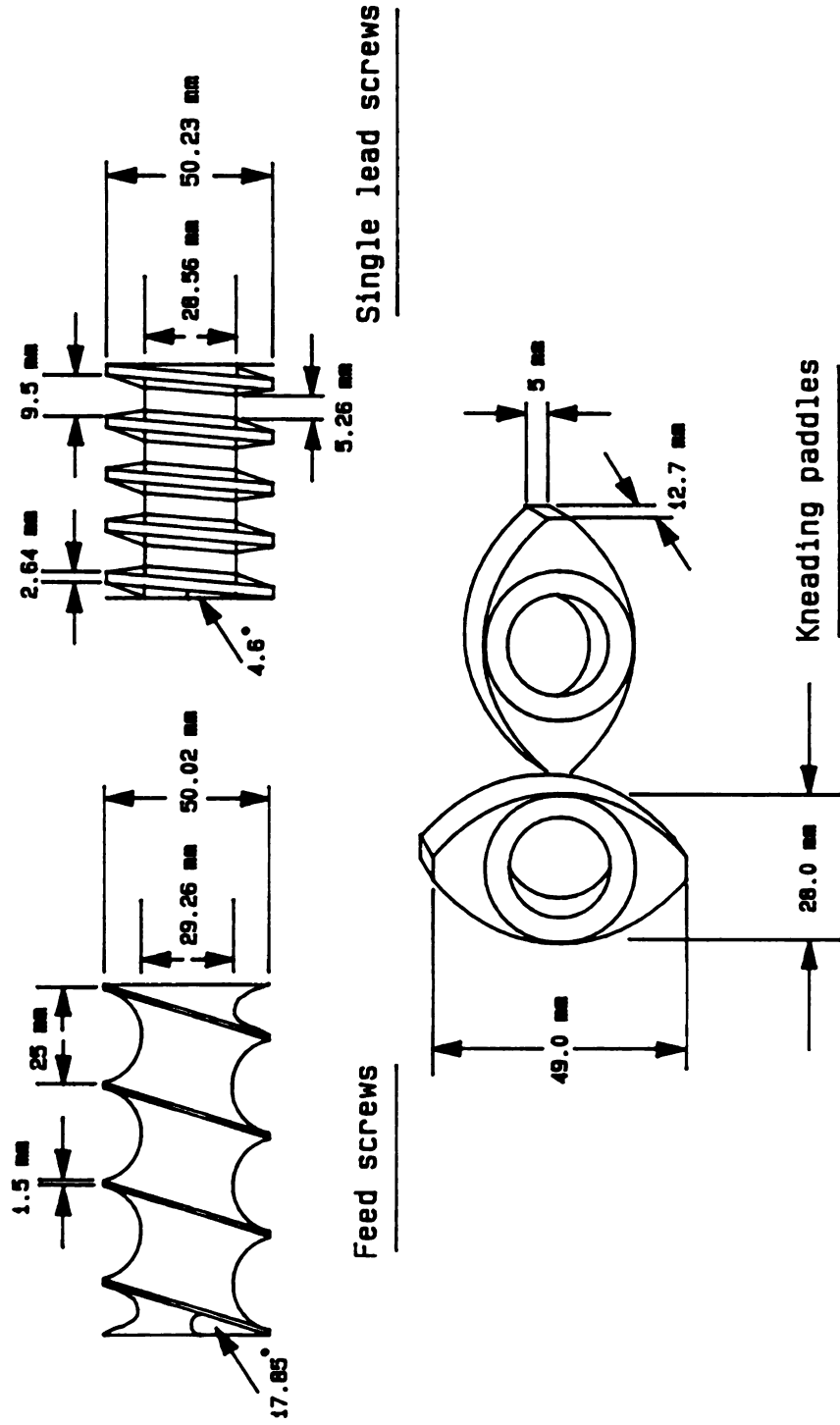


Figure 7.2 Dimensions of screw elements used in the MPF-50D Baker-Perkins twin screw extruder.

The entire experiment consisted of twenty extrusion runs. The first twelve were run at a constant length of single lead and feed screws, but variable lengths of paddles at two screw rpm, moisture contents and enzyme levels (Table 7.1). The experimental design of the last eight runs are given in Table 7.2. The schematics of screw profiles and all injection ports are shown in Figures 7.3, 7.4 and 7.5 for runs 1-12, 13-16 and 17-20, respectively. Two circular full flange dies 3.2 mm in diameter and 25.4 mm in length were used.

Pre-gelatinized corn starch (American Maize, Hammond, Indiana) was used as substrate. Liquefaction was carried out only in the paddle zone where a high level of mixing was obtained. Termamyl 120L and 240L α -amylase (Novo Laboratories, Connecticut) were used. All extrusion runs were done at a fixed mass flow rate of 10 kg/hr. Barrel temperatures in the paddle zone were fixed at 100°C for extrusion runs 1-12 and 95°C for runs 13-20. Termamyl 120L enzyme (30,000 units/ml) was diluted in deionized water, and Termamyl 240L (80,000 units/ml) was diluted in 30 mM acetate buffer at a pH of 6.0 before being fed into the extruder. Enzyme activity was determined by the DNS procedure (Saha et al., 1987). Extrusion runs 13-20 were operated at 60 rpm, 60% moisture content and 45 enzyme units (activity/g starch).

Run no.	Paddle Length (cm)	RPM	% Moisture	Enzyme level (units/g starch)
1	19.1	30	60	23
2	19.1	60	60	23
3	19.1	30	50	30
4	19.1	60	50	30
5	44.5	30	60	23
6	44.5	60	60	23
7	44.5	30	50	30
8	44.5	60	50	30
9	69.9	30	60	23
10	69.9	60	60	23
11	69.9	30	50	30
12	69.9	60	50	30

(pH = 6.0-6.5, T = 100°C and \dot{m} = 10 kg/hr.)

Run no.	L/D ratio	Length of screws, left to right (from feed port to the die), cm				Location of liquid streams (distance from feed port), cm	
		Feed	Single lead	90° disks	Single lead	Buffer	Enzyme
13	25	15.2	5.1	24.1	5.1	11.11	95.3
14							69.9
15							44.5
16							19.1
17	10	15.2	5.1	24.1	5.1	-	11.1
18	15	15.2	5.1	49.5	5.1	-	11.1
19	20	15.2	5.1	74.9	5.1	-	11.1
20	25	20.3	12.7	87.6	5.1	-	19.1

(40% starch, pH = 6.0, T = 95°C, 60 rpm, 45 enzyme units/g starch and \dot{m} = 10 kg/hr)

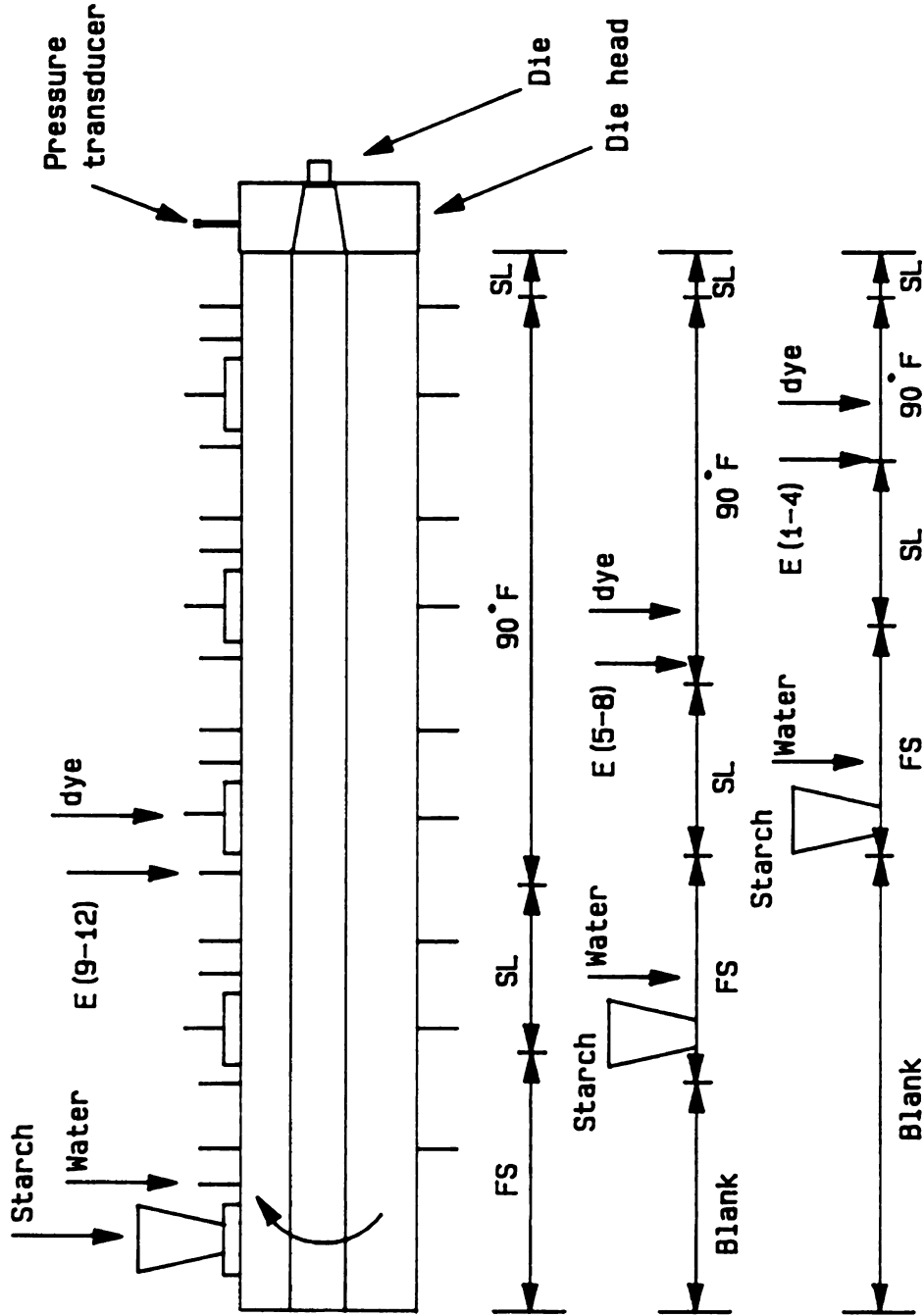


Figure 7.3 Extruder setup for experiments 1-12 showing entry points of enzyme solution (E) and tracer dyes.

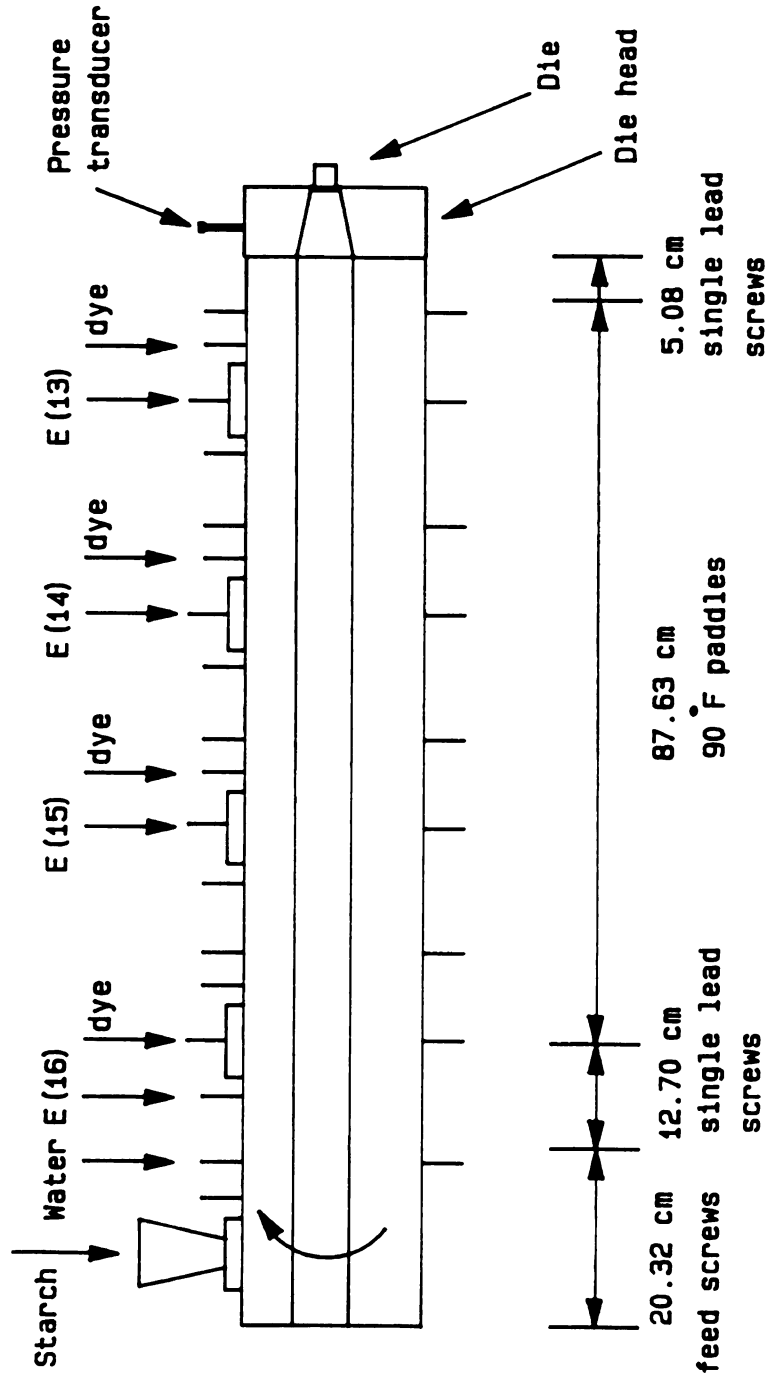


Figure 7.4 Extruder setup for experiments 13-16 showing entry points of enzyme solution (E) and tracer dyes.

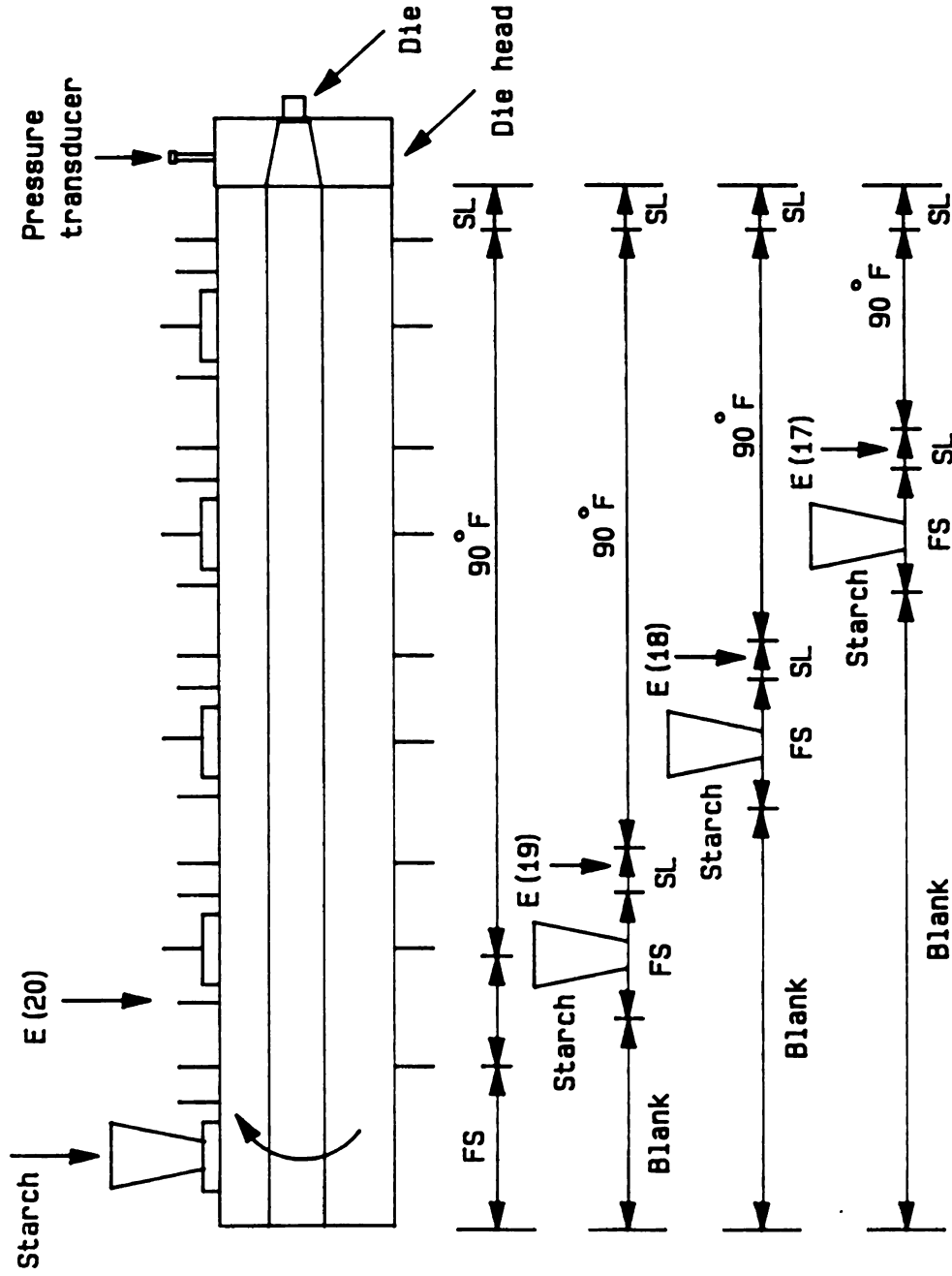


Figure 7.5 Extruder setup for experiments 17-20 showing entry points of enzyme solution (E).

The extrudate was collected after the extruder reached steady state. About 10 g of sample was collected in an aluminum pan, 5 cm in diameter and 1.5 cm in height, and immediately immersed in liquid nitrogen to freeze the enzymatic reaction. Six samples were collected from each run, three before and three after the RTD measurement. RTD measurement was performed in all runs. During run 20, three additional RTD measurements were conducted to enable determination of whether the dispersion number changes if the tracer dye is introduced at different points of the extruder for a fixed feed port (Figure 7.6). The frozen samples were stored in a household freezer maintained at -17°C for subsequent analyses. The moisture content of the extrudate was determined by the oven method at $100\text{-}105^{\circ}\text{C}$.

7.4.1 Determination of residence time distribution (RTD)

Residence time was determined by a tracer technique using an erythrosine solution (4%, w/v in water). From 0.1 to 0.5 ml of the dye solution was injected via a one ml plastic syringe through a port located near the enzyme feed port. Extrudate collection began when a slight change in color was first observed, and continued at intervals of 15s until discoloration was no longer visible.

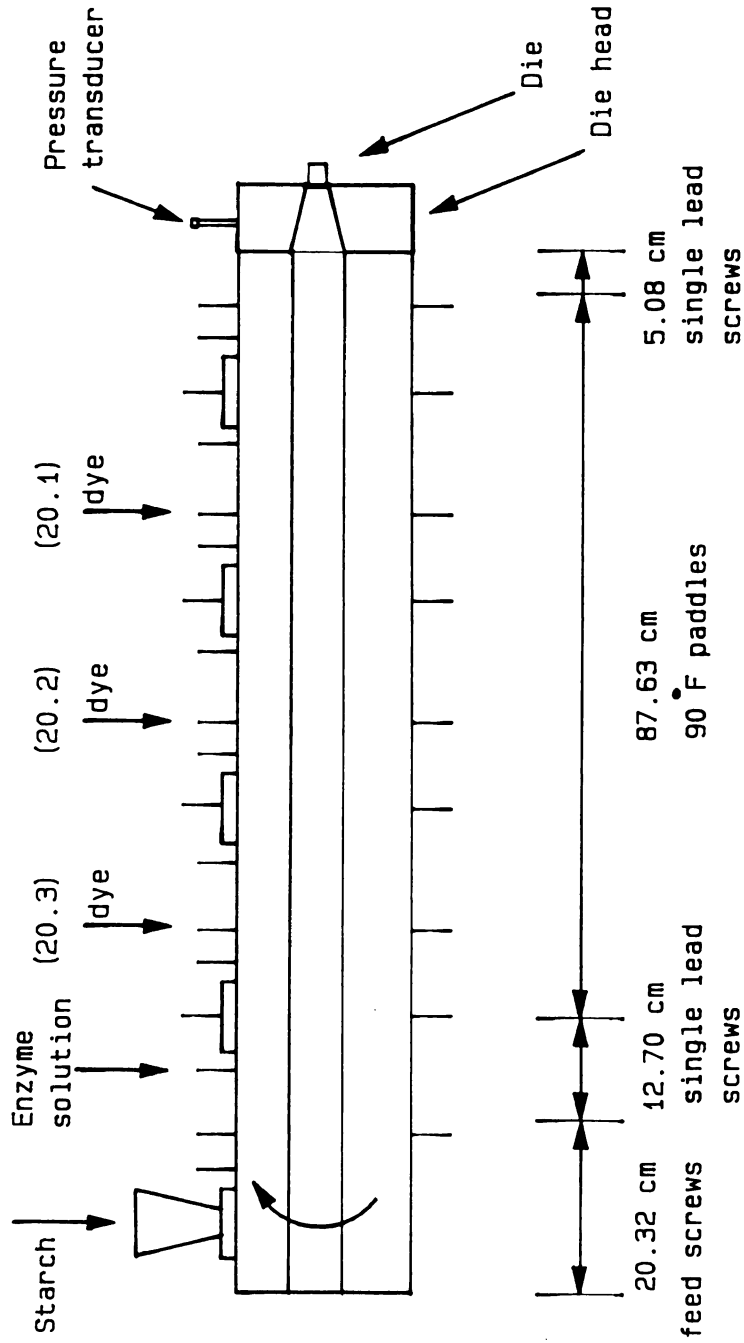


Figure 7.6 Extruder setup for experiments 20.1, 20.2 and 20.3 showing entry points of dye solution.

The extrudates were cooled at room temperature, covered with plastic wrap and placed in a household refrigerator overnight. All extrudates were removed from the refrigerator and allowed to equilibrate at room temperature for 30 minutes before analysis. Each extrudate was stirred to obtain a uniform color before measuring the intensity of dye color against a base extrudate containing no dye with a Minolta Chroma Meter model CR-200 (Minolta Camera Co., Japan). Because the meter had a small window of 8 mm in diameter, three measurements at different spots were taken, automatically averaged and recorded through a computer interface. The "a" values, which represent the degree of redness, are proportional to dye concentrations. A C-curve was obtained from a plot of the "a" values versus residence time.

The mean residence time, \bar{t} , was approximated by

$$\bar{t} = \frac{\sum_{i=1}^n t_i \Delta a_i \Delta t_i}{\sum_{i=1}^n \Delta a_i \Delta t_i} \quad (7.16)$$

where Δa_i is the redness value of the extrudate at discrete time values t_i , and Δt_i is the time step (15 s).

Based on the methods used to inject and detect the dye, the extruder could be characterized as a closed system. It is worth noting that this characterization is not in a thermodynamic sense.

7.4.2 Estimation of dispersion coefficients

Using the RTD data, the variance of the RTD curve was calculated:

$$\sigma^2 = \frac{\sum_{i=1}^n t_i^2 \Delta a_i \Delta t_i}{\sum_{i=1}^n \Delta a_i \Delta t_i} - \bar{t}^2 \quad (7.17)$$

For a closed reactor, the dispersion number (D_e/uL) could be calculated from the implicit expression (Levenspiel, 1972):

$$\frac{\sigma^2}{\bar{t}^2} = 2\left(\frac{D_e}{\bar{u}L}\right) - 2\left(\frac{D_e}{\bar{u}L}\right)^2 \left(1 - e^{-\frac{\bar{u}L}{D_e}}\right) \quad (7.18)$$

The dispersion coefficient (D_e) can be directly determined from the dispersion number if the average velocity and the reactor length are known. If the extrudates are relatively constant in density, the average velocity for the fully filled screw region may be calculated by:

$$\bar{u} = \frac{\dot{m}}{\rho A_c} \quad (7.19)$$

where \dot{m} is the mass flow rate (g/min) and A_c is the wetted cross sectional area of the extruder. However, when the extruder configuration consists of more than one screw type, estimation of A_c becomes difficult. The mean velocity must then be computed from:

$$\bar{u} = \frac{L_e}{\bar{t}} \quad (7.20)$$

where L_e is the equivalent length of a given screw section, and can be calculated as the length equivalent to that of a circular pipe containing the same volume:

$$L_e = \sum \frac{V_{wi}}{\left(\frac{\pi D_{hi}^2}{4}\right)} \quad (7.21)$$

D_{hi} in Eq. 7.21 is the hydraulic diameter of screw type i , which is 0.75 cm for single lead screws (Mohamed, 1988) and 1.04 cm for 90° paddles. The lengths of the die head and the die were neglected because they contribute equivalent lengths much shorter than that of the screws.

7.4.3 Sample preparation and analysis for reducing sugar

Frozen extrudate was thawed rapidly in a Tappan microwave oven (650 W) for 10 seconds, or thawed slowly in a plastic bag at room temperature for 15-20 min. A mixture containing 0.5-1.0 g of the sample, 0.5-1.0 ml of 0.1 N NaOH and 10 ml distilled water was homogenized using a Polytron homogenizer (Brinkmann Instruments, NY) at 15,000 rpm for 10-15 seconds and then heated at 100°C for 10 minutes. The solution was cooled and brought up to 25 g by adding water, and centrifuged at 13,000-15,000 rpm for 10-15 minutes using a Sorvall centrifuge (Dupont, IL). The supernatant was removed and subjected to sugar analyses by the DNS and %DE methods.

The quantity of total reducing sugar in the extrudate was determined using a colorimetric procedure developed by Bernfeld (1955) and modified by Saha et al. (1987). The reducing sugars liberated from the enzymatic liquefaction of starch reacted with 3,5-Dinitrosalicylic acid (DNS) and then formed a brown product upon heating. The absorbance of the brown color was measured against a blank (distilled water) at 640 nm, using a Lambda 4B Perkin-Elmer Spectrophotometer (Perkin-Elmer Corp., IL). The total amount of reducing sugars in the sample was calculated relative to the known glucose concentration, based on Beer's law.

The DE value was determined, using the procedure of Dygert et al. (1965). Upon heating, neocuproine hydrochloride (2,9-dimethyl-1,10-phenanthroline.HCl) forms a colored complex via chelation with Cu^{++} ion produced by the oxidation of reducing sugars. Glycine was used as the copper chelating agent in place of tartrate to improve the assay's precision. The colored complex was measured spectrophotometrically against a blank at 450 nm. The amount of reducing sugar in dextrose equivalent was calculated relative to a known dextrose concentration which was treated in exactly the same manner as the sample and the blank. In the analysis, the sugar extract was diluted to obtain a

solution containing 50-100 micrograms of glucose equivalent per ml. The amount of reducing sugar was estimated by using the percent reducing sugar obtained by the DNS method.

The DE value was calculated by:

$$DE = \frac{\text{amount of reducing sugar equi. to dextrose}}{\text{wt. of sample (dry basis)}} \times 100 \quad (7.22)$$

7.4.4 Estimation of the apparent viscosity of starch in the extruder

The apparent viscosity of liquefied starch in the extruder was calculated by the procedure described by Mohamed (1988). A series of extrusion runs were performed using corn syrup type C (Cleveland Syrup Corp., OH) as a Newtonian standard over a ratio of 15 L/D in a Baker-Perkins MPF 50D co-rotating twin screw food extruder. The screw profile consisted of feed screws, single lead screws and 90° forwarding paddles (Figure 7.7). Two circular dies 3.2 mm in diameter and 25.4 mm in length were used. With this screw profile, the reaction zone (paddle region) was fully filled in all extrusion runs operated at a flow rate of 7-10 kg/hr. At low rpm, the material backed up toward the feed port indicating that the channel was filled. As the rpm increased, the backup flow ceased but the screw region from the paddles to the dies remained fully filled.

Process parameters (rpm, % torque, barrel temperature, product temperature and die pressure) were recorded after the extruder reached steady state. The throughput was determined by collecting the extrudate over one minute and weighing it. The product temperature was recorded along the barrel and at the die.

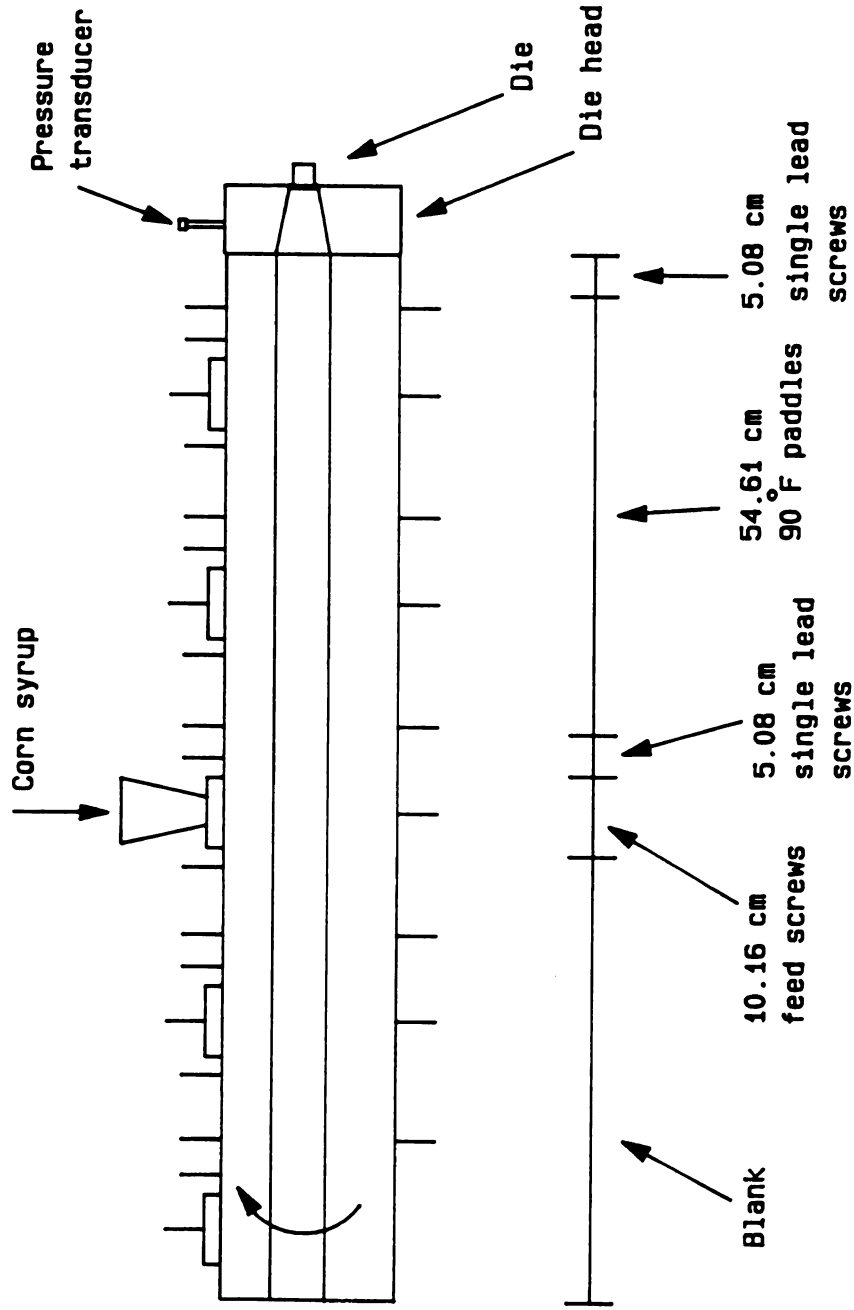


Figure 7.7 Schematic setup of the MPF-500 Baker-Perkins twin screw extruder for corn syrup experiments.

Using extrusion data, the power number for corn syrup was calculated (Mohamed, 1988) by:

$$P_o = \frac{E_v}{\rho N^3 D_k^5} \quad (7.23)$$

where

$$E_v = P_w - \Delta P Q_n \quad (7.24)$$

$$P_w = 0.354(\% \text{ Torque})N \quad (7.25)$$

The Reynolds number was calculated by (Mohamed, 1988):

$$Re = \frac{D_k^2 N \rho}{\mu} \quad (7.26)$$

A relationship between P_o and Re was developed, using regression analysis. Since the starch material used the same screw profile as the corn syrup, the Newtonian P_o and Re relationship can be used to calculate the corresponding Re (Re') for the starch material for a given P_o . The apparent viscosity (η_a) can then be calculated by:

$$\eta_a = \frac{\rho D_k^2 N}{Re'} \quad (7.27)$$

7.4.5 Rheological data

The rheological properties of corn syrup were determined using a Haake RV-12 viscometer consisting of an M-500 measuring head, SVI sensor, Haake speed programmer, Haake F3-C temperature controller, Hewlett-Packard 3495 data acquirer and Hewlett-Packard 85 computer for data collection and analysis. The samples used to collect rheological data were withdrawn from the same batch used for the extrusion runs. The rheological data were taken at five different temperatures, and over as wide a shear rate range as possible.

7.5 Results and Discussion

7.5.1 Estimation of dispersion numbers and dispersion coefficients

The C-curves of extrusion runs 1-12 are plotted in Figure 7.8 and 7.9. All the curves were similar in shape, and tended to have long tails. Using the RTD data for extrusion runs 1-12 (Appendix 8) and Eqs. 7.16-7.18 and 7.20, the mean residence time, dispersion number and dispersion coefficient were determined. The results were grouped by rpm and enzyme level and are summarized in Table 7.3.

Run no.	Length*, cm	\bar{t} (min)	σ^2 (min ²)	$\frac{D_e}{\bar{u}L_e}$ x10 ²	\bar{u} (cm/s)	D _e (cm ² /s)
1	674	4.7	0.9	2.19	2.4	35.7
5	1152	5.6	1.2	2.05	3.5	81.5
9	1630	7.0	0.9	1.00	3.9	63.1
2	674	4.5	1.5	3.84	2.5	64.1
6	1152	5.2	1.6	2.98	3.7	126.3
10	1630	6.8	0.8	0.87	4.7	56.5
3	674	5.7	2.2	3.53	2.0	46.7
7	1152	6.4	1.1	1.39	3.0	48.1
11	1630	8.8	2.2	1.39	3.1	69.6
4	674	5.3	2.3	4.23	2.1	60.6
8	1152	6.3	1.7	2.19	3.0	76.4
12	1630	8.3	2.0	1.46	3.3	78.3

* Length of equivalent path of tracer dye, calculated by Eq. 7.21.

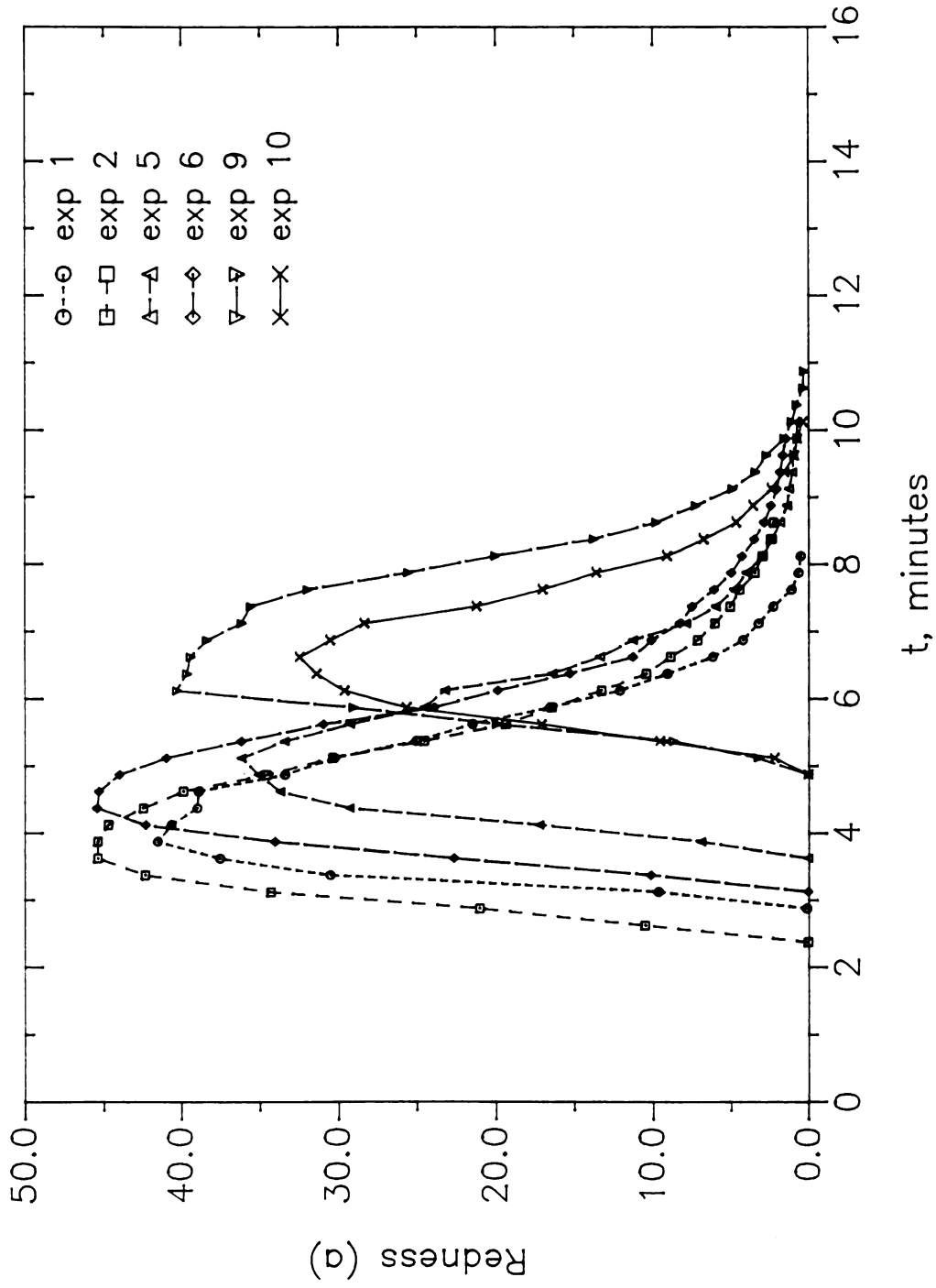


Figure 7.8 C-curves from experiments 1, 2, 5, 6, 9 and 10 at 60% moisture content.



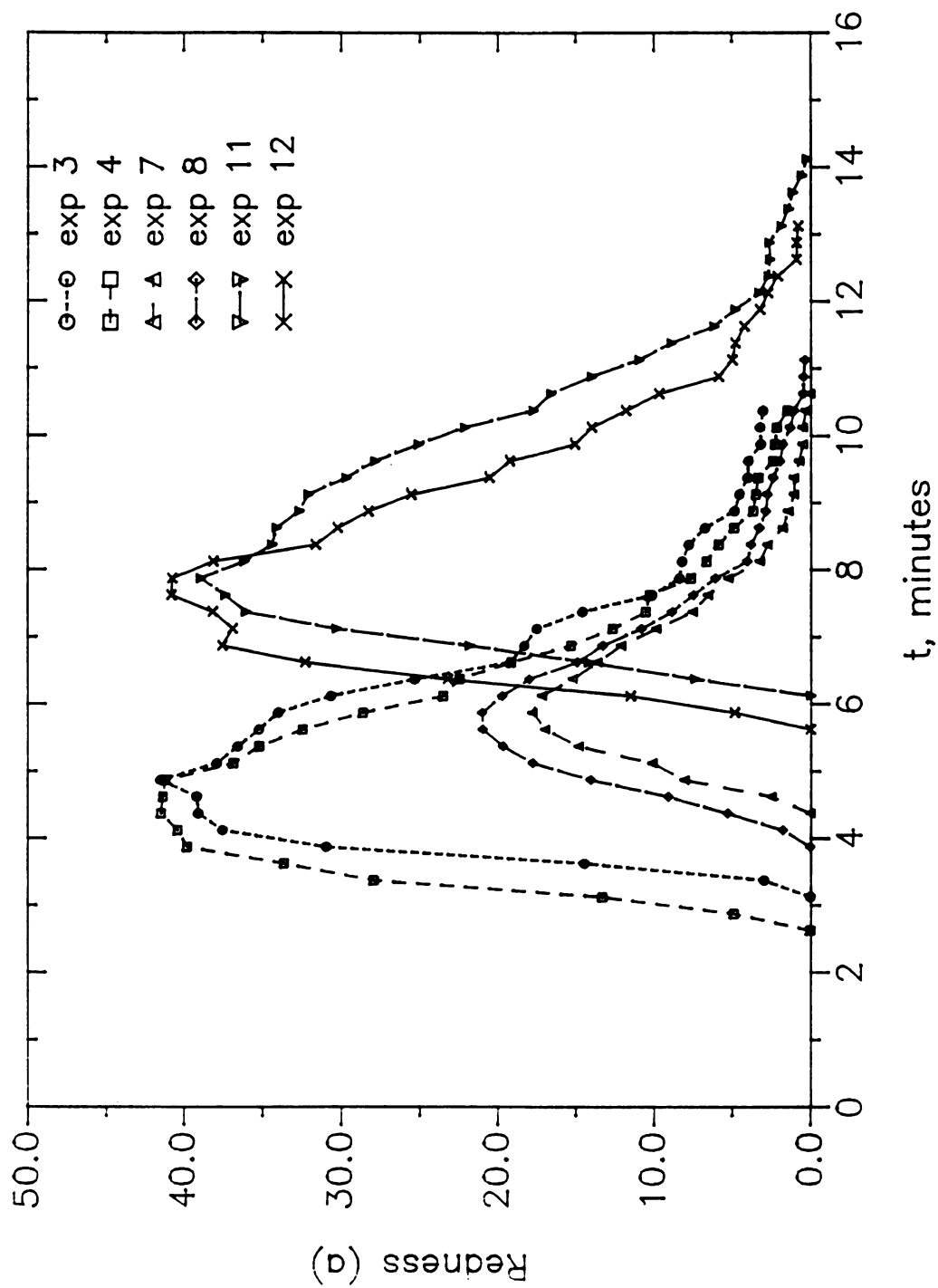


Figure 7.9 C-curves from experiments 3, 4, 7, 8, 11 and 12 at 50% moisture content.

Results from ANOVA (Appendix 9) showed that the effect of the reaction zone, moisture content and enzyme level on the mean residence time were significant at $P < .01$. The mean residence time increased with increased length of reaction zone. The effects of reactor length and screw rpm on the dispersion number were also significant (Appendix 10). The mean velocity and dispersion coefficient fluctuated, probably due to effects of screw profile and enzymatic reaction. Differences in screw profile caused the average cross-sectional area to vary, which resulted in changing the mean velocity. At short reactor lengths or residence times, the extent of starch hydrolysis was small. Therefore, the extrudate was solid-like, and the flow approached plug flow, i.e. the degree of dispersion was small. When the residence time increased, starch was more liquefied and became liquid-like; the flow deviated from plug flow, with increased mixing and dispersion.

Under the same extrusion conditions, the mean residence time during enzymatic reaction was shorter than when no enzyme was added. This effect was due to viscosity reduction, which resulted in increasing the mean velocity, thereby decreasing the residence time and increasing dispersion. The results at 60% moisture were different from those at 50% moisture. This may be due to other factors such as errors caused by truncation of the tail of the RTD curve.

C-curves of extrusion runs 13-16 and 17-20 are plotted in Figures 7.10 and 7.11, respectively. Mean residence time, dispersion number and dispersion coefficients for extrusion runs 13-20 were determined and are presented in Table 7.4.

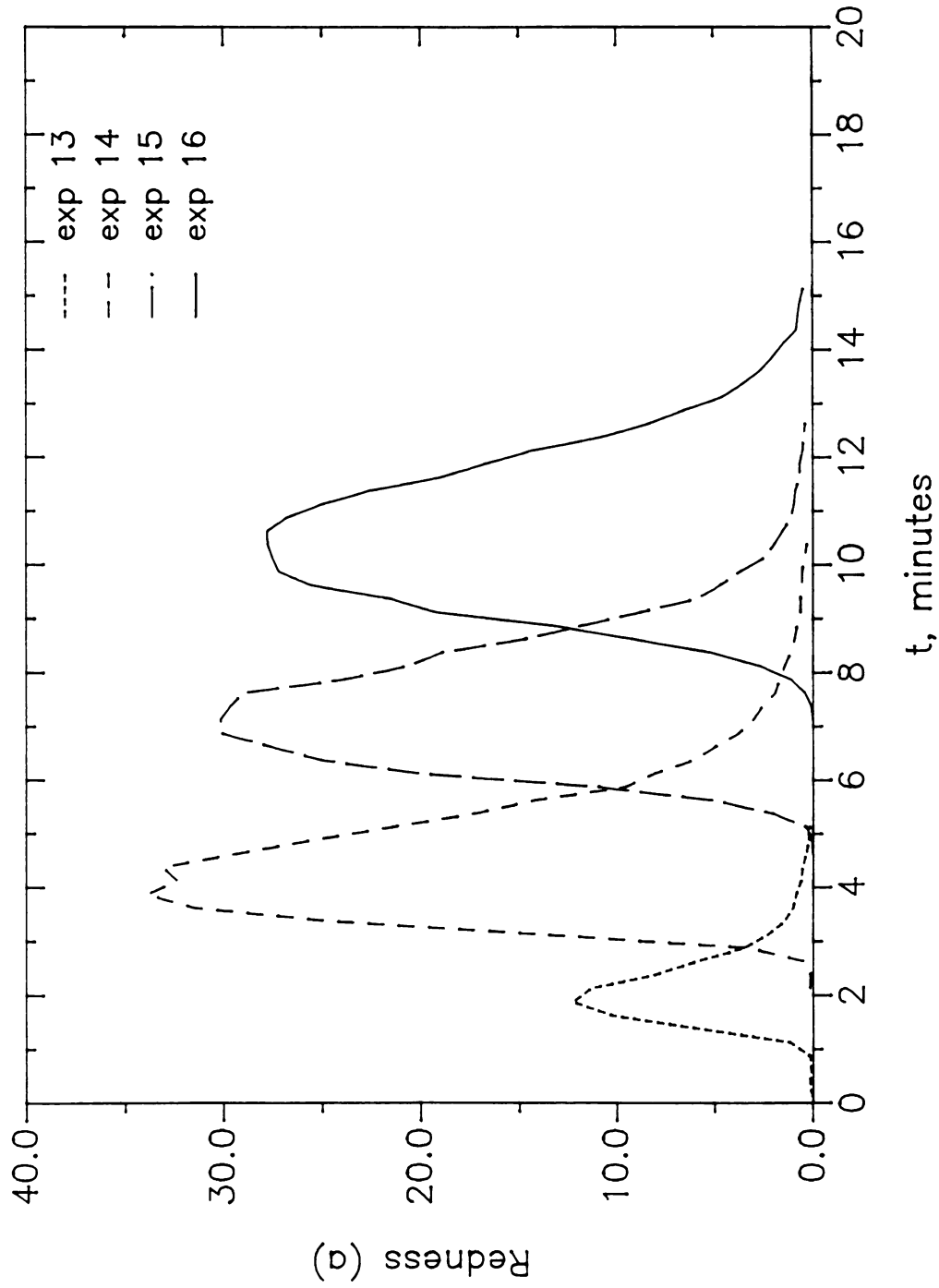


Figure 7.10 C-curves (redness versus residence time) from experiments 13–16 (mean residence times: 2.2, 4.7, 7.6 and 10.7 min, respectively).

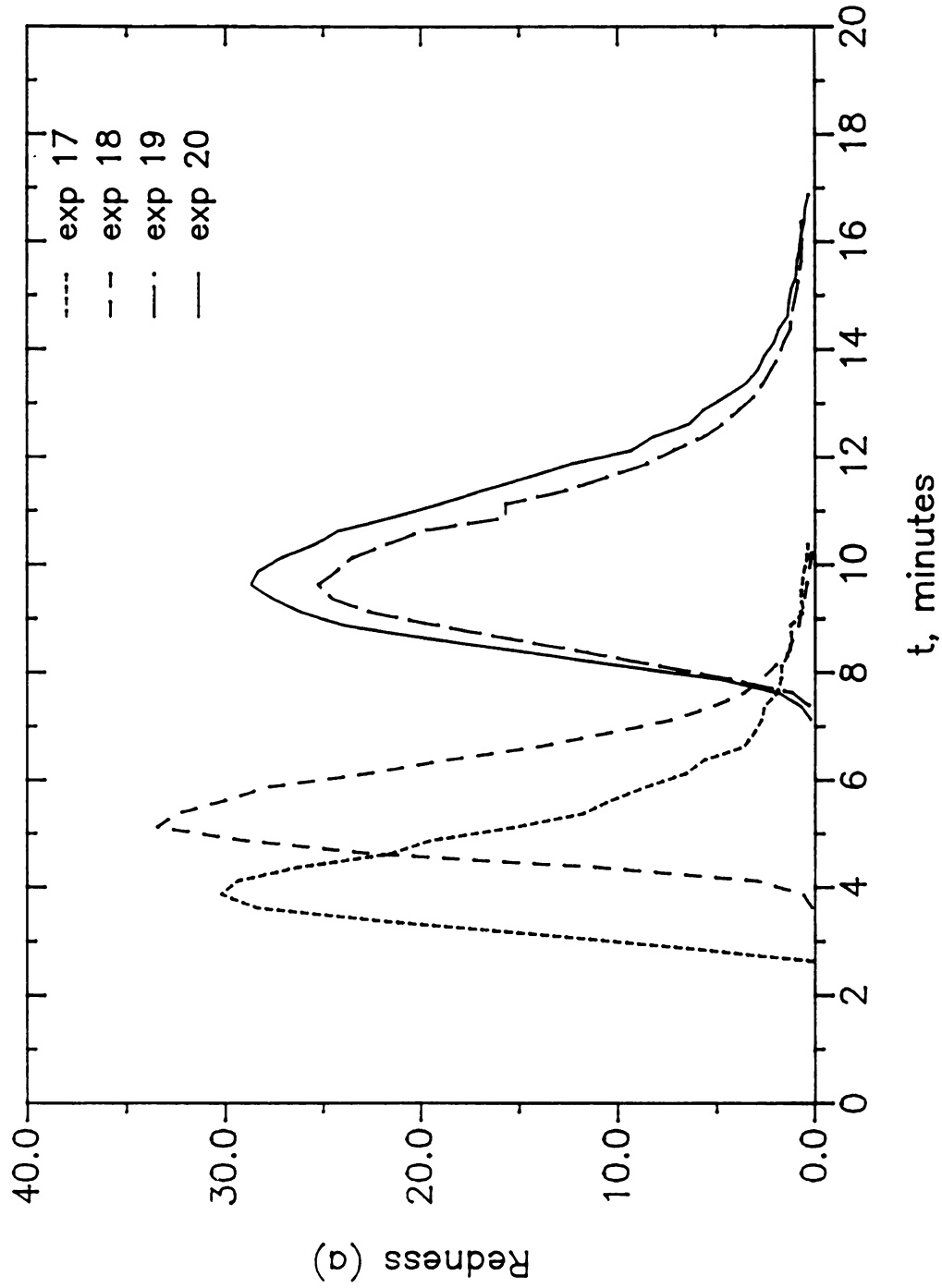


Figure 7.11 C-curves (redness versus residence time) from experiments 17–20 (mean residence times: 4.6, 5.7, 10.3 and 10.4 min, respectively).

Table 7.4. Mean residence time, dispersion number and dispersion coefficient from extrusion runs 13-20.

Run no. [*]	Length ^{**} , cm	\bar{t} (min)	σ^2 (min ²)	$\frac{D_e}{\bar{u}L_e}$ x10 ²	\bar{u} (cm/s)	D_e (cm ² /s)
13	674	2.2	0.5	5.18	5.1	179.2
14	1152	4.7	1.4	3.40	4.1	161.0
15	1630	7.6	1.4	1.21	3.6	70.9
16	2107	10.7	1.6	0.73	3.3	50.7
17	1143	4.6	1.7	4.05	4.1	189.9
18	1620	5.7	0.9	1.40	4.7	107.1
19	2098	10.3	2.3	1.09	3.4	77.6
20	2681	10.4	2.5	1.15	4.3	132.7

^{*} A dye solution was used for runs 13-16 and a dye ball for runs 17-20.

^{**} Length of equivalent path of tracer dye, calculated by Eq. 7.21.

Runs 13-20 also showed that increasing the reactor length resulted in increased mean residence time and decreased dispersion number.

In runs 13-16 the dispersion coefficients fluctuated in exactly the same manner as observed for runs 2, 6 and 10, although the magnitudes were different. For the same path length, increased enzyme levels (runs 13-16) caused the liquefaction of starch to increase, which resulted in greater dispersion. Dispersion was also expected to increase with the flow behavior index (n). The higher the extent of liquefaction, the closer n is to unity, and the closer the fluid approached Newtonian behavior.

The dispersion coefficient is a function of velocity, viscosity and the hydraulic diameter of the flow path in the extruder. It generally decreased with decreased velocity (runs 13-19). In addition, longer equivalent lengths appear to cause a significant decrease in the dispersion number, leading to smaller dispersion coefficients.

Experimental runs were made to determine if the extent of starch hydrolysis and degree of mixing depended on how the enzyme was fed into the extruder. In extrusion runs 1-16, the starch and about 80% of the water or buffer solution (pH 6.0) were pre-mixed in the extruder before adding the enzyme solution. In contrast, the enzyme solution was directly mixed in with starch in the extruder during extrusion runs 17-20. Statistical analysis (Appendix 11) showed no significant difference ($P < .05$) between the dispersion numbers obtained from the two methods.

Additional RTD data (sets 20.1-20.3) were collected during extrusion run 20. The dispersion coefficients for these runs are presented in Table 7.5.

Table 7.5. Mean velocity and dispersion coefficient at various reaction zone lengths during extrusion run 20.						
Run no.	Length*, cm	\bar{t} (min)	σ^2 (min ²)	$\frac{D_e}{\bar{u}L_e} \times 10^2$	\bar{u} (cm/s)	D_e (cm ² /s)
20.1	943	3.7	0.7	2.68	4.2	106.5
20.2	1421	6.6	1.9	2.29	3.6	117.2
20.3	1898	9.3	2.2	1.26	3.4	81.5

* Length of equivalent path of tracer dye calculated by Eq. 7.21.

With the exception of the D_e value of run 20.2 in Table 7.5, the dispersion coefficient decreased with increased length of the reactor. It is worth noting that the mean velocity varied along the barrel of the reactor, an indication that the mean velocity causes a variation in the dispersion coefficient, in the same manner as observed in Chapter 6. In fact, the change in velocity is influenced by the screw profile and the rheological properties of the fluid. Therefore, the dispersion coefficient depended on

several complex interactions. For example, D_e depends on the molecular diffusion coefficient (D_m), mean velocity and hydraulic diameter of the extruder (Eq. 7.1). From the results of this study, the dispersion number provides the best parameter for characterizing the degree of dispersion.

7.5.2 Use of the dispersion model to predict RTD

In this study, the dispersion number was estimated by using the first and second moments, which were developed theoretically from the model of flow behavior. However, it is of interest to determine whether the dispersion number could be used to predict the tracer (dye) concentration profile or F function.

The extruder was treated as a closed system with the Danckwerts boundary conditions (Eqs. 7.7-7.8). The analytical solution in terms of \bar{C} for the non-reacting tracer can be expressed (Butt, 1980) as:

$$F(\tau) = \frac{C}{C_0} = \frac{1}{2} - \frac{1}{2} \operatorname{erf} \left[\frac{1-\tau}{2\sqrt{\tau \left(\frac{D_e}{uL} \right)}} \right] \quad (7.28)$$

where

$$\operatorname{erf}(y) = \frac{2}{\sqrt{\pi}} \int_0^y \exp(-v^2) dv \quad (7.29)$$

and

$$\tau = \frac{t}{\bar{t}} \quad (7.30)$$

Eq. 7.28 was solved numerically by using the Gauss-Legendre Quadrature method (Carnahan et al., 1969). The results were compared to the experimental F values by using the linear regression:

$$F_{\text{model}} = bF_{\text{exp}} \quad (7.31)$$

Values of b and standard error for all extrusion runs are presented in Table 7.6. The " b " value is an indication of how well the two F values are related. If the " b " value equals to unity, the model is in perfect agreement with the experimental data. The deviation of the model from the experimental data was measured in terms of a standard error. The results showed that as the length of the reactor increased, b values increased while standard errors decreased ($R^2 = 0.99$ at $P < 0.05$). On the whole, the F values were within 5% of each other. An example of a comparison of F -curves of the model and the experiment is shown in Figure 7.12, and illustrates the fact that the model and the experiment became closer as the reactor length increased. This is consistent with the technical literature: the dispersion model is valid for long reactors or long residence times. These results also validate the characterization of the extruder as a closed reactor.

Table 7.6. Values of "b" (Eq. 7.31) and standard error for various extrusion runs.				
Run no.	Length* cm	$\frac{D_e}{\bar{u}L_e}$ x10³	b	Standard error
1	674	21.91	0.951	.014
5	1152	20.50	0.964	.013
9	1630	9.95	0.969	.011
2	674	38.42	0.951	.013
6	1152	29.80	0.958	.013
10	1630	8.74	0.968	.013
3	674	35.33	0.952	.012
7	1152	13.95	0.967	.012
10	1630	13.92	0.970	.009
4	674	42.25	0.953	.011
8	1152	21.90	0.962	.012
12	1630	14.60	0.967	.010
13	674	51.76	0.945	.018
14	1152	33.98	0.964	.010
15	1630	12.14	0.972	.009
16	2107	7.29	0.973	.008
17	1143	40.48	0.959	.013
18	1620	13.99	0.971	.012
19	2098	10.93	0.973	.009
20	2681	11.49	0.974	.008
20.1	942.9	26.84	0.957	.016
20.2	1420.6	22.88	0.967	.010
20.3	1898.3	12.64	0.967	.008

* Length of equivalent path of tracer dye, calculated by Eq. 7.21.

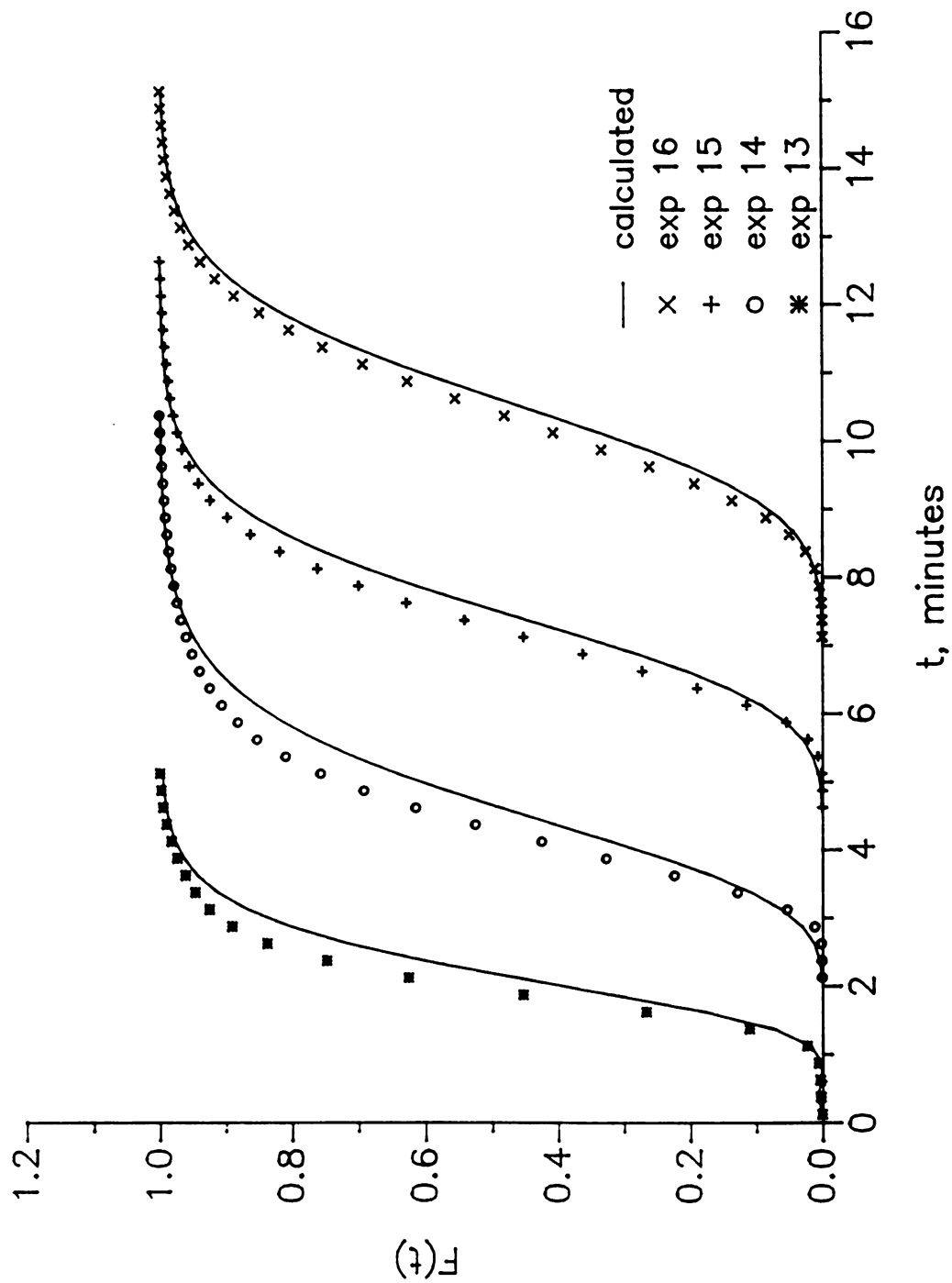


Figure 7.12 Experimental and calculated F functions versus time. Mean residence times: *, 2.19 min; o, 4.7 min; +, 7.5 min; x, 10.7 min.

7.5.3 Extent of starch liquefaction in the extruder

The extent of enzymatic starch hydrolysis (Appendix 12) were expressed in terms of %reducing sugar, %DE and fractional conversion (X). Results are shown in Table 7.7 for extrusion runs 1-12 and Table 7.8 for runs 13-20.

Since the dye could not be injected at the same port as the enzyme solution, the actual residence time of the reaction was calculated by:

$$\bar{t} = \frac{L_r^*}{\bar{u}} \quad (7.32)$$

where L_r^* is the equivalent length of the reaction zone, and \bar{u} is the mean velocity calculated from the RTD data.

Without addition of enzyme, the extrudate contained <0.7 % reducing sugar and <0.4% DE, which were produced by thermomechanical breakdown of the starch during extrusion. Since these values were small, they were ignored in the calculation of the amount of starch liquefied by the enzyme.

The effect of moisture content, residence time and enzyme level on % reducing sugar and % DE were statistically significant at $P < .05$ (Appendix 13). However, the effect of screw rotation in the range of 30-60 rpm was not significant. Starch analysis showed that initial starch concentrations were 38.8% for runs 13-16 and 42.8% for runs 17-20. Fractional conversions for runs 13-20 were calculated. Results from ANOVA (Appendix 14) showed that there was no significant differences in % reducing sugar and % DE, between runs 13-16 and runs 17-20. This is an indication that the method of introducing the enzyme solution into the extruder does not insignificantly affect the reaction at $P < .05$.

Run no.	Length*, cm	\bar{t} , min	RPM	Enzyme dosage	% Reducing sugar(s.v.)	%DE (s.v.)
1	794	5.5	30	23	3.32 (0.13)	1.94 (0.13)
5	1271	6.1	30	23	5.28 (0.16)	2.54 (0.15)
9	1749	7.5	30	23	6.62 (0.35)	3.51 (0.75)
2	794	5.4	60	23	3.61 (0.33)	1.96 (0.20)
6	1271	5.8	60	23	5.65 (0.62)	2.66 (0.31)
10	1749	6.2	60	23	6.71 (0.26)	3.54 (0.51)
3	794	6.8	30	30	6.31 (0.64)	3.30 (0.45)
7	1271	7.0	30	30	7.98 (0.52)	3.37 (0.18)
11	1749	9.5	30	30	8.43 (0.71)	4.40 (0.35)
4	794	6.2	60	30	6.32 (0.83)	3.03 (0.42)
8	1271	7.0	60	30	8.67 (0.42)	3.52 (0.17)
12	1749	8.9	60	30	8.43 (0.34)	4.12 (0.48)

* Length of equivalent path of enzyme, calculated by Eq. 7.21.

Run no.	Length*, cm	\bar{t} , min	%un-reacted starch	% Total reducing sugar (s.v.)	% DE (s.v.)	X
13	794	2.4	34.3	8.52(0.80)	3.28(0.26)	0.12
14	1271	5.2	34.4	9.98(0.88)	3.43(0.44)	0.11
15	1749	8.1	30.8	12.28(1.10)	4.69(0.76)	0.21
16	2227	11.3	27.6	15.12(0.90)	6.27(0.89)	0.29
17	1143	4.6	34.7	10.44(1.00)	2.75(0.56)	0.18
18	1620	5.7	33.0	17.71(1.32)	5.88(0.42)	0.23
19	2098	10.3	32.7	15.66(0.79)	4.44(0.61)	0.23
20	2681	10.4	31.4	20.36(1.28)	7.05(0.73)	0.27

* Length of equivalent path of enzyme, calculated by Eq. 7.21.



7.5.4 Relationship between power number and Reynolds number for mixed screws

The consistency coefficients for corn syrup at various temperatures were determined by regression analysis ($R^2 = 0.99-1.00$) and are presented in Table 7.9.

Temperature, °C	Consistency coefficient, K (Pa.s)
23	66.71
25	55.53
34	15.86
50	3.17
65	0.86

A plot of $\log K$ versus $1/T$ (Figure 7.13) shows an Arrhenius relationship, with an R^2 of 0.998. Since for Newtonian fluids, the consistency coefficient and the viscosity are identical, the viscosity may be expressed as:

$$\mu = 2.73 \times 10^{-14} e^{\left(\frac{10480}{T}\right)} \quad (7.33)$$

A hydraulic diameter of 0.98 cm was calculated for the mixed screws (combination of single lead screws and 90° forwarding paddles) by:

$$D_h = \frac{4 \sum V_{wi}}{\sum A_{wi}} \quad (7.34)$$

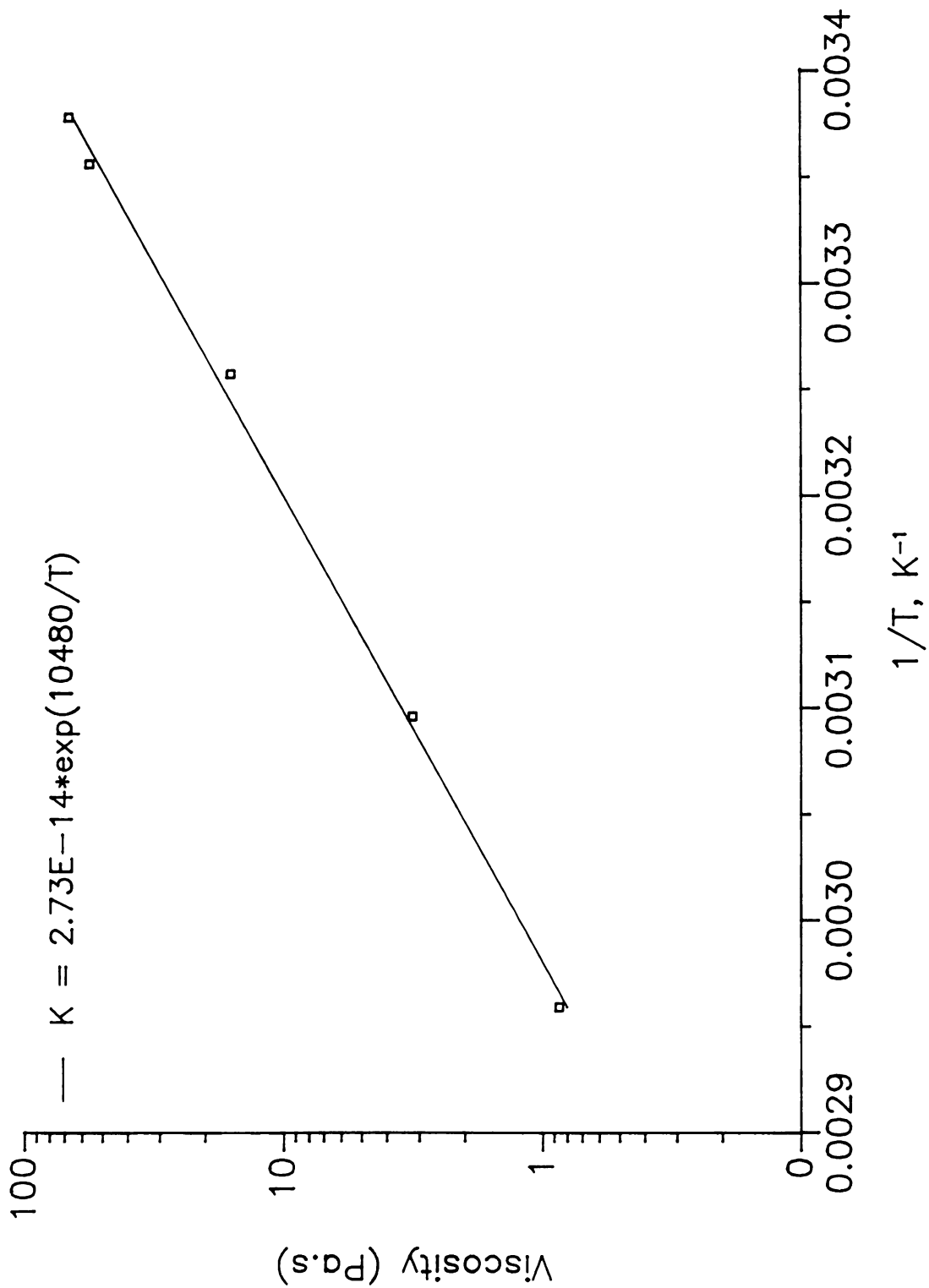


Figure 7.13 Viscosity versus inverse temperature for corn syrup.

From extrusion data, P_o and Re were calculated using equations 7.23 to 7.26, and are summarized in Table 7.10.

RPM	% Torque	Pressure drop, kPa	Avg. Temp, °C	m , kg/hr	$P_o \times 10^{-7}$	$Re \times 10^3$
60	14.0	275.8	19.7	7.0	4.0	1.3
100	14.5	275.8	22.1	9.4	1.0	3.1
150	15.5	206.8	23.2	9.6	0.7	5.3
200	15.5	137.9	24.6	9.9	0.4	8.3

A plot of $\log P_o$ against $\log Re$ is given in Figure 7.14, and yields the relationship ($R^2 = 1.00$):

$$\log P_o = 3.96 - 1.26 \log Re \quad (7.35)$$

This result is similar to that reported by Mohamed (1988) who used a homogeneous screw profile. The apparent viscosity was calculated by Eq. 7.27. Since the calculated values may not represent the true viscosities, each is referred to as a viscosity index (η_i) instead. It is a relative value that describes how the viscosity changes during extrusion.

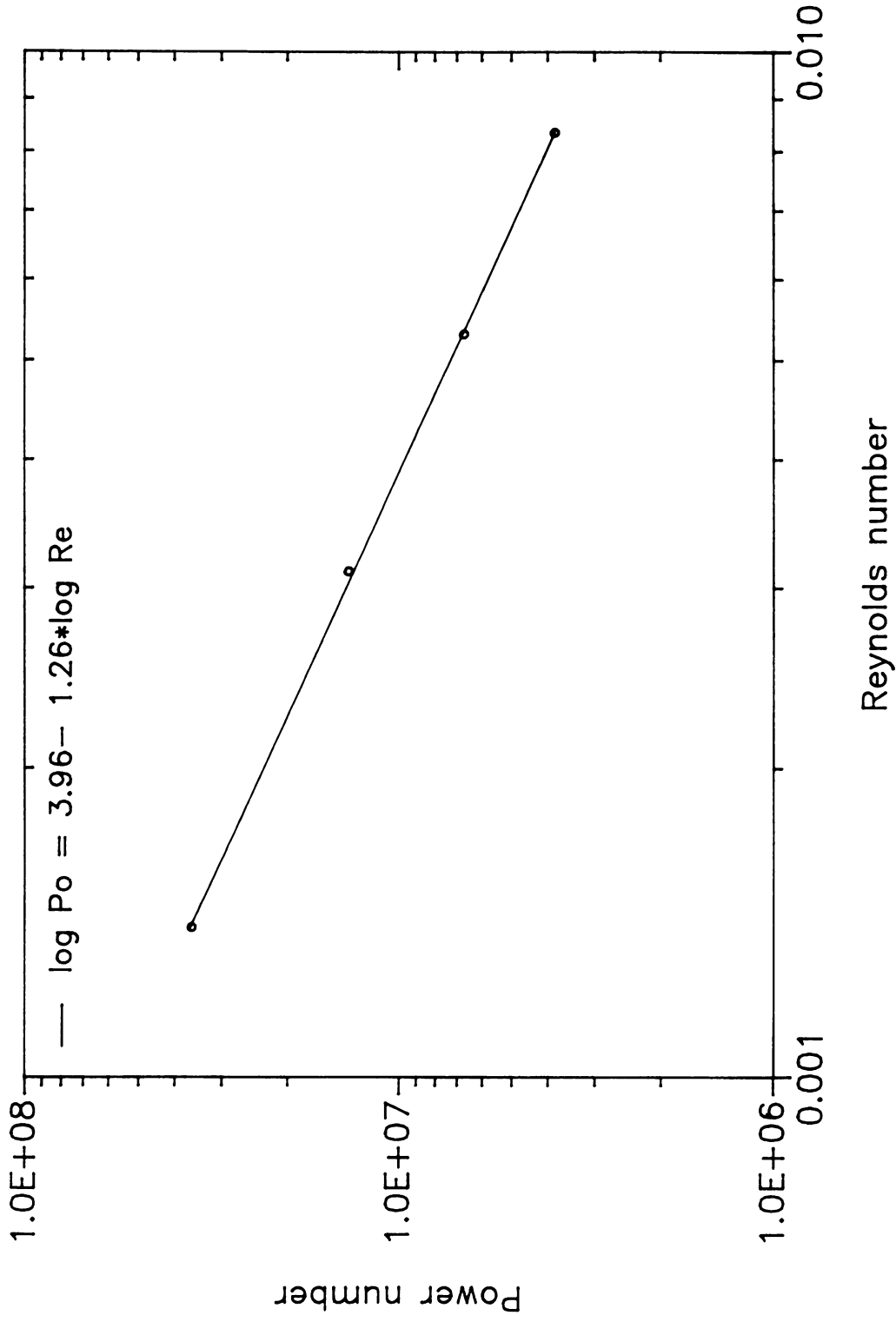


Figure 7.14 Power number versus Reynolds number for corn syrup (Newtonian standard).

7.5.5 Effect of rheology on extent of reaction

Using extrusion data (Appendix 8) with Eqs. 7.23-7.27 and Eq. 7.35, viscosity indices of extrudates at various conditions were estimated. The viscosity indices were normalized by the viscosity index of a base extrudate. The results are shown in Table 7.11 for extrusion runs 1-12 and Table 7.12 for runs 13-20.

Run no.	Avg. temp., °C (s.v.)	% Reducing sugar (s.v.)	% DE (s.v.)	$\frac{\eta_t}{\eta_b}$
1	96.9 (3.6)	3.32 (.13)	1.94 (.13)	0.85
5	96.3 (3.1)	5.28 (.16)	2.54 (.15)	0.81
9	95.6 (2.3)	6.62 (.35)	3.51 (.75)	0.72
2	96.3 (3.3)	3.61 (.33)	1.96 (.20)	0.67
6	96.8 (3.1)	5.65 (.62)	2.66 (.31)	0.58
10	96.3 (2.7)	6.71 (.26)	3.54 (.51)	0.62
3	96.7 (3.3)	6.32 (.64)	3.30 (.45)	0.71
7	96.4 (3.1)	7.98 (.52)	3.37 (.18)	0.75
11	95.8 (2.4)	8.43 (.71)	4.40 (.35)	0.68
4	96.7 (3.6)	6.32 (.83)	3.03 (.42)	0.54
8	96.6 (3.2)	8.67 (.42)	3.52 (.17)	0.50
12	96.7 (2.3)	8.43 (.34)	4.12 (.48)	0.54



Table 7.12. Normalized viscosity indices of starch extrudates from extrusion runs 13-20.

Run no.	Avg. temp., °C (s.v.)	% reducing sugar (s.v.)	% DE (s.v.)	X	$\frac{\eta_t}{\eta_b}$
13	91.6 (2.9)	8.52(0.80)	3.28(0.26)	0.12	0.95
14	91.3 (2.9)	9.98(0.88)	3.43(0.44)	0.11	0.84
15	91.3 (2.4)	12.28(1.10)	4.69(0.76)	0.21	0.68
16	90.9 (2.8)	15.12(0.90)	6.27(0.89)	0.29	0.56
17	89.3 (3.1)	10.44(1.00)	2.75(0.56)	0.18	0.97
18	89.5 (3.7)	17.71(1.32)	5.88(0.42)	0.23	0.72
19	90.2 (2.9)	15.66(0.79)	4.44(0.61)	0.23	0.84
20	92.0 (2.6)	20.36(1.28)	7.05(0.73)	0.27	0.52

The results show that the normalized viscosity index decreases with increased extent of starch hydrolysis, measured in terms of reducing sugars and amount of un-reacted starch (Table 7.12). However, the rate of viscosity reduction was not directly proportional to the extent of hydrolysis because of the varying molecular weights of products formed.

7.5.6 Dispersion model for predicting starch hydrolysis in reactive extrusion

Since RTD measurement was performed during starch hydrolysis in the extruder, it was assumed that the dispersion number of the dye used was the same as that of the starch, even though the dye is a non-reacting tracer, and the starch was fed continuously while the dye was not. The dispersion equation with a reaction term included was used, incorporating the appropriate boundary conditions. If the starch is subjected to the same boundary conditions as the dye, the dispersion equation could be solved in terms of starch

concentrations, which depended on the reaction kinetics of the enzyme.

The reaction kinetics of α -amylase in Chapter 4 were determined from data obtained from runs 13-20, and the results showed that the enzyme reaction could be characterized by a modified first order reaction with a rate constant of 0.033 min^{-1} . The kinetics obtained were used to predict the extent of reaction for extrusion runs 13-20 and compared with the analytical solution from the axial dispersion model (Eq. 7.13). It is worth noting that thermal inactivation of the enzyme was insignificant because the mean product temperatures of $89\text{-}92^\circ\text{C}$ (Table 7.10) were below the maximum tolerable temperature of the enzyme (105°C); and also the residence time in the extruder was relatively short (11 minutes or less). Shear inactivation of the enzyme was assumed to be small and was neglected, due to the shielding effect of the enzyme by the starch molecules, in a manner similar to that of soy polysaccharide (Chapter 5).

The fractional conversion was calculated by Eqs. 7.13 and 7.15. The predicted profiles of fractional conversion for extrusion runs 13-16 and 17-20 are shown in Figures 7.15 and 7.16, respectively. It was apparent that slope of the profile increased with increased length of reactor. Therefore, the rate of fractional conversion increases with increased length of the reactor, while the dispersion number decreases. This is true for runs 13-16 (Figure 7.15), but not for runs 17-20, where there is no clear trend (Figure 7.16).

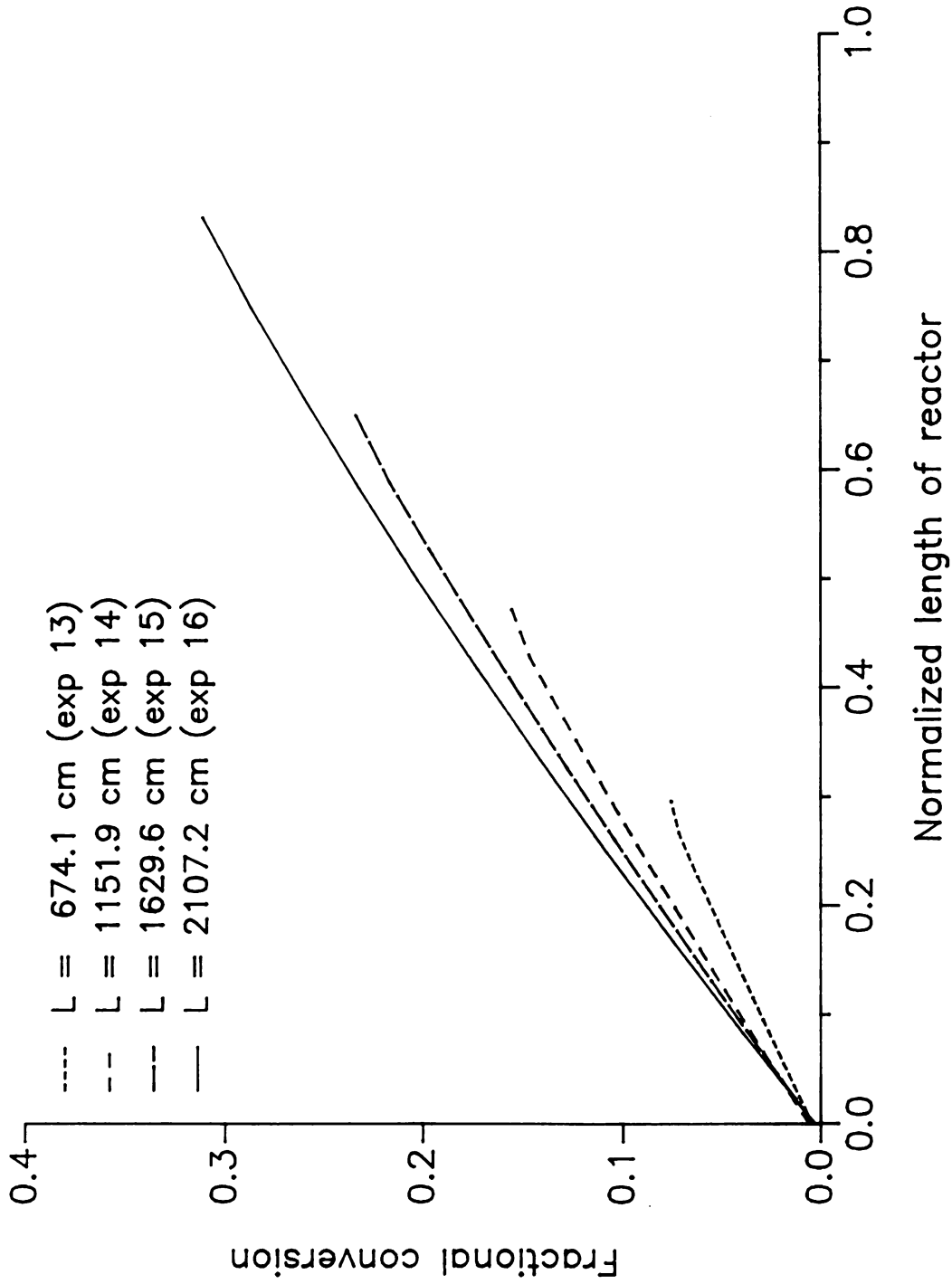


Figure 7.15 Predicted fractional conversion versus normalized length of reactor from experiments 13–16.

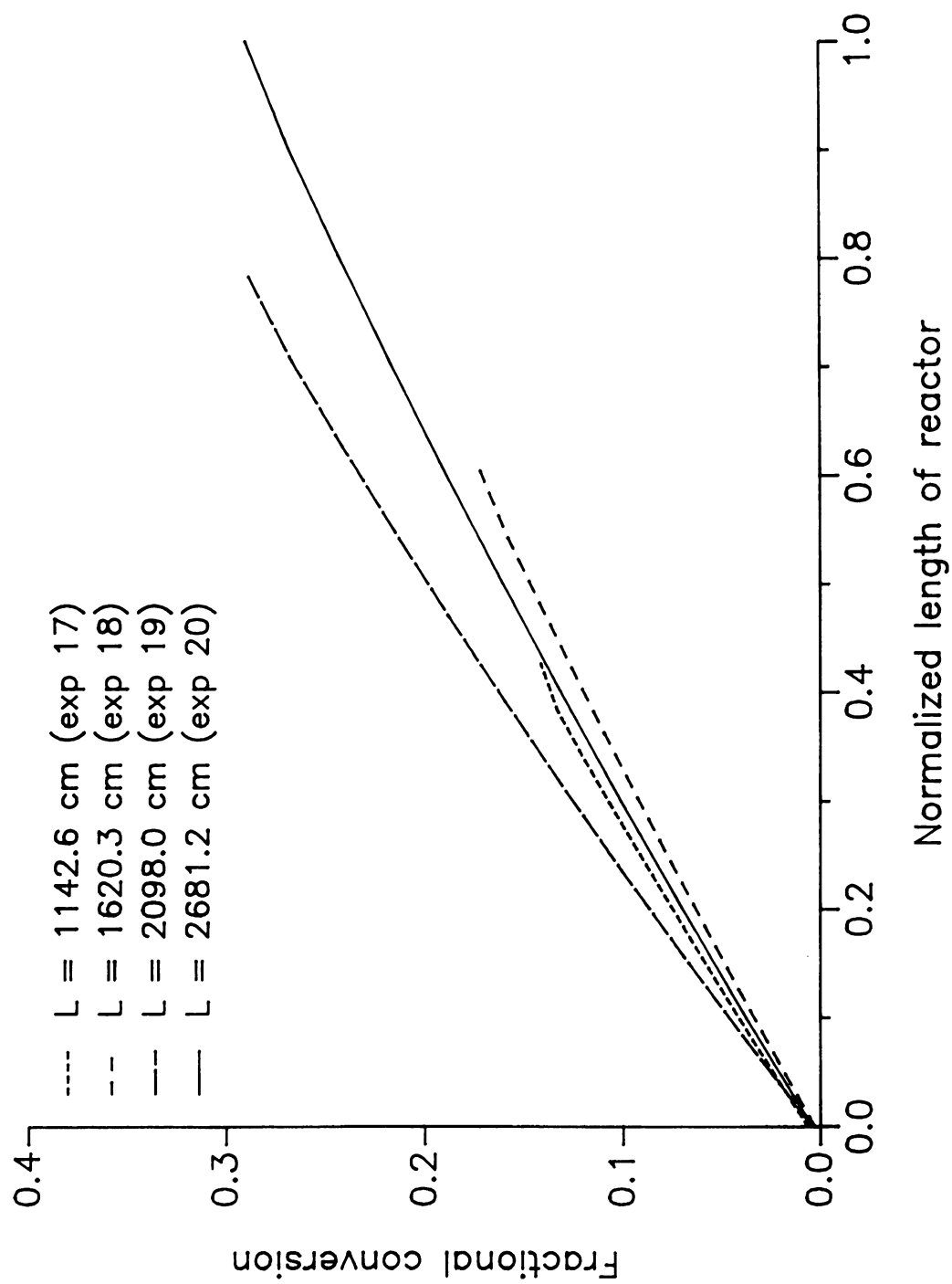


Figure 7.16 Predicted fractional conversion versus normalized length of reactor from experiments 17–20.

The observed and predicted fractional conversion (X) of extrusion runs 13-20 are presented in Table 7.13.

Table 7.13. Observed and predicted fractional conversion (extrusion runs 13-20).

Run no.	$\frac{D_e}{\bar{u}L_e} \times 10^3$	\bar{t}^* , min	Observed X	Predicted X
13	51.8	2.4	0.12	0.07
14	34.0	5.2	0.11	0.14
15	12.1	8.1	0.21	0.22
16	7.3	11.3	0.29	0.30
17	40.5	4.6	0.18	0.14
18	14.0	5.7	0.23	0.17
19	10.9	10.3	0.23	0.29
20	11.5	10.4	0.27	0.29

There is generally good agreement between the predictions and experimental data, especially at long residence times. It is possible that the large variations at short residence times were due to lack of complete mixing. Using regression analysis, it was found that the predicted and the experimental data have good agreement ($R^2 = 0.96$, at $P < 0.05$). The experimental results from runs 13-20 were super-imposed and are plotted against the predicted profiles of runs 16 and 20 in Figure 7.17.

Because the reaction was characterized as first order, the effect of dispersion was not significant. For example, at a constant residence time, the outlet fractional conversion did not change significantly when the dispersion number increased ten-fold. On the whole, the extent of liquefaction depended significantly on the residence time, as expected.

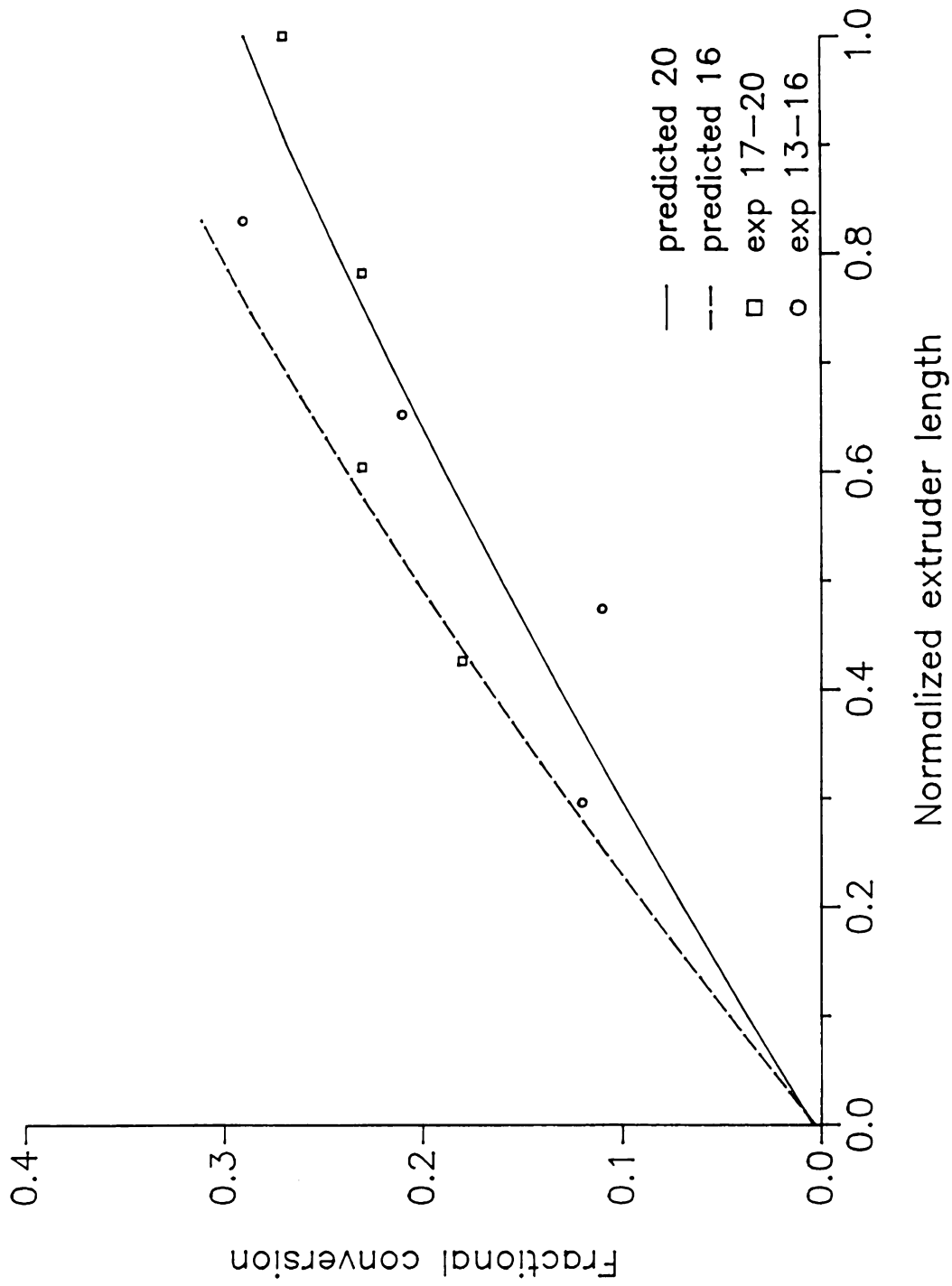


Figure 7.17 Predicted and observed fractional conversion versus normalized length of reactor from experiments 13-20.

7.6 Conclusions

A dispersion model was used to characterize the flow behavior of a twin screw extruder during starch hydrolysis by thermostable α -amylase. The flow behavior was determined by an impulse-response experiment, using erythrosine as a tracer. The dispersion number was calculated from RTD data, using the first and second moments. The extruder was characterized as a tube, and a closed system. This characterization as a closed system is not in the thermodynamic sense. Analysis showed good agreement between the concentration profile of the tracer calculated from the model of a closed system and the one obtained from experiment ($P < .05$).

The experimental results show that the dispersion number depends on the screw rpm and length of the reactor. Therefore, it is also a function of the mean velocity. Also, the dispersion number depends on the dispersion coefficient, which is a function of molecular diffusion, velocity and geometry of the extruder. The effects of interactions between these parameters complicates the analysis and may make the dispersion model difficult to apply to enzymatic starch liquefaction.

The above complication occurs when the effect of each parameter is considered separately. However, if all effects are lumped in terms of the dispersion number, several trends are easily observed. For example, it was apparent that the dispersion number decreases with increased length of reactor, and that at long residence times, the extent of reaction increases while the dispersion number decreases.

The dispersion number obtained from RTD data was assumed to be the same as that of the extrudate. Therefore, it was used to predict the extent of liquefaction. The enzymatic reaction was described by a modified first order reaction, allowing the

dispersion equation to be solved analytically. The analytical solution gave results comparable to experimental data, especially at low dispersion numbers (long residence times). This is in agreement with what has been reported in the literature.

As expected, increases in enzyme levels resulted in increased extents of starch liquefaction. At an enzyme activity of 45 units/g of starch, the maximum fractional conversion was 0.3 at a residence time of 11 minutes. Because enzymes are expensive, increasing enzyme dosage offers limited prospects. Since under the extrusion conditions used, thermal and shear inactivation was negligible, liquefaction should be continued in a batch system, in a longer extruder, or in multi-passage systems. Because the twin screw extruder is very flexible, other conditions may be used to increase the extent of starch conversion. Additional study in this area would be helpful.

Theoretically, the axial dispersion model is valid for a system with a constant dispersion number. Results in this study indicate that the model can also be used under conditions of variable dispersion numbers if the reaction is linear. It would be of interest to examine the effect of varying dispersion numbers on the extent of reaction under unsteady state conditions. The result will be useful and may explain process instabilities when the dispersion number changes along the extruder. It is also recommended that the dispersion equation be studied under unsteady state conditions. The solution of the unsteady state equation is likely complex; it is an eigenvalue problem and may require numerical methods.

7.7 Nomenclature

A_c	Cross-sectional area, cm^2
A_{wi}	Wetted area of screw i , cm^2
a	Redness value, from Chroma Meter

b	Slope (Eq. 7.31), dimensionless
C_0	Concentration of substrate at time = 0, g/g
C, C_t	Concentration of substrate at time t , g/g
C_s'	Modified starch concentration, g/g
\bar{C}	Normalized starch concentration, dimensionless
D	Tube diameter, cm
D_e	Effective axial dispersion coefficient, cm^2/s
D_h	Hydraulic diameter, cm
D_m	Molecular diffusion coefficient, cm^2/s
DE	Dextrose equivalent, dimensionless
E_v	Viscous dissipation of mechanical energy, W
F	F-function, dimensionless
k	Rate constant, min^{-1}
K	Consistency coefficient, $\text{Pa}\cdot\text{s}^n$
L	Axial length of reactor, cm
L_e	Equivalent length of screws used during RTD measurement, cm
L_e^*	Equivalent length of the screws in the reaction zone, cm
\dot{m}	Throughput, g/min
n	Flow behavior index, dimensionless
N	Screw speed, rps
Pe	Peclet number, dimensionless
Po	Power number, dimensionless
P_w	Power input, W
Re, Re'	Reynolds number, dimensionless

r_s	Rate of starch consumption, g/g/min
t	Residence time, min
\bar{t}	Mean residence time from RTD data, min
\bar{t}^*	Corrected mean residence time of the reaction, min
\bar{u}	Mean velocity, cm/s
V_{wi}	Wetted volume of screw i, cm ³
x	Axial length of the reaction vessel or extruder, cm
X	Fractional conversion, dimensionless
y	Variable, Eq. 7.24
z	Normalized length, dimensionless

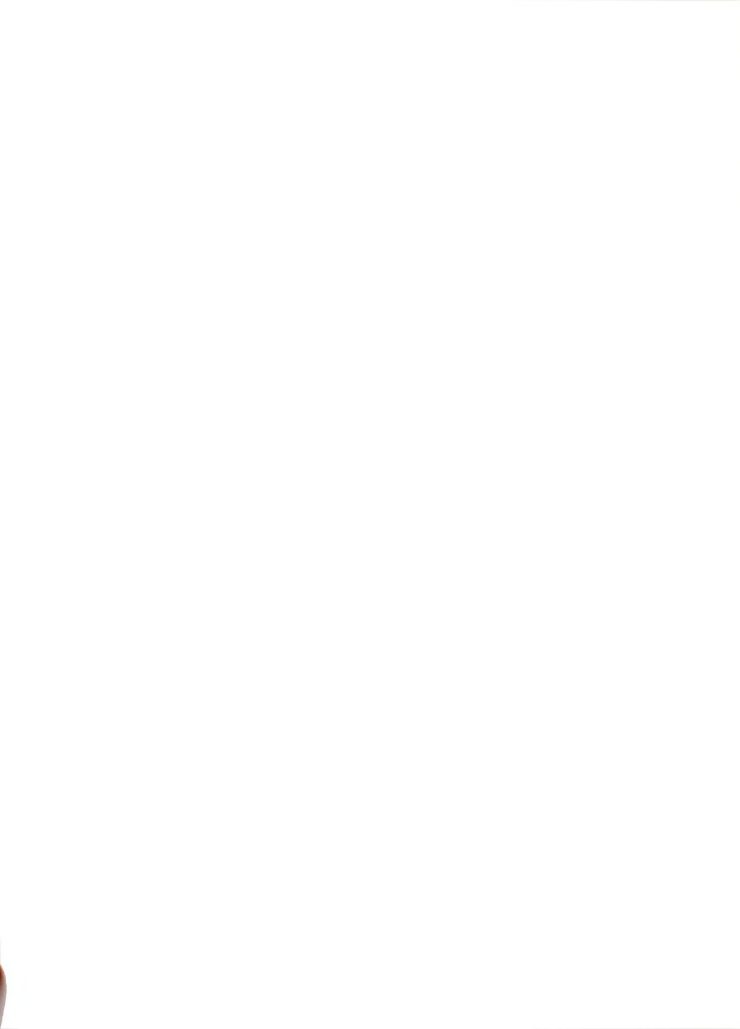
Greek symbols

η_a	Non-Newtonian apparent viscosity, Pa.s ⁿ
η_i	Non-Newtonian viscosity index, Pa.s ⁿ
μ	Newtonian viscosity, Pa.s
v	Variable, Eq. 7.24
ρ	Density of extrudate , g/ml
σ^2	Variance of the RTD curve, min ²
τ	Dimensionless residence time
ζ	Variable, Eq. 7.14

7.8 References

- Aris, R. 1956. On the dispersion of a solute in a fluid flowing through a tube. Proc. Roy. Soc. London. Series A. 235:67.
- Bernfeld, P. 1955. Amylase, α , β . Methods Enzymol. 1:149.
- Bischoff, K.B. 1968. Accuracy of the axial dispersion model for chemical reactors. AIChE J. 14(5):820.
- Bischoff, K.B. and Levenspiel, O. 1962. Fluid dispersion - generalization and comparison of mathematical models. Chem. Eng. Sci. 17:245.
- Booras, G.S. and Krantz, W.B. 1976. Dispersion in the laminar flow of power-law fluids. Ind. Eng. Chem. Fundam. 15(4):249.
- Bounie, D. 1988. Modeling of the flow pattern in a twin-screw extruder through residence-time distribution experiments. J. Food Eng. 7:223.
- Butt, J.B. 1980. Reaction Kinetics and Reactor Design. Prentice-Hall, New York.
- Carnahan, B., Luther, H.A. and Wilkes, J.O. 1969. Applied Numerical Methods. John Wiley & Sons, New York.
- Danckwerts, P.V. 1953. Continuous flow systems, distribution of residence times. Chem. Eng. Sci. 2(1):1.
- Dygert, S., Li, L.H., Florida, D. and Thoma, J.A. 1965. Determination of reducing sugar with improved precision. Anal. Biochem. 13:367.
- Froment, G.F. and Bischoff, K.B. 1979. Chemical Reactor Analysis and Design. John Wiley & Sons, New York.
- Gibilaro, L.G. 1978. On the residence time distribution for systems with open boundaries. Chem. Eng. Sci. 33:487.
- Gill, W.N. 1967. A note on the solution of transient dispersion problems. Proc. Roy. Soc. London. Series A. 298:335.

- Gill, W.N. and Sankarasubramanian, R. 1970. Exact analysis of unsteady convective diffusion. Proc. Roy. Soc. London. Series A. 316:341.
- Komolprasert, V. and Ofoli, R.Y. 1989. A dispersion model of enzyme-catalyzed reaction-kinetics in a twin screw extruder. Proceeding of the International Conference on Engineering and Food (ICEF), Cologne, W. Germany, June 1989.
- Kreft, A. and Zuber, A. 1978. On the physical meaning of the dispersion equation and its solutions for different initial and boundary conditions. Chem. Eng. Sci. 33:1471.
- Levenspiel, O. 1972. Chemical Reaction Engineering. 2nd edition. John Wiley & Sons, New York.
- Levenspiel, O. and Smith, W.K. 1957. Notes on the diffusion - type model for the longitudinal mixing of fluids in flow. Chem. Eng. Sci. 6:227.
- Linko, P. and Linko, Y.Y. 1983. Extrusion cooking and bioconversions. J. Food Eng. 2:243.
- Linko, P., Hakulin, S. and Linko, Y.Y. 1983. Extrusion cooking of barley starch for the production of glucose syrup and ethanol. J. Cereal Science. 1:2745
- Linko, P., Hakulin, S. and Linko, Y.Y. 1984. HTST - extrusion cooking in ethanol production from starchy materials. Enzyme Microb. Technol. 6:457.
- Michelsen, M.L. and Ostergaard, K. 1970. The use of residence time distribution data for estimation of parameters in the axial dispersion model. Chem. Eng. Sci. 25:583.
- Michelsen, M.L. 1972. A least - squares method for residence time distribution analysis. Chem. Eng. J. 4:171.
- Mohamed, I.O. 1988. Modeling shear rate and heat transfer in a twin screw co-rotating food extruder. Ph.D. Dissertation. Dept. Agri. Engr. Michigan State University. East Lansing, MI.



- Nauman, E.B. 1981. Residence time distributions and micromixing. *Chem. Eng. Commun.* 8:53.
- Ofoli, R.Y., Komolprasert, V., Saha, B.C. and Berglund, K.A. 1989. Production of maltose by reactive extrusion of carbohydrates. *Lebens. Wissen. und Technol.* In print.
- Parimi, K. and Harris, T.R. Identification of residence time models by reacting tracer experiments. *Can. J. Chem. Eng.* 53:175.
- Pham, Q.T. and Keey, R.B. 1977. The use of graphical transfer-function methods for residence time distribution studies. *Chem. Eng. Sci.* 32:786.
- Reinikainen, P., Suortti, T., Olkku, J., Mälkki, Y. and Linko, P. 1986. Extrusion cooking in enzymatic liquefaction of wheat starch. *Starch.* 1:20.
- Saha, B.C., Shen, G.J. and Zeikus, J.G. 1987. Behavior of a novel thermostable β -amylase on raw starch. *Enzyme Microb. Technol.* 9:598.
- Sankarasubramanian, R. and Gill, W.N. 1972. Dispersion from a prescribed concentration distribution in time variable flow. *Proc. Roy. Soc. London. Series A.* 329:479.
- Subramanian, R.S. and Gill, W.N. 1976. Unsteady convective diffusion in non-Newtonian flows. *Can. J. Chem. Eng.* 54:121.
- Subramanian, R.S. 1977. On generalized dispersion theory. *Chem. Eng. Sci.* 32:788.
- Taylor, G. 1953. Dispersion of soluble matter in solvent flowing slowly through a tube. *Proc. Roy. Soc. London. Series A.* 219:186.
- Van der Laan, E.T. 1958. Notes on the diffusion - type model for the longitudinal mixing in flow. *Chem. Eng. Sci.* 7:187.

8 CONCLUSIONS

An MPF 50D Baker-Perkins twin screw food extruder was used as a bioreactor to carry out liquefaction of pre-gelatinized corn starch by thermostable α -amylase. The reaction occurred in a fully-filled zone configured with 90° paddles. A one-dimensional axial dispersion model was used to predict the extent of starch liquefaction. The model was evaluated with several extrusion data obtained during studies designed to address the following:

1. Starch hydrolysis kinetics of α -amylase;
2. Effect of shear on enzyme activity;
3. Effect of rheology on dispersion of fluids in the extruder; and
4. Effect of moisture content, screw rpm, enzyme level and dispersion number on the extent of starch liquefaction.

Based on an initial rate experiment at low starch concentrations (1-8%, w/w), the kinetics of α -amylase was found to follow the classical Michaelis-Menten model. A continuous rate study at a high starch concentration of 40% showed that the enzyme kinetics may be described by a modified first order reaction equation.

Effect of shear on enzyme activity was performed in both a concentric cylinder viscometer and the extruder. In the viscometer, strain history had the most significant effect on loss of activity. However, loss of activity in the extruder depended on a combination of strain history, shear rate and specific energy consumption (SEC). About a 20% loss of activity was observed. This loss of activity was less than expected, possibly due to the shielding effect of SPS during extrusion.

Effect of rheological behavior on the dispersion coefficient (D_e) was explained by a model developed on the basis of the Taylor-Aris model. Several extrusion runs were performed using corn syrup, 30% SPS in honey and 2.5% methocel in water. Corn syrup

is a Newtonian fluid ($n=1$), while the SPS-honey ($n=.416$) and the methocel-water ($n=.3$) systems are pseudoplastic fluids. The methocel solution had the largest dispersion coefficient, followed by corn syrup; SPS-honey had the smallest dispersion. The mean velocity was dominant and governed the degree of dispersion. The viscoelastic properties of the fluids did not show a clear effect on the dispersion coefficient.

The extent of reaction, measured by percent DE and percent reducing sugar, was significantly affected by moisture content, enzyme level and residence time; the effect of screw speeds (30-60 rpm) was not apparent. Dispersion numbers were calculated from RTD data and increased with screw rpm but decreased with length of the reaction zone.

Several extrusion data were super-imposed to obtain a profile of the extent of conversion. Since the enzymatic reaction was first order, an analytical solution was obtained and compared to the experimental data; there was good agreement between the predictions and the experimental data at $P<.05$. In general, the axial dispersion model is suitable for the modeling of reactions involving starch hydrolysis.

9 RECOMMENDATIONS FOR FURTHER RESEARCH

Further studies are required to extend the understanding of enzymatic starch hydrolysis in twin screw extruders. These include:

1. Initial rate studies at various high starch concentrations in the extruder.
2. Determination of the effect of temperature on the kinetics of α -amylase.
3. Effect of shear on enzyme activity under various extrusion conditions.
4. Effect of viscoelastic properties on the dispersion coefficient.
5. Evaluation of the validity of the axial dispersion model with other screw configurations.
6. Assessment of the axial dispersion model as a tool for predicting the extent of other reactions, such as saccharification by β -amylase.
7. Effect of the dispersion number on the stability of the extrusion processes.



10 APPENDICES

Appendix 1. Shear deactivation data from Haake viscometer.	
Strain history x 10⁴	% Residual enzyme activity
2.80	100.0 96.6
4.20	100.0 100.0
5.60	100.0 98.4
8.40	87.6 93.6
9.80	89.7 95.7 86.7 100.0
11.20	93.2 93.2
14.00	92.6 100.0
14.70	97.1 93.5
15.40	97.2 86.3
19.60	99.5 99.3 96.9 79.7
22.40	93.2 86.7
25.20	96.6 95.1
30.80	100.0 85.4
34.30	93.0 91.2
39.20	82.8 86.7
49.00	83.9 82.8

Appendix 1. (Cont'd).

53.91	81.0 74.0
58.81	86.3 88.6
72.81	82.5 82.0
84.01	75.9 76.6
92.41	70.2 66.8
126.02	65.1 64.8

Appendix 2. Analysis of variance (SAS program) of effect of strain history on % residual enzyme activity from Haake viscometer data.					
Source	DF	Sum of Square	Mean Square	F value	Pr > F
Model					
strain	21	3948.2	188.0	7.31	0.0001
Error	26	668.3	25.7		
Corrected Total	47	4616.5			
R square	C.V.	Root MSE	Mean % activity		
0.8552	5.702	5.070	88.92		



Appendix 3. Shear deactivation data from extrusion runs.	
RPM	Residual activity x 10 ⁻³ , units
60	27.6 28.1 27.6 29.5 32.3
100	33.3 31.1 31.8 30.3 26.4
150	30.3 28.4 28.3 23.7 25.6
200	29.1 26.2 27.8 29.4 28.9
250	20.7 30.6 29.5 21.5 25.7
300	28.1 30.5 29.3 27.1 27.6
400	25.2 31.0 26.1 28.9 29.1

Appendix 4. Analysis of variance* (SAS program) of effect of strain history on enzyme activity during extrusion.					
Source	DF	Sum of Square	Mean Square	F value	Pr > F
Model					
strain	6	640.85	106.81	1.76	0.1436
Error	28	1697.44	60.62		
Corrected Total	34	2338.29			
R square	C.V.	Root MSE	Mean % activity		
0.2741	9.21	106.81	84.5		

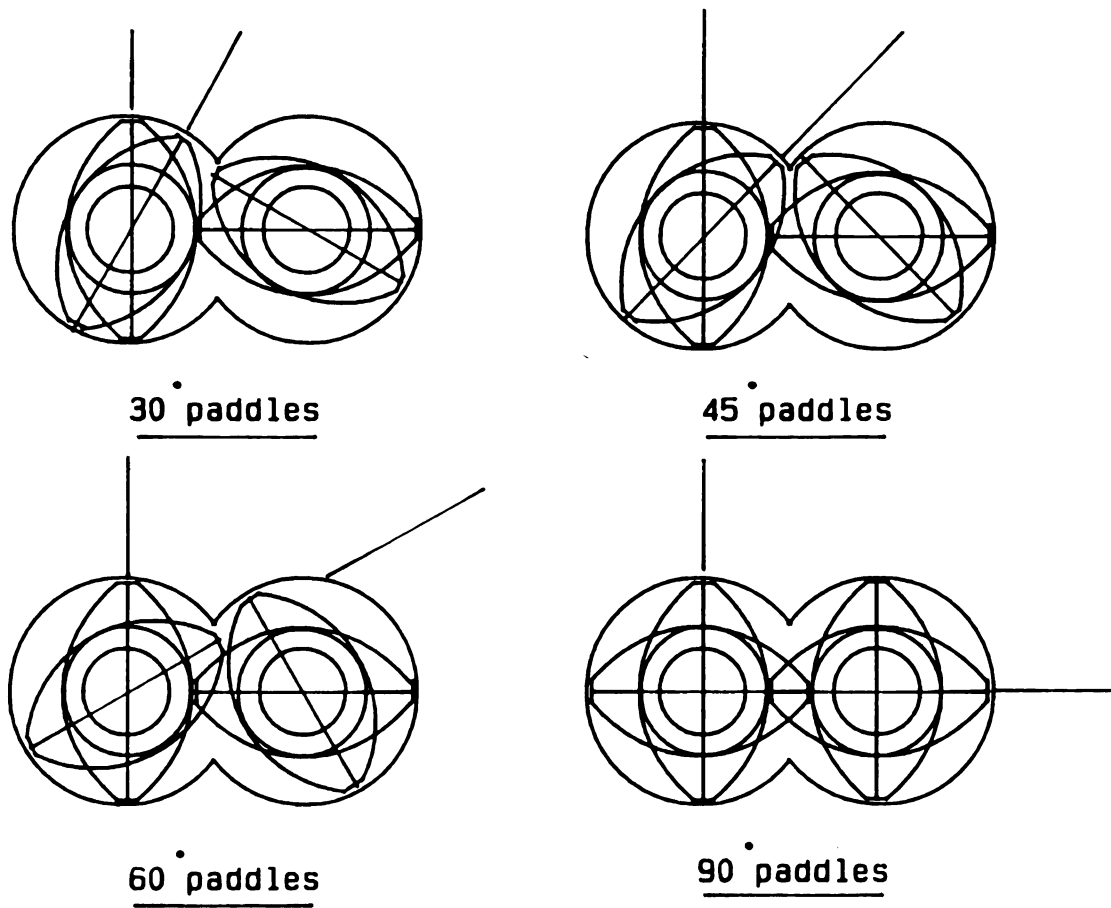
* The same result was obtained for shear rate and SEC.

Appendix 5. Analysis of variance (SAS program) of effect of strain history, shear rate and SEC on enzyme activity during extrusion.

Source	DF	Sum of Square	Mean Square	F value	Pr > F
Model	18	1922.56	106.81	4.11	0.0110
strain	6	640.85	106.81	4.11	0.0110
shear rate	6	640.85	106.81	4.11	0.0110
SEC	6	640.85	106.81	4.11	0.0110
Error	16	415.74	25.98		
Corrected Total	34	2338.29			
R square	C.V.	Root MSE	Mean % activity		
0.8222	6.03	5.10	84.5		



Appendix 6. Extrusion data for corn syrup, 7% SPS in honey and 2.5% Methocel.					
Material	RPM	% Torque	Pressure drop (psi)	Flow rate, kg/hr	Avg. temp., C (s.v.)
Corn syrup	100	14.0 15.0	35	9.37	23.5(0.8) 22.1(0.9)
	150	15.5	30	9.63	23.2(1.1)
7% SPS in honey	100	14.0	30	9.23	26.6(0.9) 23.7(0.6)
	150	15.5	30	9.62	24.0(0.7) 23.8(2.0)
2.5% Methocel	150	7.0	5	8.40	18.3(0.7)
				9.18	22.3(0.4)

Appendix 7. Paddle configurations in the twin screw extruder.

Cross-sections of the extruder barrel with different forwarding paddle configurations.

Appendix 8. Extrusion data on starch liquefaction (extrusion runs 1-20).						
Run no.	RPM	% Torque	Pressure drop, psi	Flow rate (kg/hr)	Avg. temp., C	% MC (out)
1	30	9	50	10.98	96.9	55.4
2	60	11	60	11.10	96.3	55.4
3	30	17	70	10.74	96.7	49.4
4	60	20	70	10.98	96.7	49.4
5	30	10	30	10.08	96.3	57.2
6	60	10	30	10.32	96.8	57.2
7	30	20	40	10.38	96.4	46.0
8	60	20	40	10.20	96.6	46.1
9	30	8	40	11.10	95.6	60.9
10	60	12	40	10.98	96.3	60.9
11	30	27	40	10.74	95.8	46.5
12	60	25	50	10.32	96.7	45.3
13	60	14.5	20	10.05	91.6	56.0
14	60	12.5	20	10.11	91.3	56.0
15	60	9.5	20	10.08	91.3	56.8
16	60	7.5	20	9.99	90.9	57.3
17	60	11.0	30	9.90	89.3	56.0
18	60	8.5	20	10.68	89.5	55.7
19	60	12.0	30	9.60	90.2	57.1
20	60	7.5	20	10.59	92.0	53.0



Appendix 9. Analysis of variance (SAS program) of mean residence time (RTD, \bar{t}) for extrusion runs 1-12.

Source	DF	Sum of Square	Mean Square	F value	Pr > F
Variable:RTD					
Model	5	19.743	3.949	192.33	0.0001
L _o	2	15.095	0.021	367.63	0.0001
% MC	1	0.295	0.295	14.35	0.0091
Enz. dose	1	4.107	4.106	200.03	0.0001
RPM	1	0.247	0.247	12.01	0.0134
Error	6	0.123	0.008		
Corrected Total	11	19.866			
R square	C.V.	Root MSE	Mean RTD		
0.9938	2.304	0.1433	6.22		



Appendix 10. Analysis of variance (SAS program) of dispersion number (DI, $\frac{D_e}{\bar{u}L_e}$) for extrusion runs 1-12.					
Source	DF	Sum of Square	Mean Square	F value	Pr > F
Variable:DI					
Model	5	0.0011839	0.0002368	5.93	0.0256
L_e	2	0.0002397	0.0001198	12.96	0.0066
% MC	1	0.0000008	0.0000008	0.02	0.8955
Enz. dose	1	0.0000132	0.0000132	0.33	0.5859
RPM	1	0.0001347	0.0001347	3.37	0.1160
Error	6	0.0002397	0.0000399		
Corrected Total	11	0.0014236			
R square	C.V.	Root MSE	Mean DI		
0.8316	27.97	0.0063	0.0226		



Appendix 11. Analysis of variance (SAS program) of dispersion number ($DI, \frac{D_p}{uL_c}$) for extrusion runs 13-20.

Source	DF	Sum of Square	Mean Square	F value	Pr > F
Variable:DI					
Model					
Method	1	0.00010	0.00010	0.32	0.5925
Error	6	0.00188	0.00031		
Corrected Total	7	0.00198			
R square	C.V.	Root MSE	Mean DI		
0.0505	77.8	0.0177	0.0228		

Appendix 12. Percent reducing sugar and DE from extrusion runs 1-20.						
Run no.	L _e	% MC	Enz. dose	RPM	% Reducing sugar	% DE
1	674	60	23	30	3.48	2.03
					3.12	2.01
					3.20	1.74
					3.37	2.10
					3.39	1.88
					3.36	1.88
2	674	60	23	60	3.99	2.12
					3.20	1.75
					3.55	1.87
					3.98	2.28
					3.33	1.88
					3.59	1.86
3	674	50	30	30	6.28	3.09
					6.84	3.93
					6.30	3.24
					6.12	3.19
					7.09	3.68
					5.26	2.66
4	674	50	30	60	6.34	3.09
					5.74	2.60
					5.53	2.73
					6.30	2.97
					6.13	2.99
					7.88	3.81
5	1152	60	23	30	5.35	2.61
					5.31	2.76
					4.96	2.48
					5.38	2.30
					5.39	2.56
					5.31	2.52
6	1152	60	23	60	6.09	2.89
					5.75	2.63
					5.71	2.55
					5.23	2.41
					4.68	2.32
					6.43	3.16
7	1152	50	30	30	8.42	3.16
					7.58	3.33
					7.36	3.38
					8.15	3.29
					7.67	3.37
					8.69	3.70

Appendix 12. (Cont'd).

8	1152	50	30	60	8.66 8.80 8.19 9.39 8.31 8.67	3.76 3.50 3.63 3.26 3.46 3.52
9	1630	60	23	30	6.61 6.15 6.45 7.22 6.64 6.64	4.58 3.33 4.31 2.80 2.89 3.15
10	1630	60	23	60	6.62 6.59 6.36 7.11 6.68 6.91	3.36 3.27 3.25 4.56 3.33 3.46
11	1630	50	30	30	8.66 8.89 7.65 9.39 7.58 8.40	4.33 4.88 4.04 4.45 4.00 4.69
12	1630	50	30	60	8.22 8.98 8.22 8.49 8.62 8.03	4.01 4.20 4.03 4.23 4.87 3.38
13	674	60	45	60	7.15 8.93 8.60 8.13 9.43 8.88	2.94 3.48 3.57 3.10 3.49 3.10
14	1152	60	45	60	9.59 9.46 8.91 10.08 11.45 10.39	3.34 3.18 2.97 3.24 4.22 3.63

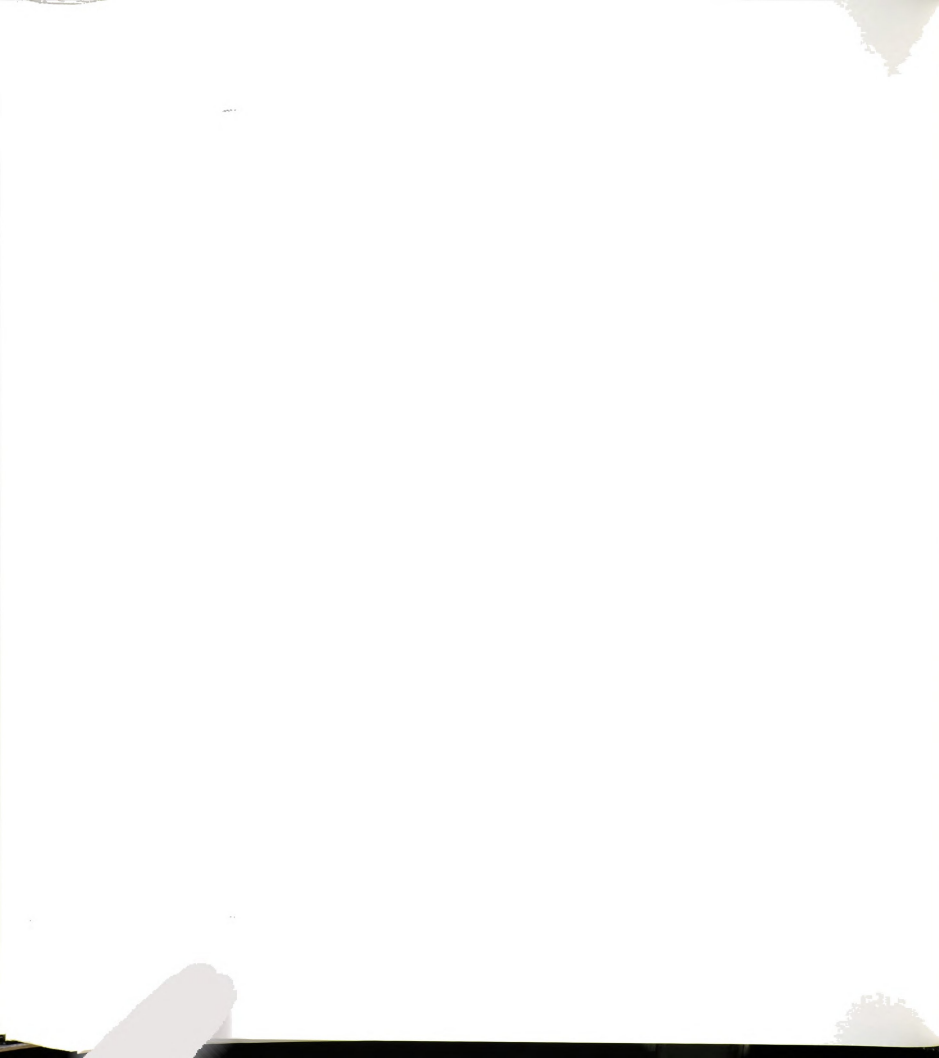
Appendix 12. (Cont'd).

15	1630	60	45	60	11.72 10.53 12.84 11.96 13.59 13.04	4.26 3.85 5.21 4.37 5.94 4.53
16	2107	60	45	60	14.84 14.34 15.43 14.52 16.80 14.81	5.82 5.32 6.58 5.39 7.39 7.11
17	1143	60	45	60	8.87 9.93 10.10 11.00 11.57 11.19	1.81 2.58 2.81 2.68 3.20 3.43
18	1620	60	45	60	18.54 19.34 17.31 15.95 18.59 16.53	6.10 6.50 5.73 5.84 5.90 5.22
19	2098	60	45	60	15.83 15.38 16.83 14.45 15.42 16.06	4.19 4.25 5.13 3.47 4.56 5.04
20	2681	60	45	60	20.43 20.48 22.13 21.28 18.93 18.91	7.10 7.95 7.70 7.07 6.04 6.43

Appendix 13. Analysis of variance (SAS program) of effect of moisture content, screw rpm and enzyme level on % reducing sugar (RS) and % DE for extrusion runs 1-12.					
Source	DF	Sum of Square	Mean Square	F value	Pr > F
Variable:RS					
Model	3	224.539	74.846	9355.61	0.0001
MC	1	111.751	111.751	13968.62	0.0001
Enz. dose	1	111.751	111.751	13968.62	0.0001
RPM	1	1.037	1.037	129.60	0.0001
Error	68	0.544	0.008		
Corrected Total	71	225.083			
R square	C.V.		Root MSE	Mean % RS	
0.9976	1.3888		0.0894	6.44	
Variable:DE					
Model	3	31.330	10.443	42.72	0.0001
MC	1	15.652	15.652	64.03	0.0001
Enz. dose	1	15.652	15.652	64.03	0.0001
RPM	1	0.025	0.025	0.10	0.7486
Error	68	16.624	0.224		
Corrected Total	71	47.953			
R square	C.V.		Root MSE	Mean % DE	
0.6533	15.66		0.4944	3.15	



Appendix 14. Analysis of variance (SAS program) of effect of method of enzyme addition on % reducing sugar (RS) and % DE for extrusion runs 13-20.					
Source	DF	Sum of Square	Mean Square	F value	Pr > F
Variable:RS					
Model					
Method	1	41.68	41.68	3.21	0.1234
Error	6	77.93	11.07		
Corrected Total	7	119.61			
R square	C.V.		Root MSE	Mean % RS	
0.3485	26.19		3.604	13.76	
Variable:DE					
Model					
Method	1	0.76	0.76	0.28	0.6150
Error	6	16.15	2.69		
Corrected Total	7	16.90			
R square	C.V.		Root MSE	Mean DI	
0.0448	34.74		1.640	4.72	



MICHIGAN STATE UNIV. LIBRARIES



31293005706944